Steering and control of a CVT based hybrid transmission for a passenger car

Steering and control of a CVT based hybrid transmission for a passenger car

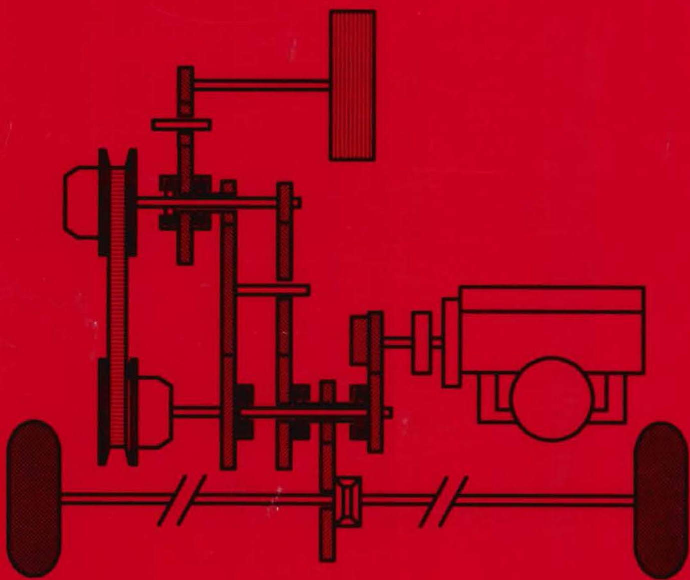

E. Spijker

Steering and control of a CVT based hybrid transmission for a passenger car

CIP-GEGEVENS KONINKLIJKE BIBLIOTHEEK, DEN HAAG

Spijker, Engbert

Steering and control of a CVT based hybrid transmission
for a passenger car / Engbert Spijker. - Eindhoven:
Technische Universiteit Eindhoven
Proefschrift Eindhoven. - Met lit. opg. - Met samenvatting
in het Nederlands.
ISBN 90-386-0173-5
Trefw.: aandrijftechniek; motorvoertuigen.

Druk: Wibro, Helmond

Steering and control of a CVT based hybrid transmission for a passenger car

PROEFSCHRIFT

ter verkrijging van de graad van doctor aan de Technische Universiteit Eindhoven, op gezag van de Rector Magnificus, prof. dr. J.H. van Lint, voor een commissie aangewezen door het College van Dekanen in het openbaar te verdedigen op vrijdag 15 april 1994 om 14.00 uur

door

ENGBERT SPIJKER

geboren te Oldemarkt

Dit proefschrift is goedgekeurd door de promotoren

prof.dr.ir. R.F.C. Kriens
prof.dr.ir. J.J. Kok

en de co-promotor

dr.ir. F.E. Veldpaus

voor Judith

Summary

At the Eindhoven University of Technology a hybrid drive line concept is developed, with a high speed flywheel, an internal combustion engine and a Continuously Variable Transmission (CVT), which is aimed at the reduction of fuel consumption and exhaust gas emissions of road vehicles. In order to realize this concept, a controller is essential which includes the dynamic behaviour of the drive line. The output torque which is to be controlled depends on the driver's requests and the vehicle load. A good vehicle driveability and high levels of passenger comfort should be obtained. The hybrid drive line concept is significantly different from conventional vehicle drive lines on two specific points. First, by means of accelerating or decelerating the flywheel, an output torque can be generated. This is realized by continuously varying the ratio of the CVT. Second, the lowest resonance frequency of the hybrid drive line is significantly lower than the corresponding resonance frequency in conventional drive lines.

A hierarchical steering and control scheme has been formulated to control the complete drive line. This scheme gives the flow paths by which the demands of the driver are translated into torques and speeds. By means of this scheme the design specifications for both the drive line controller and the CVT controller have been derived, where the drive line controller sets the desired rate of CVT ratio change.

The CVT controller contains two independent parallel control loops. The first loop has to realize the desired rate of ratio change by means of an axial displacement of the hydraulically actuated pulley sheave of the driving pulley. The second loop has to realize the required clamping force on the driven pulley to prevent belt slip. The closed-loop response of the CVT is fast compared to the drive line controller and, hence, the CVT can be considered as an independent component in the drive line.

It is sufficient to model the drive line as a nonlinear two-masses-spring system with dampers. The nonlinearity originates from the varying transmission ratio of the CVT. With this model a drive line controller has been designed. A feedback linearization is applied to compensate for the nonlinear characteristics of the drive line. A linear control law, combined with a reference model, is sufficient to obtain the required torque response. The designed controllers have been tuned by means of numerical simulations and experimentally verified on a test-rig. The approach used in this thesis yields an adequate torque response of the hybrid drive line. The controller operates satisfactory and good vehicle driveability and high levels of passenger comfort can be achieved.

Samenvatting

Op de Technische Universiteit Eindhoven wordt een concept voor een hybride aandrijving, met sneldraaiend vliegwiel, een verbrandingsmotor en een Continu Variabele Transmissie (CVT), ontwikkeld dat moet leiden tot brandstofbesparing en vermindering van de uitlaatgasemissies van personenvoertuigen. Voor de realisatie van dit concept is een regeling die rekening houdt met het dynamisch gedrag van deze aandrijving van essentieel belang. Het te regelen uitgaande koppel is afhankelijk van de bestuurderswens en de last. Hiermee dient een comfortabel en soepel rijgedrag, de zogenaamde driveability, van het voertuig te worden verkregen. Het concept van de hybride aandrijving verschilt op twee punten wezenlijk van dat van een conventionele voertuigaandrijving. Ten eerste kan door het vertragen of het versnellen van het vliegwiel een aandrijvend c.q. remmend koppel worden gegenereerd. Dit wordt gerealiseerd door middel van het continu variëren van de overbrengingsverhouding van de CVT. Ten tweede is de laagste resonantie frequentie van de aandrijflijn significant lager dan de overeenkomstige resonantie frequentie van een conventionele voertuigaandrijving.

Om de gehele voertuigaandrijving te kunnen besturen is in het verleden een hiërarchisch stuur- en regelschema opgezet. Dit schema beschrijft hoe de wensen van de bestuurder vertaald kunnen worden in fysisch realiseerbare grootheden als koppels en snelheden. Door middel van dit schema zijn de ontwerpeisen voor de regeling van zowel de aandrijflijn als de CVT afgeleid, waarbij de regeling van de aandrijflijn de gewenste opregelsnelheid van de CVT bepaalt.

De CVT regeling is opgebouwd uit twee onafhankelijke parallelle regellussen. De eerste regellus realiseert de gewenste opregelsnelheid van de CVT met behulp van een axiale verplaatsing van een hydraulisch beweegbare en geactiveerde poeliehelft van de aandrijvende poelie. De tweede regellus verzorgt de benodigde aandrukkracht op de aangedreven poelie zodat bandslip wordt voorkomen. De gesloten lus regeling van de CVT is snel in vergelijking tot de regeling van de aandrijflijn en daarom kan de CVT als een onafhankelijke component worden beschouwd in de aandrijflijn.

Het is voldoende om de aandrijflijn te modelleren als een niet-lineair twee-massa-veersysteem met dempers. De niet-lineariteit wordt veroorzaakt door de variërende overbrengings-verhouding van de CVT. Met behulp van dit niet-lineaire model is een regeling voor de aandrijflijn is ontworpen. De niet-lineaire eigenschappen van de aandrijflijn zijn met behulp van een terugkoppellinearisatie verdisconteerd. Een lineaire regelwet in combinatie met een referentiemodel volstaat voor het realiseren van de gewenste koppelresponsie. De ontworpen regelingen zijn met behulp van numerieke simulaties verfijnd en experimenteel geverifieerd op een proefstand. De gehanteerde aanpak levert een goede koppelresponsie van de hybride aandrijflijn. De regeling functioneert goed en hiermee kan een comfortabel en soepel rijgedrag van het voertuig worden verkregen.

Contents

Chapter 1

General introduction

In the last decade alternative vehicle propulsion systems have gained an increasing interest. In the late sixties interest in these systems was initiated because of high levels of exhaust pollution of the cars. The oil crises of the mid seventies shifted the motivation towards reduced fuel consumption. Subsequent price rises emphasised the dependence of vehicles on a single type of fuel and an additional aspect was the growing awareness of limited oil resources. The general opinion was that consumption of fossil fuels had to be reduced. Therefore, more efficient vehicle propulsion systems were necessary. In the eighties the interest shifted again because of the increased need to protect the environment. The traffic in most metropolitan areas was congested by increasing numbers of vehicles. The resulting exhaust emissions of the stop-start driving polluted these cities. At present both aspects, energy conservation and reduced exhaust emissions, are of interest (Myers, 1992) and are subject of extensive research. At the Eindhoven University of Technology research into vehicle drive line concepts in which both aspects are covered has been in progress since the early eighties.

1.1. Search for alternative drive lines

Present vehicles are powered by a relatively large internal combustion (i.c.) engine. This is dictated by the performance criteria for modern vehicles. However, because of low steady state and low average power demands of a vehicle, the engine operates mainly at partial load. In this operating region, the engine performs inefficiently. The torque-speed characteristics of an i.c. engine are fundamentally mismatched to the vehicle characteristics for minimum fuel consumption (Bullock, 1989; Whitelaw, 1971). Figure 1.1 shows the engine speed versus engine torque characteristics of a typical i.c. engine. The constant power curve represents the power required at

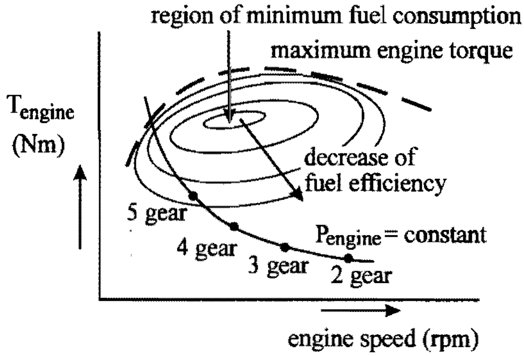

Figure 1.1. Schematic i.c. engine fuel efficiency map.

constant vehicle velocity. This curve shows that the engine operates at low efficiency when the vehicle is driving at constant speed. Moreover, the engine's operating region for minimal fuel consumption is not utilised at constant vehicle speeds. Because fuel consumption is predominantly determined by this kind of engine operation, a consequence is a propulsion system with low overall efficiency. Another cause for increased fuel consumption is traffic congestion because of the high number of vehicles. This congestion results in a stop-start driving pattern. The kinetic energy of the vehicles is dissipated at each stop. The subsequent power required to accelerate these vehicles results in increased fuel consumption and in raised environmental pollution levels because of the increased exhaust emissions. Thus, a result of increased vehicle density in (sub)urban areas is an increased power demand per covered distance.

In order to match a power source to the energy demand of a vehicle, regenerative braking in combination with an energy storage device can be employed. During deceleration the vehicle's kinetic energy is recuperated and stored. This stored energy can be used to power the vehicle during the subsequent acceleration. In electrically driven vehicles the above mentioned features are easily incorporated. During regenerative braking the batteries are recharged. Unfortunately, the power and energy density of nowadays batteries are insufficient to meet the power demands of a medium sized passenger vehicle with a reasonable battery weight. Therefore, medium sized electrical passenger cars with a reasonable quantity of traction batteries have only limited performance and range.

Thus, alternative vehicle propulsion systems are being investigated to realize more efficient, high capacity drive lines. One of the promising options for a more efficient drive line is the so-called hybrid drive line, which combines two or more sources in a single drive line. Many of these propulsion systems have a prime mover, i.e. a main power source, which has been matched to the average power demand of the vehicle. An additional short term energy storage device is used to achieve good performance and can often be used as a regenerative source. Numerous combinations are conceivable. For instance:

Figure 1.2. The M.A.N. Hydrobus (Martini, 1984).

- The M.A.N Hydrobus (Martini, 1984) where a pneumatic short term storage device has been used and an i.c. engine as a prime mover, Figure 1.2.
- The XA-100 (Reuyl, 1992), a retrofitted Chevrolet Corsica, is a battery electric/heat engine hybrid drive line. The traction battery can be used for short term regenerative energy storage and as energy source to deliver the energy for propulsion. The heat engine can in this case be seen as a range extender of the electric vehicle.
- The ika-Hybrid II, an i.c. engine-battery electric hybrid vehicle which can drive on the i.c. engine, the electric motor or on both simultaneously (Harbolla and

Buschhaus, 1991). This vehicle can drive in the inner city on the electrical motor for short periods of time. It normally uses the traction battery for regenerative energy storage and as source for the electrical motor to boost the performance of i.c. engine (Figure 1.3).

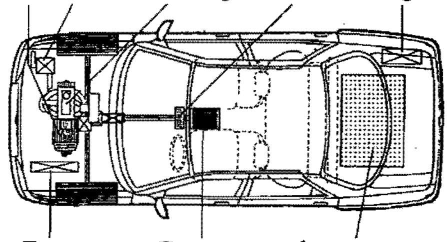

Figure 1.3. The ika-Hybrid II (Harbolla and Buschhaus, 1991).

- A flywheel energy storage system for trolley buses, described by Mitcham (1984), is a flywheel/ battery electric hybrid. The flywheel has been used only as a short term energy storage device which can handle high power densities and, therefore, fully exploits regenerative braking. The prime mover in this case is pure electric.
- A flywheel/i.c. engine hybrid which uses the flywheel as a short term energy storage device and the i.c. engine as prime mover (Schilke et al., 1984; van der Graaf, 1987).

With the current exhaust gas emission regulations of the Air Resources Board in California, USA, interest and research in electric and electric-hybrid vehicles is boosted (McGuinness, 1992). The electric hybrid has been considered primarily as a range extender of the pure electric vehicle, providing purely electric traction in urban areas and still has the capability to cover long distances. In the Netherlands, the Dutch government has adopted the E.G. guidelines for emission levels for vehicles. The government supports the 'best technical means' and encourages these to be used. The government also promotes these 'best technical means' to become the new standards in emission legislation (Nationaal Milieubeleidsplan, 1990; Nationaal Milieubeleidsplan-plus, 1992).

As a result of the continuous research efforts in industry to enhance vehicles having conventional drive lines, i.e. vehicles with an i.c. engine, a clutch or torque converter, and a transmission, every new model is a further improvement of the previous model. Further developments in the fuel efficiency of the i.c. engine can be expected (Oetting, 1992). A reduction of vehicle mass by using new and light weight materials (Hoogovens, 1992) reduces fuel consumption. In general, 10% mass reduction yields approximately 10% fuel savings for a medium sized passenger car (Schaik, 1992). Further reductions of fuel consumption can be expected by using engine transmission management systems. The engine and transmission controls are integrated. The transmission is used to select an engine operating point for minimum fuel consumption (Höhn, 1989; Narumi et al., 1990). Therefore, reduced fuel consumption and a reduced level of exhaust gases can be expected in the future. Improvements in vehicles with a conventional drive line will usually hold for an i.c. engine-hybrid vehicle as well. As the efficiency of the corresponding components in these latter drive lines will improve to the same amount. Therefore, efficiency improvements of a hybrid drive line, compared to a conventional drive line, will in general be preserved.

A clear disadvantage of hybrid drive lines is the complexity and their increased manufacturing costs. In order to compete successfully with conventional vehicles, hybrid vehicles must have apparent advantages. They must not only yield fuel savings and reduce emissions, but also they must be attractive to consumers (Masding, 1988). Therefore, these vehicles must have good driveability, performance and range.

1.2. Various designs of hybrid vehicle drive lines

Many concepts of hybrid propulsion systems have already been proposed, Whitelaw (1971) and Sampson and Killian (1972) published in the early seventies. Extensive simulation studies demonstrated the reduced fuel consumption potentials of these systems. However, only a limited number of the design studies have been carried out or prototypes have been build, for instance by Gelb et al. (1971), Trummel et al. (1984), Bullock (1985), and Reuyl (1992).

A parallel hybrid-electric power train was designed and tested by Gelb et al. (1971). This drive line consisted of an i.c. engine driving the wheels through a planetary gear train. An electrical engine/generator and traction battery pack was fitted parallel to the i.c. engine in the drive line. The propulsion system was a dual mode system, at low vehicle velocities the vehicle was well suited for a stop-start driving pattern. At higher vehicle velocities the system was conceived for highway cruising. One of Gelb's conclusions was that a parallel configuration yields a more efficient drive line. In the parallel configuration mechanical energy from the i.c. engine is applied towards the wheels, whereas in a series configuration all mechanical energy is converted into electrical energy and back into mechanical energy for vehicle propulsion. Gelb also observed fuel savings and exhaust emission reduction because of the near steady state operation of the i.c. engine with high thermal efficiency. Furthermore, improvements of the efficiency of the gear train should increase the drive line efficiency.

Bullock (1985 and 1989) showed that vehicles which incorporate regenerative braking are more efficient. Electrical vehicles can easily incorporate this feature. However, because of the additional mass of the batteries, the range of these vehicles is limited. Therefore, a segmentation should be made according to the operating range of vehicles. For short range, low and medium performance vehicle applications, the electric vehicle is one of the best options. Nevertheless, for long range and high performance applications, hybrid vehicles offer the best prospects as a short term solution (Bullock, 1989; Harbolla and Buschhaus, 1991). Bullock (1985) described the advantages of dedicated designs of hybrid vehicle drive lines. The drive lines were designed to meet the requirements for specific vehicle application. A potential saving of 30 to 50% was expected and these figures have been confirmed experimentally with prototypes.

A research project aiming at the design of an i.c. engine-flywheel hybrid drive system has been performed by Schilke et al. (1984). They concluded that expected efficiency improvements of a dual mode hybrid system are small compared to the much simpler single mode hybrid. The dual mode hybrid was capable of driving in a stop-start mode at a low vehicle speed and had a high speed mode for highway cruising. In addition, it was felt that the expected fuel improvements of the two mode hybrid did not justify the construction of a prototype for experimental validation. The fuel economy of the single mode series hybrid system was compared to a 1984 production model car. An overall improvement of 13% in fuel consumption was predicted. The relatively small improvement in fuel economy was mainly due to relatively high losses in the drive line.

1.3. The EUT hybrid

In order to design a high efficiency drive line for passenger cars, a hybrid vehicle drive line has been proposed (van der Graaf, 1987). It has been designed specifically for mixed city traffic and highway driving, as can be observed in the Netherlands. This system features regenerative braking, a short term storage device and optimum utilisation of an i.c. engine. Van der Graaf showed that by a careful selection of components, a high efficiency drive line can be designed. The drive line uses a flywheel as a short term energy storage device. A mechanical continuously variable transmission (CVT) is employed to transport the energy from flywheel to the wheels and vice versa during regenerative braking. A small i.c. engine serves as prime mover. The hybrid system has been designed to optimize the engine's operation. This results in a dual mode hybrid system, a 'low speed' mode in which the engine is used in a on/off mode and a 'high speed' mode in which the engine continuously operates near its maximum efficiency. The dual mode hybrid system of Schilke et al. (1984) can functionally be compared to the current hybrid system under study. However, due to a significantly smaller number of components, a much better efficiency is expected. An additional advantage of this concept, as compared to other hybrid systems, is that only mechanical energy is used. No conversions are made from mechanical to electric or hydraulic energy, and hence, conversion losses are avoided. Therefore, a high drive line efficiency can be expected. A disadvantage is that, because of its complexity and because of the use of a CVT, control of this drive line is rather complicated.

1.4. Context of this thesis

This thesis describes the design of a controller for the EUT i.c. engine-flywheel hybrid drive line with a CVT. It shows how a hybrid drive line consisting of an i.c. engine, a flywheel and a CVT can be controlled. A systematic design path is devised and the resulting dynamic controllers are validated and are shown adequate for this application. To our knowledge, a systematic control strategy that also includes control of the dynamic behaviour of the drive line has not been developed previously. Other researchers and developers of hybrid vehicles established the high efficiency potential of the flywheel-mechanical CVT combination, for instance Thoolen (1993). However, they did not choose for this specific combination because the CVT was not commercially available and its control is inherent more complex than the control of other types of transmission.

The contents of the remainder of this thesis is structured as follows. Chapter 2 describes the i.c. engine/flywheel hybrid drive line, which is under development. The realization of this drive line is explained and the control problem is stated. A formulation for a suitable hierarchical control strategy is given. The overall drive line steering is partitioned in an engine controller and a drive line controller. The CVT and the flywheel are key elements in the current hybrid drive line.

In Chapter 3 mathematical models for the drive line are given. These complex models are reduced in size. A simplified simulation model and a controller design model are obtained.

Chapter 4 describes the test-rig that is used for controller evaluation. This test-rig has been designed for the CVT controller evaluation. Adapting this test-rig to the hybrid drive line, by means of incorporating the drive line resonance frequency, enables the drive line controller to be experimentally verified.

In Chapter 5 the CVT is discussed. The CVT is a key element in the drive line and its implications for this drive line are discussed. In order to obtain high levels of passenger's comfort, good performance and driveability, accurate control of the CVT is imperative. The CVT is considered as an isolated component in the drive line and its required response is stated. The CVT is analyzed and models are derived for controller design. The controller is experimentally verified.

In Chapter 6 the design of the dynamic drive line controllers is given. The nonlinearities in the drive line are compensated for by the controller. The limited torque capacity of the CVT and risk of structural damage to this transmission element are taken into account. Numerical simulations are used to optimize and to evaluate the proposed drive line controller.

Chapter 7 shows the experimental validation of the drive line controller. The drive line closed-loop torque response is analyzed. Passengers comfort and driveability are considered. For this purpose the response at steady state driving and during load reversal is analyzed.

Finally, in Chapter 8 the research presented in this thesis is summarized and the conclusions of this thesis are given. Suggestions for future research are formulated. These suggestions concern not only this particular flywheel-hybrid transmission but also the application of CVT's in more conventional drive lines.

Chapter 2

The flywheel-hybrid vehicle

2.1. Introduction

In the preceding chapter, the Eindhoven University of Technology (EUT) hybrid drive line was introduced. Numerical simulations (Devens, 1984) showed that the hybrid drive line configuration has a high fuel saving potential, low emissions characteristics and a good performance and driveability. In the present chapter the hybrid drive line under study is described. First, the main goals and objectives of the hybrid concept are given and the drive line is explained. A schematic layout of the drive line is given and the expected fuel savings and exhaust gas emissions are presented. Second, the realization of this concept is demonstrated. Finally the control issue that arises with this type of drive line is stated and the problem which is addressed in this thesis is defined.

2.2. Development of the flywheel-hybrid vehicle

The Laboratory for Automotive Engineering of the Eindhoven University of Technology is developing a system concept and proto-type for a hybrid drive line system for passenger cars. The main objectives are reduced fuel consumption and low exhaust emissions. This hybrid drive line concept is described in detail by van der Graaf (1987). The prototype in his paper was designed for a rear wheel driven vehicle. Since a vehicle dissipates most of its kinetic energy at the front wheel brakes, this concept could recover only a limited amount of kinetic energy. In order to take full advantage of energy recuperation through regenerative braking, the current prototype hybrid drive line has been realized for a front wheel driven vehicle (Figure 2.1). Although the configuration was modified, the hybrid concept is identical. The specifications of the components in the drive line, i.e. the i.c. engine, high speed flywheel and a CVT are given in Table 2.1. The relatively high powered engine has been chosen

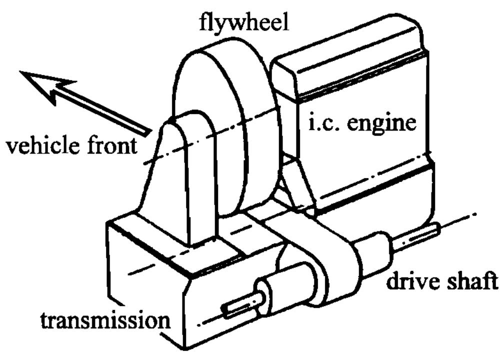

Figure 2.1. The EUT hybrid engine and transmission unit for a front wheel driven vehicle (van der Riet, 1988).

because it enables the vehicle to drive at rather high speeds over long distances and because this power is sufficient to drive the vehicle in a non-hybrid mode with acceptable performance.

Table 2.1. Hybrid vehicle drive line components.

vehicle:	medium size passenger car of 1100 kg.
prime mover:	1.4 litre single point injection i.c. engine, maximum power 47 kW at 5500 rpm.
transmission:	CVT with metal V-belt of Transmatic type and gear-shifting part with wet plate-clutches.
starting device:	multiplate wet slip coupling.
storage device:	high speed glass fibre composite flywheel with energy contents of 180 Wh and maximum running speed 19000 rpm.

The flywheel has been chosen as a short term storage device because of its high power density and durability. The flywheel has been made of a glass fibre composite. It is a fail safe design, providing sufficient protection of the vehicles' passengers. The flywheel is surrounded by a steel containment ring, kept in an aluminium caving. In case of a catastrophic event, the flywheel is maintained inside this aluminium housing. It has been designed to enable low cost mass production. The transmatic type CVT has been chosen because of its high efficiency. It has been used in series production cars for several years now without complications. It is a reliable transmission and can be used in vehicles without reservation (Liebrand, 1992). A disadvantage of the CVT, the complexity of its control in a drive line, is addressed in this thesis.

The drive line has several operating modes. Depending on the driver's choice, it can operate as a conventional vehicle or in a hybrid configuration. In the basic or 'engine' mode, shown in Figure 2.2b, the drive line functions as a drive line in a conventional vehicle equipped with a CVT. This type of propulsion system has been reported by several authors (Falzoni, 1984; Main, 1986; Wade, 1984), and is currently still subject of research (Höhn, 1991; Narumi et al., 1990). The accelerator pedal position is interpreted as an output power signal representing the desired wheel power by the driver (Douven, 1984; Hermans, 1985). This desired output power is interpreted as a desired engine power which is obtained by selection of engine speed and torque combinations. The engine's optimum operating line can be fully utilized with the aid of the CVT, which allows continuous changes of the transmission ratio.

Figure 2.2c shows the mode for flywheel loading. The flywheel is accelerated up to its operating speed by the engine. The engine is operated at maximum thermal efficiency and it takes about 30 seconds to reach the maximum flywheel speed of 19000 rpm. In the context of this thesis, the primary CVT shaft is defined as the shaft (Shaft 3) on engine side and the secondary CVT shaft (Shaft 4) as the outgoing shaft towards the vehicle's wheels.

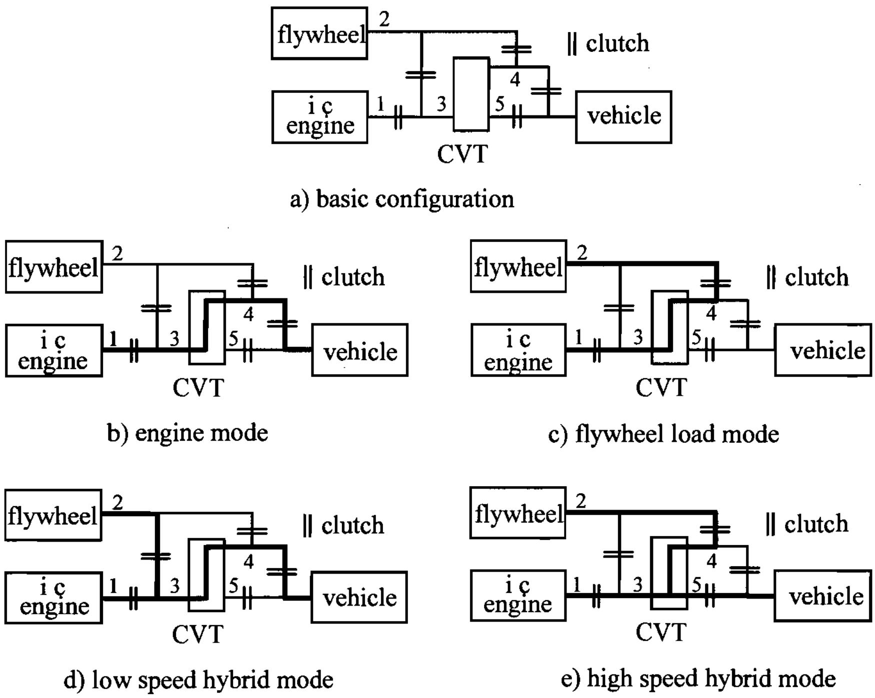

Figure 2.2. Power flow paths for four different operating modes in the hybrid vehicle drive line.

In the hybrid mode, the flywheel is coupled to the CVT. This hybrid mode is split into a 'low speed' and a 'high speed' mode, because of the limited transmission ratio of the CVT. In the 'low speed' mode, as shown in Figure 2.2d, the engine (Shaft 1) is coupled in series with the flywheel (Shaft 2) to the CVT input shaft (Shaft 3). For the lower speed range, for speeds ranging from 0 to 55 km/h, the flywheel is used as the main power source for the vehicle. During braking kinetic energy of the vehicle is being recovered in the flywheel. The engine is needed only for short periods and is shut down, and disconnected, when inoperative. A wet-plate clutch is used as starting device (Hermans, 1984), allowing the vehicle to accelerate from standstill.

In the 'high speed' mode, for the speeds lying between 55 and 120 km/h the engine (Shaft 1) is coupled directly to the output shaft (Shaft 5), see Figure 2.2e. In this case the engine is considered as the main power source. The flywheel (Shaft 2) and the CVT (Shaft 4) are connected to the output shaft (Shaft 5). These components are coupled in parallel with the engine to the output shaft, a parallel hybrid configuration. To save fuel and reduce emissions, the engine is shut down when the energy contents of the flywheel is sufficient to maintain a desired output torque. The flywheel is used to recover the kinetic energy of the vehicle during braking. Above 120 km/h, the flywheel is disconnected from the output shaft.

The basic philosophy behind our concept is conservation of energy in the drive line. The kinetic energy of the vehicle is recovered during braking and re-used to accelerate the vehicle. Kinetic energy is continuously being exchanged between the flywheel and the vehicle (van der Graaf, 1987). The transfer of kinetic energy between vehicle and flywheel is mathematically expressed by:

$$\frac{1}{2} J_{fkw} \omega_{flw}^{2} + \frac{1}{2} m_{veh} v_{veh}^{2} = \text{constant}, \tag{2.1}$$

where the vehicle velocity is represented by v_{veh} and vehicle mass by m_{veh}, the flywheel rotational speed is represented by ω_{flw} and flywheel inertia is denoted by J_{flw}. This relation, which does not include drive line losses, can be considered as the essence of the power steering strategy for this drive line. Dissipated energy, such as rolling resistance, air drag, and transmission losses is replenished by the engine. The engine basically delivers the average power necessary for vehicle propulsion. Because this engine, if in operation, operates along its optimum operating line (OOL), the expected overall efficiency of the drive line is high.

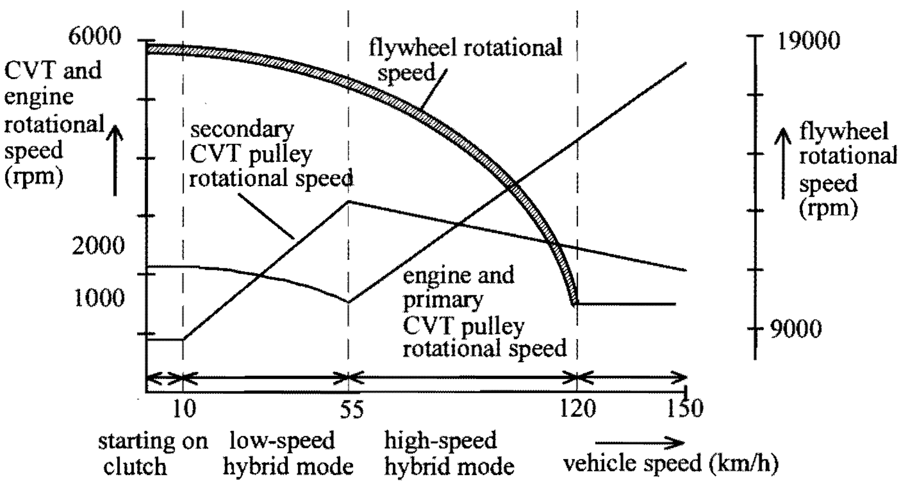

Figure 2.3. Vehicle speed and engine/flywheel rpm diagram.

The relation between vehicle velocity and flywheel rotational speed, as shown in Equation 2.1, is illustrated in Figure 2.3. This figure, which corresponds to the hybrid modes of Figures 2.2d and 2.2e, also shows the rotational speeds of the corresponding primary and secondary CVT shaft. The flywheel rotational speed is shown as a zone bounded by a minimum and maximum value in Figure 2.3. This range enables the practical realization of the transmission. The speed ratio between flywheel speed and output shaft speed can be covered by the CVT ratio range. Due to the drive line losses, the engine has to be occasionally used. The engine is started when the lower bound of the flywheel speed is reached and after a short period of time the engine is stopped when the upper limit is reached.

2.3. Expected fuel savings and exhaust emission reductions

Devens (1984) assessed the feasibility of the proposed hybrid vehicle system by means of numerical simulations. The results of this study showed a considerable dependence on system parameters such as flywheel losses and CVT efficiency (Devens, 1984 and van der Graaf, 1987). The fuel consumption of the hybrid vehicle was compared to the fuel consumption of the same vehicle propelled by the same i.c. engine only and in conjunction with a manual 5 speed gearbox. It was assumed that the vehicle was equipped with an engine start/stop facility to prevent the engine from running idle. The simulations showed that a reduction of 15 - 25 % can be achieved by the hybrid concept, for city traffic only.

A few comments on these predicted fuel savings have to be made. The calculated savings of 15 - 25 % are fully on account of the hybrid concept. Fuel savings due to the automatic fuel cut off with an engine start/stop facility are not included in these numbers. Hofbauer et al. (1983) showed that the Volkswagen ECO-Golf with its engine start/stop facility yields approximately 10 - 15% fuel savings. The fuel savings were achieved without any loss in vehicle performance. Greve and Liesner (1993) showed that even a 21% fuel saving was achieved by the Golf Ecomatic. An additional advantage of this (diesel engine) concept was a substantial reduction in CO and $HC+NO_x$ emissions because of the constant temperature of the catalytic converter. For the hybrid vehicle, exhaust gas emissions are expected to decrease due to a lower fuel consumption. Furthermore, a reduction in CO and C_xH_y is anticipated because of the avoidance of low-load running conditions. For NO_x emission no estimate could be made, this depends on the specific operating conditions of the engine. Experiments should clarify this issue (van der Graaf, 1987).

2.4. Hierarchical steering and control

To control the complete drive line, a hierarchical strategy has been developed. In this strategy several levels of control can be defined. This strategy controls not only the power flow through the drive line, but also supervises the drive line status and provides an interface towards the driver of the vehicle.

At the top of this hierarchical control is the driver, who may look at a control and display panel very similar to the ones of current production vehicles. The only modification is the additional 'hybrid mode' option at the transmission selector lever. The driver commands the vehicle by manipulating the accelerator pedal, braking pedal and drive selector. He decides in what mode the vehicle has to operate; as a hybrid vehicle or as a conventional vehicle, i.e. on the engine only. The driver's commands are translated and used to select an operating mode of the vehicle while the accelerator (or brake) position is translated into a desired transmission output torque (Douven, 1984; Hermans, 1985).

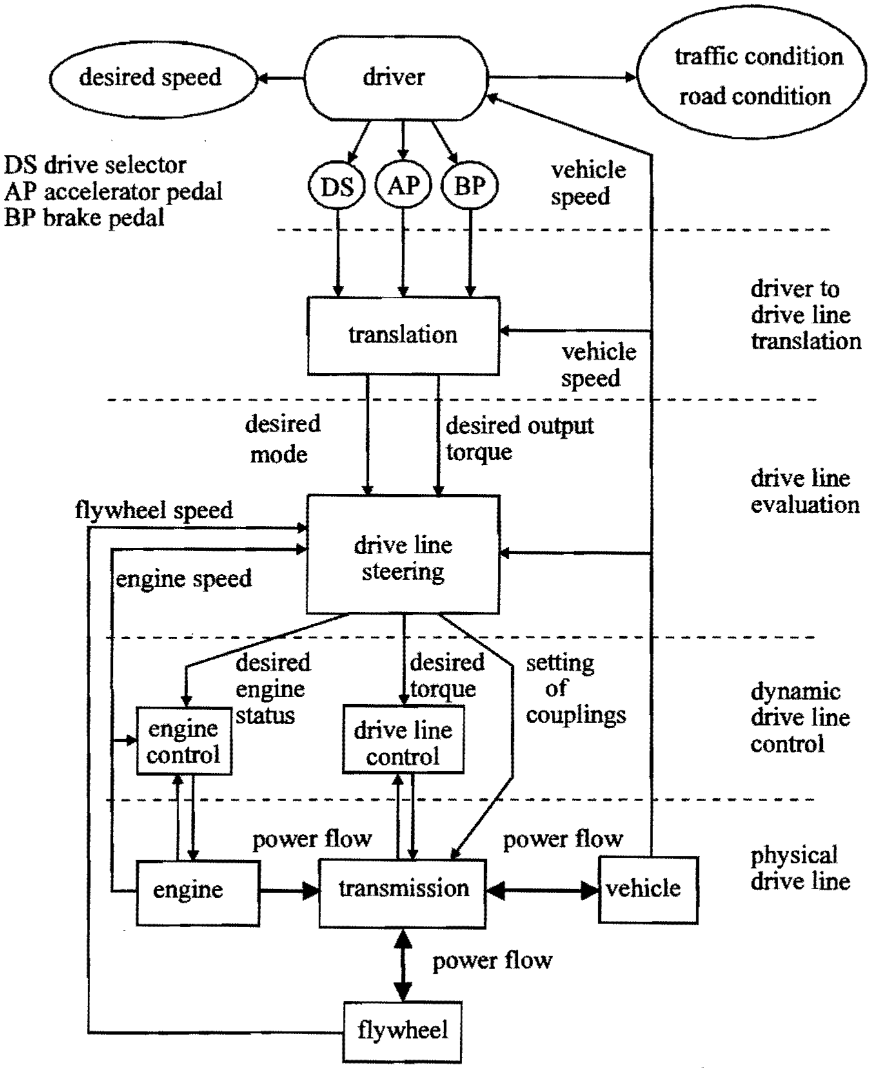

Figure 2.4. Hierarchical steering and control strategy for hybrid vehicle.

The following stage in the hierarchical steering scheme is the examination of the drive line configuration. If a new drive line configuration is required, or if one of the drive line components reaches a boundary in its operating range, it is decided what the next configuration of the hybrid drive line should be (Hermans, 1985). Shifts from the present drive line configuration to a new configuration are achieved by opening and closing appropriate clutches (van Nijnatten, 1986).

The permissible shifts are schematically shown in Figure 2.5 as arrows between the modes. The modes shown in Figure 2.5 are a more detailed extension of the configurations shown in Figure 2.2. An example is the low speed hybrid mode in Figure 2.2d, it is divided into two modes in Figure 2.5 according to the components that have to be controlled. The corresponding rotational speeds for these modes are shown in the speed-rpm diagram of Figure 2.3. By limiting the shift possibilities, only a very small number of allowable shifts per operating mode have to be monitored. For instance, when the vehicle is driving in 'Flywheel mode 3', only the transitions to 'Flywheel mode 2' and 'Engine/Flywheel mode 3' are allowed. Consequently only vehicle parameters corresponding to these allowable shift conditions have to be monitored. The 'safety' mode in Figure 2.5 is an additional mode in which all clutches are released and the engine is shut down. This mode is entered only if an exceptional or an unexpected event occurs within the drive line.

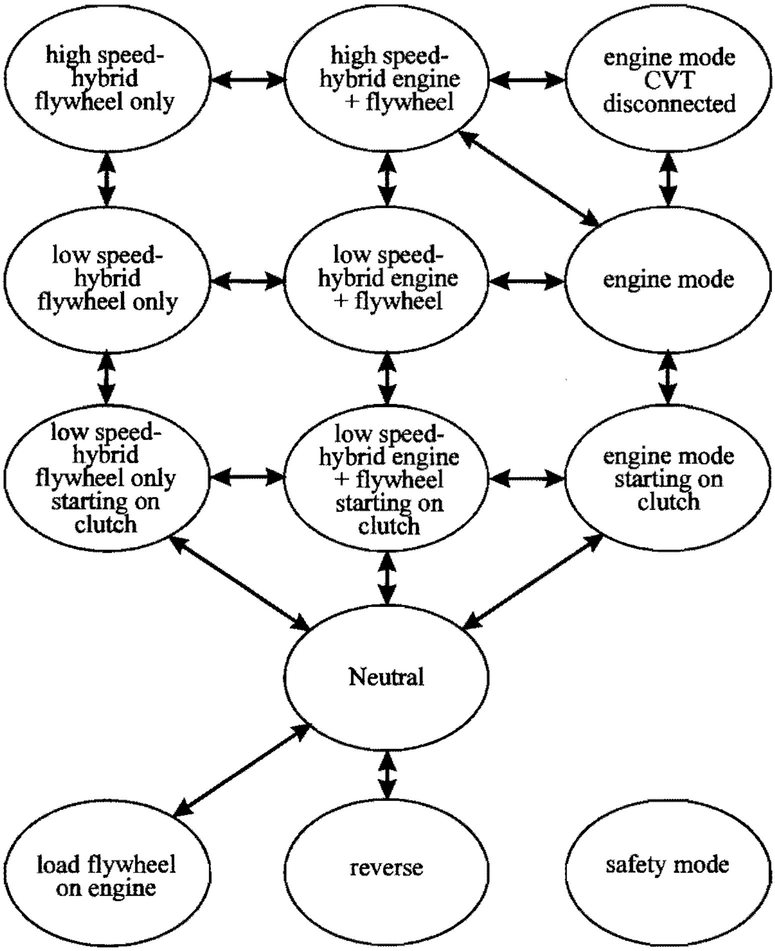

Figure 2.5. Mode shift diagram of the hybrid vehicle.

The drive modes of the vehicle, shown as oval-shaped boxes in Figure 2.5, are to be applied to the lowest hierarchical level (Figure 2.4). In these modes, the drive line dynamics are controlled. The drive line controller has to realize the desired output torque by controlling the engine torque and by changing the transmission ratio continuously. The engine controller governs the throttle opening, fuel injection and spark advance. Transients in the output torque due to the on/off nature of the engine operating mode should be compensated for by the drive line controller.

The dynamic properties of the hybrid drive line are characterized by its various components and their interactions. If the engine is running, it operates along its OOL, which is close to wide open throttle (WOT). Because the engine rotational speed is determined by the slowly varying flywheel rotational speed, the engine is considered as a steady torque source. In the (engine-)flywheel hybrid mode, the transmission output torque is generated by decelerating the flywheel inertia. This deceleration is accomplished by a varying rate of change of the CVT ratio. If the rate of change is used as a parameter to characterize the CVT dynamics in the drive line, the physical processes in the CVT, the shifting of the pulley sheaves and metal V-belt, are not required for the drive line description. A relatively simple mathematical description can be used for describing the output torque response of the drive line. Furthermore, if the CVT can realize the desired rate of ratio change within a very short time, the drive line and the CVT can be considered as independent. This enables the CVT and the drive line to be controlled independently.

A clear separation should be made between 'control of the power flow' in a hybrid drive line and the 'dynamic control' of the hybrid drive line. In automotive literature, 'steering of power flow' is often referred to by using the term 'control strategy of hybrid vehicles'. The paper of Beachly (1984) is such an example. An explicit distinction between the notation of steering and control is not used in this literature. In general, control involves feedback, i.e. a comparison between desired output and realized output combined by a corrective action. Steering on the other hand does not include feedback. For the power flow in hybrid vehicles, basically event driven steering is used. If certain boundaries are exceeded, the power flow is redirected from source to load by using a different power path in the vehicle, as demonstrated by the operating modes in Figure 2.2. A simple example is regenerative braking, the power flow through the vehicle is reversed when a driver touches the brake pedal.

In order to avoid confusion between steering and control, the term 'steering strategy' will be used for the power flow in the hybrid drive line. The term 'control strategy' will be used for the dynamic control of the drive line.

2.5. Problem definition

In order to obtain reduced fuel consumption and low exhaust emissions while maintaining high comfort levels, the dynamic behaviour of the drive line has to be controlled accurately. The dynamic properties of the EUT hybrid drive line are significantly different from those found in conventional vehicle drive lines:

- the output torque is generated by accelerating or decelerating the flywheel inertia (inertia torque),
- transients occur in the output torque due to the on/off nature of the i.c. engine operating mode,

- the high speed flywheel causes a low resonance frequency in the drive line, which varies with the transmission ratio and is of the same order of magnitude as the closed loop bandwidth of the drive line.

In order to control the dynamic behaviour of the drive line a strategy must be developed which incorporates the engine, CVT and flywheel. The output torque of the drive line is considered the main output variable of the system and must be controlled. The CVT is the main governing device in the drive line and only limited adjustments in the engine output torque are allowed, because the engine operates along its OOL.

A set of performance specifications has been formulated for the hybrid vehicle. These specifications include the output torque response, output torque disturbance rejection and consideration for the limitations of components. For the drive line a desired response can be expressed:

- a steady state accuracy for the desired output torque should be within 5-10% (Douven, 1984).
- to obtain high comfort levels, vehicle acceleration ripples should be below 0.08 m/s^2 (Ketelaars, 1991),
- the output torque should be available within 0.2 - 0.3 seconds (Langerijs, 1985),
- output torque fluctuations due to disturbances, for instance resonances caused by displacements of the power unit in the vehicle body or engine start up transients, should not be noticed by the passengers,
- the limited torque capacity of the CVT should be taken into account (Van Doorne's Transmissie, 1988).

Chapter 3

Modelling of the flywheel-hybrid drive line

3.1. Introduction

The design of a drive line controller requires two mathematical models of the rotational dynamics in the drive line. The first model is a controller design model, which contains the essential characteristics of the drive line. This model is used explicitly in the design of the drive line controller. The second model is required to evaluate the controller performance. This simulation model is more detailed and contains additional information about the drive line rotational dynamics which has not been included in the controller design model, for instance wheel spin on a wet surface.

The basic model used in this thesis, to derive the two previous mentioned models, is obtained by modelling the drive line components and the interactions between these components. This results in a model which is too complex for simulations and, moreover, it is too complicated to be used in the design of the drive line controller. Therefore, the size of this model is reduced and a model that is suitable for simulations is obtained. Further reduction of this simulation model yields the controller design model.

3.2. Objectives and requirements

The hierarchical control structure of the hybrid drive line, as explained in Chapter 2, enables the design of dynamic controllers for each of the operating modes of the vehicle. In these operating modes the structure of the drive line does not change. Shifts between operating modes are carried out by opening and closing the appropriate clutches at near synchronous speed. To realize these shifts, steering of the hydraulic pressure of the clutches is used (van Nijnatten, 1986).

Because high passenger comfort levels must be achieved, the controller design model for the analysis of the dynamic response should predict the occurrence of vehicle acceleration shocks which are caused by torque fluctuations in the drive line. In order to minimize these shocks, the drive line output torque has to be controlled to eliminate these fluctuations. The frequency range to be covered by the controller design model can be specified by considering several aspects. The model should be accurate at steady state and the upper frequency bound of the model must be beyond the range of the closed-loop bandwidth of the controller. Additionally, the controller design model must be suitable for use in an on-line control algorithm. In Chapter 2, Section 2.5, and Chapter 6, Section 6.2.2, the required output torque response is given. Because the necessary closed-loop bandwidth of the drive line controller is 2.5 Hz, an upper frequency boundary of 10 Hz is considered sufficiently high as reduction boundary and will be used in this Chapter.

Circumstances which have not been included in the controller design but are important for controller evaluation should be incorporated in the simulation model. For this simulation model accuracy is essential. Unmodelled phenomena, for instance wheel spin on a slippery road surface or high frequencies which are excited by actions of the control system, are to be considered in this simulation model. The reason is that these phenomena can degrade controller performance or even destabilize the closed-loop. Computation time and complexity are less important. Laschet (1988) states that, in general, the highest resonance frequency of a drive line model must be above the maximum excitation frequency.

3.3. A hybrid drive line model

A schematic diagram of the hybrid drive line is given in Figure 3.1. It shows the main components, being the i.c. engine, the flywheel and the vehicle, as well as the corresponding connecting elements such as clutches, shafts, gear trains and the CVT.

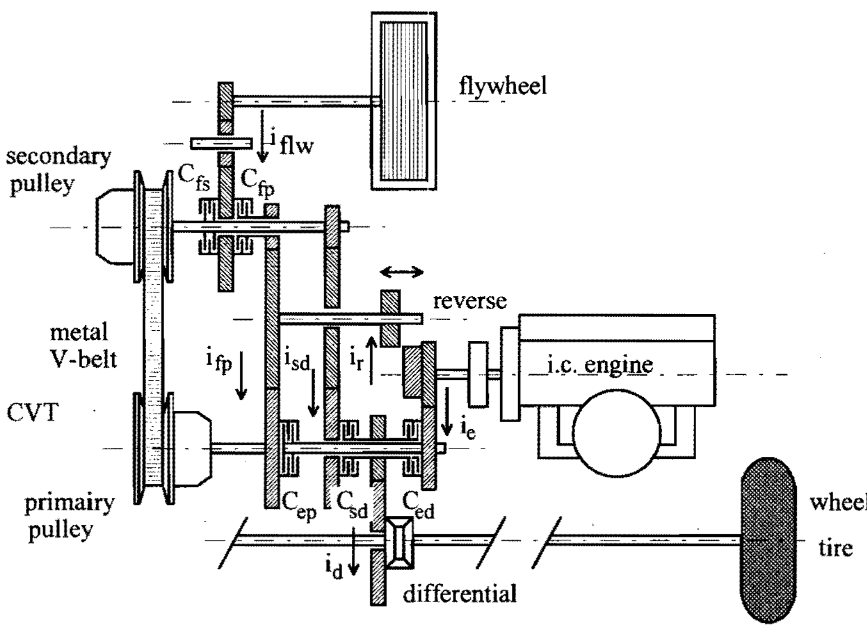

Figure 3.1. Schematic diagram of the flywheel-hybrid drive line.

The gear ratios are denoted by the ratio i and are identified by their indices; i_{flw} (flywheel), i_{fp} (flywheel to primary pulley), i_{sd} (secondary pulley to differential),

i_e (engine), i_d (differential) and i_r (reverse). These gear ratios are necessary to match the different operating speeds of the main components. With the clutches C_{fp} (flywheel to primary pulley), C_{fs} (flywheel to secondary pulley), C_{ep} (engine to primary pulley) and C_{ed} (engine to differential) the different components can be linked. Clutch C_{sd} (secondary pulley to differential) is used as starting device, enabling the vehicle to start from a standstill.

3.3.1. The nonlinear model

The physical hybrid drive line in each of the operating modes can be modelled as a series connection of rigid inertias, massless torsional springs and massless torsional dampers. Van der Ven (1988) analyzed the hybrid drive line and developed models for several operating modes.

A torsional model for the 'low speed' hybrid mode is shown in Figure 3.2. The flywheel and engine are coupled to the primary pulley by the clutches C_{fp} and C_{ep}, respectively. The secondary pulley is coupled to the output shaft by the clutch C_{sd}.

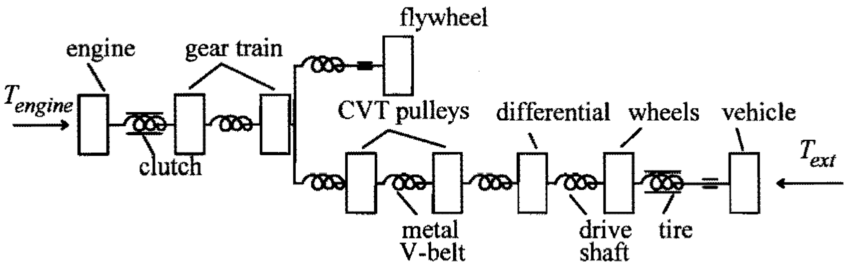

Figure 3.2. Model of the 'low speed' hybrid mode. Only discrete masses, torsional springs and relevant dampers are shown.

In this model the engine and its flywheel are modelled as a single inertia, coupled to the high speed flywheel through a gear train. The produced engine torque T_{engine} is considered to be a known torque acting upon this system. For this analysis a mean value engine torque model is used. This torque represents the average torque over several crankshaft rotations and excludes the periodic nature of the i.c. engine (Hendricks and Sörenson, 1990; van den Berg, 1993).

The CVT is modelled as two inertias connected by a torsional spring, representing the metal V-belt. In the model, the primary CVT shaft is chosen as the basis to which all rotational elements are transformed, thereby eliminating the gear ratios in the transmission (cf. Appendix A). The CVT ratio is defined as the ratio of the secondary pulley rotational speed $\omega_{secondary}$ over the primary pulley rotational speed $\omega_{primary}$. The mechanical efficiency η is taken into account in the torque ratio over the CVT. The CVT model includes only the properties of the CVT which are relevant for the dynamic behaviour in the drive line. The internal physical phenomena in the CVT are not considered.

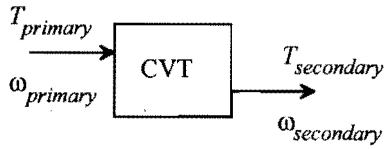

$$\begin{aligned} \omega_{secondary} &= i\,\omega_{primary} \\ T_{primary} &= \frac{i}{\eta}\,T_{secondary} \end{aligned} \tag{3.1}$$

Figure 3.3. CVT definition.

A CVT efficiency $\eta = 1$ is used in the torsional model of Figure 3.2, because it is not essential for the torsional analysis. Since, the CVT ratio is varying in time, all elements to the right of the primary CVT pulley inertia depend on the CVT ratio explicitly. The rate of ratio change is an input variable to the drive line. This ratio change introduces a torque in the drive line. A detailed analysis is given in Appendix A. With this input the drive line can be controlled. The dynamic behaviour of the CVT, including the hydraulic characteristics and its response to input signals, is not modelled here. It is discussed in Chapter 5.

The vehicle's mass is represented by a single inertia and the vehicle acceleration is transformed into a rotational acceleration. Significant damping phenomena are the engine's clutch dry friction damping, the rubber damping of the tires, the flywheel and vehicle air drag, and the vehicle rolling resistance. The external torque, for instance due to hill climbing, is represented in the torque T_{ext}.

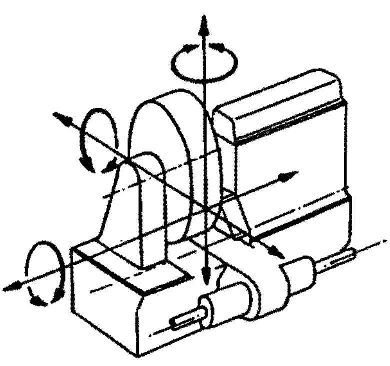

Figure 3.4. The EUT transmission unit, including the flywheel (Hendrikx, 1993).

The drive line model includes rotating elements only. The engine unit in its supports is not modelled because there is no kinematic link between the rotating bodies and the engine unit. The coupling between the torsional bodies and the engine unit is modelled by the engine torque (van der Riet, 1988; Hendrikx, 1993). Displacements and velocities of the engine unit (see Figure 3.4) are very small compared to the rotational speeds and, hence, they are negligible.

3.3.2. The linear model

Available reduction techniques are usually based on linear models. Therefore, linear models are derived for this drive line. These linear models are written in a form suitable for the reduction techniques. Van der Ven (1988) linearized the general model, shown in Figure 3.2, in a suitable operating point. The nonlinear torsional elements and damping elements have been replaced by appropriate linear elements and the CVT ratio has been assumed constant. The equations of motion for the linearized model can be derived, using Newton's second law:

$$\boldsymbol{J}\,\ddot{\varphi} + \boldsymbol{R}\,\dot{\varphi} + \boldsymbol{K}\,\varphi = T_{in}\,. \tag{3.2}$$

The components of the vector φ are the angular displacements of the inertias, reduced to the primary CVT axis. The symbols $\boldsymbol{J}$, $\boldsymbol{R}$ and $\boldsymbol{K}$ represent the mass matrix, the damping matrix and the stiffness matrix respectively. The vector T_{in} represents the external torques which act upon the system. The system's kinetic energy can be expressed as:

$$E_{kin} = \tfrac{1}{2}\dot{\varphi}^T \boldsymbol{J}\,\dot{\varphi}, \tag{3.3}$$

and the potential energy as:

$$E_{pot} = \tfrac{1}{2}\varphi^T \boldsymbol{K}\,\varphi. \tag{3.4}$$

The stiffness matrix $\boldsymbol{K}$ is singular because the model is not connected to the reference frame by a stiffness element. Therefore, a solution of the eigenvalue problem exists for which $\varphi \neq 0$ while $E_{pot} = 0$. This solution is called the rigid-body mode of the system. This mode does not give any information on the torsional behaviour of the drive line. Decoupling of the rigid-body mode from the other modes of a damped system can not always be achieved. However, because of the inherently low drive line damping, the damping can be considered as a second order effect and decoupling can be achieved (Meirovitch, 1967). Eliminating this rigid-body motion reduces the system's degrees of freedom by one. A transformation $\boldsymbol{T_C}$ can be obtained which relates the (n-1) new coordinates φ^* of the reduced system without the rigid-body mode to the n old coordinates φ (Meirovitch, 1967):

$$\varphi = \boldsymbol{T}_c \varphi^*. \tag{3.5}$$

The resulting system without rigid-body mode can be used in the analysis of the torsional behaviour.

In control literature models are represented in sets of first order ordinary differential equations. In order to comply with this form of notation, the set of second order ordinary differential equations of Equation 3.2 is transformed into a set of first order ordinary differential equations in the state x:

$$x = \begin{bmatrix} x_1 \\ x_2 \end{bmatrix} = \begin{bmatrix} \varphi \\ \dot{\varphi} \end{bmatrix}. \tag{3.6}$$

This results in the state space description:

$$\begin{aligned} \dot{x} &= \begin{bmatrix} 0 & 1 \\ \boldsymbol{J}^{-1}\boldsymbol{K} & \boldsymbol{J}^{-1}\boldsymbol{R} \end{bmatrix} x + \begin{bmatrix} 0 \\ \boldsymbol{J}^{-1} \end{bmatrix} T_{in}, \\ y &= \boldsymbol{C}x, \end{aligned} \tag{3.7}$$

where the output y represents the wheel torque. This model can also be rewritten as:

$$\begin{aligned} \dot{x} &= \boldsymbol{A}x + \boldsymbol{F}w + \boldsymbol{B}u, \\ y &= \boldsymbol{C}x, \end{aligned} \tag{3.8}$$

where the external torque T_{in} consists of two separate terms. The first is the control input u, which represents the CVT ratio change. This ratio change introduces a torque in the drive line, as shown in Appendix A. The second input is the disturbance w, which contains the engine torque T_{engine} and the external torque T_{ext}. In Equation 3.8 the matrix A represents the system matrix, B the input matrix for the control input u, F an identical input matrix for the disturbance w, and C the output matrix.

3.4. Model reduction

In order to optimize mechanical components for the drive line, van der Ven (1988) analyzed the resonance frequencies of the mechanical structure. The model of Figure 3.2 is rather detailed and has a frequency range of 0 - 1 kHz. A controller design model, however, requires a limited frequency range. For a vehicle drive line model the lower characteristic frequency is in the 0 - 5 Hz range (Catchpole et al., 1978; Muiderman, 1991; Ogasawara and Yonekawa, 1987). Reduction of the extensive model without loss of accuracy in the lower frequency range, is necessary.

The hybrid drive line model consists of two linear submodels connected by a time varying element, i.e. the varying CVT ratio. With well known reduction techniques, reduction of the linear submodels can be carried out immediately (van den Bosch, 1993). A combination of the reduced submodels with the nonlinear element, followed by a final reduction into a controller design model could prove to be advantageous. This option has not been pursued for the drive line model because the modal shapes of the drive line at high eigenfrequencies are strongly influenced by the CVT ratio. This indicates that only limited reduction of the submodels is allowed, which leaves a fairly extensive final model. Therefore, the complete drive line, with a predetermined constant CVT ratio, is reduced towards the controller design model.

The models of van der Ven (1988) have been verified and are taken as the starting point for model reduction. A model of the 'low speed' hybrid mode is reduced in the present chapter. Models of other modes are given in Appendix B. Two reduction techniques are used. The first one is based on modal analysis and related to engineering practice. It yields a qualitative model of lower order. The second is based on input-output response analysis and yields a reduced quantitative model.

The simulation model is obtained as an intermediate result during the reduction process. This model is of lower order than the original model but is still too complex for controller design and is therefore reduced further. In the next sections the reduction from the basic model into the controller design model is carried out.

3.4.1. Modal analysis

The analytic method as given by Laschet (1988) is based on an analysis of the system matrices and yields a reduced model. The method considers undamped drive lines, consisting of series connections of inertias and torsional springs. Application of this method seems justified because eigenfrequencies and resonance frequencies of the drive line almost coincide since damping in the drive line is very small. Eigenfrequencies and the corresponding eigenvectors are interpreted as resonance frequencies and modal shapes. Inertia and torsional spring combinations which are excited at high eigenfrequencies are eliminated and the remaining inertias and springs are modified in order to preserve the lower frequency characteristics.

The homogeneous linear differential equation for the undamped linear model follows from Equation 3.2:

$$\boldsymbol{J}\,\ddot{\varphi} + \boldsymbol{K}\,\varphi = 0. \tag{3.9}$$

The eigenfrequencies ω_m (m = 1,2,...,n-1) and the corresponding eigenvectors λ_m follow from the eigenvalue problem:

$$(\omega_m^2 \boldsymbol{J} - \boldsymbol{K})\lambda_m = 0. \tag{3.10}$$

It is assumed that the eigenvalues are normalized, such that the (in absolute value) maximum component of λ_m equals 1. In order to identify the particular inertia-spring combination which is sensitive for a given eigenfrequency, the eigenvectors are interpreted as the kinetic and potential energy of the elements for a given eigenfrequency. After reduction, the modal shapes at lower frequencies must be preserved. Therefore, a systematic approach is followed to keep the lower resonance frequencies and corresponding modal shapes. A mass and torsional stiffness combination which is sensitive to the highest eigenfrequency is eliminated. The mass is distributed to its adjoining masses and the torsional spring is combined with the remaining torsional spring to a combined equivalent torsional spring. This procedure can be carried out recursively until a reduction boundary is reached. The reduction boundary has to be chosen and can be a highest frequency of interest or a desired model order (Laschet, 1988).

Modification of the reduction process, as given by Laschet (1988), allows the influence of the CVT ratio on the eigenfrequencies to be analyzed. The diagonal mass matrix $\boldsymbol{J}$ has been modified and includes the CVT ratio:

$$\boldsymbol{J} = \mathrm{diag}\left[J_1 \quad \ldots \quad J_k \;\middle|\; i^2 J_{k+1} \quad \ldots \quad i^2 J_n \right]. \tag{3.11}$$

The stiffness matrix $\boldsymbol{K}$ is modified similarly to incorporate the CVT ratio dependency. This modification allows the CVT ratio to be varied from its minimum to its maximum value. Once the modal shapes are obtained, the algebraic reduction technique enables the CVT ratio to be used directly in the expressions for the reduced model. However, a different CVT ratio can change the modal shape of the drive line. Thus, the reduction should be carried out cautiously. Because the modal shapes do not depend on the CVT ratio for the lower resonance frequencies, the reduction is straightforward.

This reduction technique has been applied to the drive line model of Figure 3.2. In order to obtain the modal shapes, a CVT ratio $i = 1$ is used in Equation 3.10. These modal shapes are used for the reduction process. The obtained two mass model is shown in Figure 3.5. This model contains only the lowest resonance frequency (2 Hz). The next unmodelled resonance frequency is located at 25 Hz, which is above the reduction boundary.

In Figure 3.5 the remaining inertias J_{flw} and J_{veh} are dominated by, respectively, the flywheel inertia and vehicle inertia. The CVT ratio i can be time dependent. The torsional stiffness k_t is dominated by the combined stiffness of the drive shaft and tire. It is concluded that this reduced model is accurate enough for control design. This is based on the close correspondence between the lowest resonance frequency of the original model and the reduced model and because the next unmodelled resonance frequency is larger than the reduction boundary of 10 Hz.

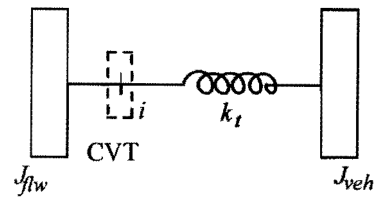

Figure 3.5. Undamped reduced drive line model obtained through modal analysis.

3.4.2. Balanced truncation

The balanced truncation technique as presented by Moore (1981), is implemented in the MATLAB Control Toolbox. This technique analyzes the controllability and observability of the model. The responses of the model for certain input signals are analyzed, and, only states which contribute significantly to the output response of the model are selected.

For the single input single output (SISO) system of Equation 3.8, with zero initial conditions, the output $y(t)$ is given by:

$$y(t) = \int_0^t h(t-\tau)\,u(\tau)\,d\tau, \qquad h(t) = \boldsymbol{C}e^{\boldsymbol{A}t}\boldsymbol{B}, \tag{3.12}$$

where $h(t)$ represents the impulse response and $u(\tau)$ the input of the system. The response $y_r(t)$ of the reduced model with matrices $\boldsymbol{A_r}$, $\boldsymbol{B_r}$ and $\boldsymbol{C_r}$, obtained by the reduction algorithm, is given by a similar expression. The difference $y - y_r$ is the error e:

$$e(t) = y(t) - y_r(t) = \int_0^t \big(h(t-\tau) - h_r(t-\tau)\big)u(\tau)d\tau. \tag{3.13}$$

A measure for the magnitude of the error is given by the relative reduction error χ, defined by:

$$\chi^2 = \frac{\int_0^\infty e^T e\,dt}{\int_0^\infty h^T h\,dt}, \tag{3.14}$$

Application of the balanced truncation reduction technique to the drive line model of Figure 3.2 requires a definition of inputs and outputs of the linear system. As before, the torque generated by the CVT is chosen as input signal. The wheel torque in the drive line is chosen as output signal. In order to keep the model linear, the CVT is assumed to be functioning at a fixed operating point with the CVT ratio $i = 1$. The MATLAB routine requires an asymptotically stable model. After elimination of the rigid body motion the drive line model is asymptotically stable. A second order model is chosen as the required reduced model order. The reduction result is expressed in a second order state space model description:

$$\begin{aligned} \dot{x} &= \boldsymbol{A}_r x + \boldsymbol{B}_r u, \\ y &= \boldsymbol{C}_r x + \boldsymbol{D}_r u. \end{aligned} \tag{3.15}$$

This reduced model has a relative reduction error χ of 2%. This error is small and it can be concluded that a second order model can be used to represent the vehicle drive line. However, in the model reduction process the link with the physical quantities is lost.

3.4.3. Discussion

In order to detect which states are relevant for the input-output relation, both reduction techniques use different criteria to compare the states objectively. The analytical technique considers the kinetic and potential energy of the elements and the numerical technique uses internal balancing. The obtained reduced drive line models for both methods are second order models. Because the modal analysis can not account for drive line damping direct comparison of the models is not correct. However, Bodeplots of the original model and of the reduced models enable a qualitative comparison. In order to obtain a Bodeplot of the reduced model obtained by modal analysis, linear dampers ($b_{flw,lin}$ and $b_{veh,lin}$) must be included in this model. The reduced model, including the linear viscous dampers, is shown in Figure 3.6.

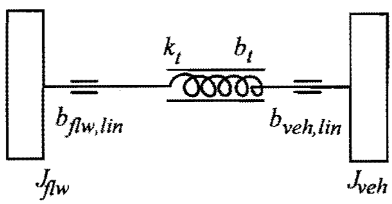

Figure 3.6. Reduced linear model obtained by modal analysis with damping.

The Bodeplots are shown in Figure 3.7. Several conclusions can be drawn from these plots. The lowest resonance frequency of the reduced models closely matches the resonance frequency of the original model. However, for frequencies above the resonance frequency, the reduced models diverge from the original model.

The model obtained by modal analysis is modified by adding damping after the reduction process. Correct choices yield a response very close to that of the original model. The reduced model is accurate over a large frequency range for both amplitude and phase. The modal analysis reduction method enables the incorporation of a time varying parameter, i.e. the CVT ratio, which is essential for a drive line with a CVT. The balanced truncation method is very effective because it yields a reduced model, including damping and a corresponding relative reduction error. However, the reduced model is only valid for one specific CVT ratio.

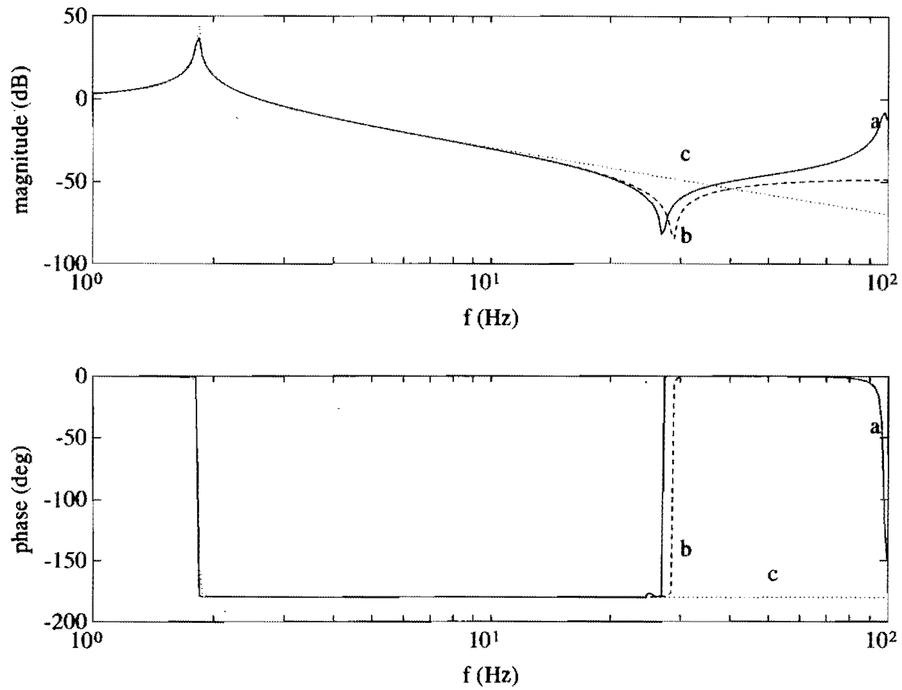

Figure 3.7 *Bodeplot, with magnitude and phase of the transfer function of the drive line model, for a) original model (solid line), b) reduced by balanced truncation (dashed line) and c) reduced by modal analysis (dotted line).*

The model reduction based on modal analysis is used in this thesis to obtain a reduced drive line model. This is because the response of the reduced model accurately matches the response of the original model over a large frequency range, see the Bodeplot of Figure 3.7. Furthermore, it yields a reduced drive line model which includes the CVT as a nonlinear element.

Jones et al. (1986) developed a similar model for the simulation of a Perbury CVT based conventional drive line. They used two inertias to represent the drive line inertia and the vehicle inertia respectively. These inertias were connected by a spring representing the drive line compliance. The Perbury CVT dynamics was described by a non-linear function, which was determined by measurements.

Sakai (1990), Yang and Frank (1985) and Chan et al. (1984) used even simpler models for a CVT based drive line. They modelled the drive line as inertias connected through a CVT, neglecting the drive line compliance. Their main concern was to model the effect of the inertia torque of the engine. The vehicle is accelerated on engine torque only, the torque resulting from the accelerating or decelerating engine inertia, due to the CVT ratio change, is considered an undesired effect which has to limited.

3.5. Controller design model and simulation model

The reduced model obtained by the modal analysis reduction technique is used as controller design model. The air drag is modelled proportional to the squared rotational velocity. The mechanical efficiency of the CVT is assumed to be constant and is used in the expression for the transmitted CVT torque.

The controller design model, shown in Figure 3.8, has been obtained previously. The two inertias are connected by a linear viscous torsional damper with damping coefficient b_t in parallel with a linear elastic spring with stiffness k_t. The CVT ratio is denoted by i. The air drag of flywheel and vehicle are modelled by b_{flw} and b_{veh} respectively. The rolling resistance and the hill climbing resistance is represented by the torque T_{ext}, and the engine by the mean engine torque T_{engine}.

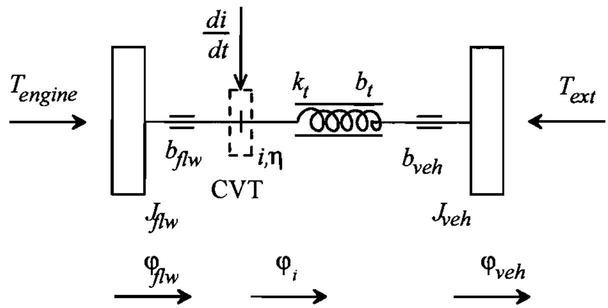

Figure 3.8. Controller design model for hybrid drive line.

The relations describing this drive line model follow from the equations of motion for both inertias. In terms of angular velocities $\dot{\varphi}_{flw}$ of J_{flw} and $\dot{\varphi}_{veh}$ of J_{veh} these equations of motion are given by:

$$J_{flw}\ddot{\varphi}_{flw} = T_{engine} - b_{flw}\dot{\varphi}_{flw}^2 - \frac{i}{\eta}\left(k_t\varepsilon + b_t\dot{\varepsilon}\right), \qquad (3.16)$$

$$J_{veh}\ddot{\varphi}_{veh} = \left(k_t\varepsilon + b_t\dot{\varepsilon}\right) - b_{veh}\dot{\varphi}_{veh}^2 - T_{ext}, \qquad (3.17)$$

where the deformation ε is defined as the relative angle over the torsional spring:

$$\varepsilon = \varphi_i - \varphi_{veh}, \qquad (3.18)$$

and the CVT ratio i is defined by:

$$i = \frac{\dot{\varphi}_i}{\dot{\varphi}_{flw}}, \qquad (3.19)$$

The new variable ε, the relative angle over the torsional spring, allows a compact notation of the equations. Furthermore, this relative angle eliminates the rigid body motion of the vehicle. The absolute coordinate, i.e. the distance travelled by the vehicle is not relevant. Substitution of Equations 3.17 and 3.19 into Equation 3.16 yields:

$$J_{flw}\ddot{\varepsilon} = -(k_t\varepsilon + b_t\dot{\varepsilon})\left(\frac{i^2}{\eta} + \frac{J_{flw}}{J_{veh}}\right) - b_{flw}i\dot{\varphi}_{flw}^2 + iT_{engine} + \frac{J_{flw}}{J_{veh}}T_{ext} + \ldots$$
$$+\frac{J_{flw}b_{veh}}{J_{veh}}\left(i\dot{\varphi}_{flw} - \dot{\varepsilon}\right)^2 + J_{flw}\dot{\varphi}_{flw}\frac{di}{dt}. \tag{3.20}$$

In this relation the deformation ε is expressed in a second order differential equation. This deformation is proportional to the torque T_{out} in the drive line:

$$T_{out} = k_t\varepsilon + b_t\dot{\varepsilon}. \tag{3.21}$$

The input to this model is the rate of ratio change of the CVT. The CVT is assumed to be ideal, i.e. any required rate of ratio change is realized immediately. This idealisation of the CVT results in a simple CVT model:

$$i = \int_0^t u\,dt, \quad u = \frac{di}{dt}. \tag{3.22}$$

This assumption holds because the rate of change is realized much faster than the drive line can respond. The CVT response time is determined mainly by the CVT hydraulics. In Chapter 5 where the CVT response is investigated these assumptions are shown to be valid. Therefore, the rate of change can be used directly as input to the drive line model.

In order to clarify the control objective and to specify the input and outputs of the controller design model, the following short hand notation is introduced:

$$\begin{aligned} \dot{x} &= f(x,w) + g(x,u), \\ y &= h(x). \end{aligned} \tag{3.23}$$

In this equation, the state vector x is given by:

$$x = \begin{bmatrix} x_1 & x_2 & x_3 & x_4 \end{bmatrix}^T = \begin{bmatrix} \varepsilon & \dot{\varepsilon} & i & \dot{\varphi}_{flw} \end{bmatrix}^T, \tag{3.24}$$

which is the deformation ε, the time derivative of ε, the CVT ratio i and the flywheel rotational speed $\dot{\varphi}_{flw}$. These variables are sufficient to describe the state of the system. It is noted that the rigid body motion of the system is not represented with this model. The function $f(x,w)$ and the input function $g(x,w)$ are given:

$$f(x,w,t)=\begin{bmatrix} x_2 \\ -(k_t x_1 + b_t x_2)\left(\frac{x_3^2}{\eta J_{flw}}+\frac{1}{J_{veh}}\right)-\frac{b_{flw} x_3 x_4^2}{J_{flw}}+\frac{x_3 w_1}{J_{flw}}+\ldots \\ \frac{b_{veh}}{J_{veh}}(x_3 x_4 - x_2)^2+\frac{w_2}{J_{veh}} \\ 0 \\ \frac{1}{J_{flw}}\left(-b_{flw} x_4^2 - \frac{x_3}{\eta}(k_t x_1 + b_t x_2)+w_1\right) \end{bmatrix}, \tag{3.25}$$

with: $w=\begin{bmatrix} T_{engine} \\ T_{ext} \end{bmatrix}$.

$$g(x,u)=\begin{bmatrix} 0 \\ x_4 u \\ u \\ 0 \end{bmatrix}. \tag{3.26}$$

The disturbance w consists of the engine torque T_{engine} and the external torque T_{ext}. The input of this system is the input u, which is the rate of CVT ratio change: $u=\frac{di}{dt}$. The output of the system, the output torque T_{out} is given by the function $h(x)$:

$$h(x)=k_t x_1 + b_t x_2 . \tag{3.27}$$

The above derived controller design model is relatively simple. In order to evaluate the controller performance a more realistic vehicle model is used. This enables the analysis of phenomena which are not essential for controller design but can deteriorate the controller performance or can destabilize the closed-loop. As an intermediate result during the reduction process, an appropriate simulation model is obtained. This model, given in Figure 3.9, is used for controller evaluation only. It contains higher resonance frequencies and enables the incorporation of wheel spin on a slippery surface (Custers, 1992).

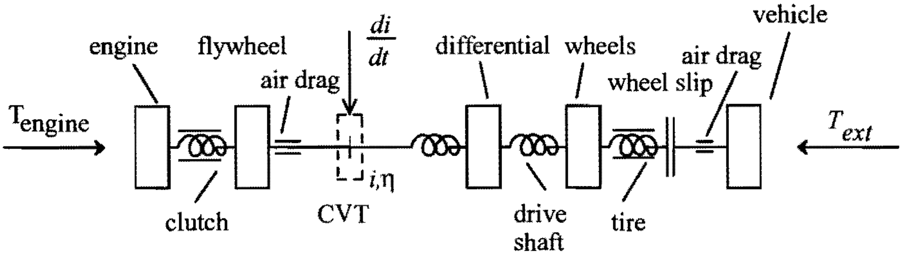

Figure 3.9. Drive line simulation model.

Chapter 4

Experimental set-up for controller validation

4.1. Introduction

A test-rig has been designed and constructed for experimental verification of the control of the hybrid transmission. The test-rig enables the simulation of the 'low speed' mode of the hybrid drive line. It consists of a mechanical part, a hydraulic actuating system and an electronic control and data acquisition system. The test-rig has been used for two different sets of experiments, one being the CVT response analysis and its validation, and the other being the drive line controller performance verification. The test-rig has been adapted to each set of experiments.

4.2. Test-rig for CVT controller validation

4.2.1. Validation objectives

The main purpose of the CVT controller response analysis and validation is to asses its applicability in a hybrid transmission. The CVT behaviour has to be determined quantitatively, i.e. its response time and its accuracy must be measured.

4.2.2. Measurement methods and signals

The CVT behaviour is described by its ratio and its rate of ratio change. A detailed description of the CVT is given in Chapter 5. The CVT ratio is derived from the shaft speed signals. The rotational speeds are measured with Hall-sensors, which are triggered by toothed discs mounted on the input and output shaft of the CVT.

The CVT pulley pressures are measured by means of pressure sensors, which are placed in the hydraulic pressure line close to the pulley pressure chamber. The torque is measured by means of a torque sensor in the CVT output shaft. The measurement accuracy (including signal conditioners and prefilters) are given in Table 4.1.

Table 4.1. Measurement accuracy.

	range	abs. error	bandwidth
torque signal	-200...200 Nm	1 Nm	25 Hz
pressure signal	0...60 bar	0.3 bar	150 Hz
speed signal	120...6000 rpm	3 rpm	20 Hz

With the speed sensors and the slotted discs on the CVT shafts, the CVT ratio can be calculated and the rate of ratio change can be obtained (Spijker et al., 1992). The accuracy depends on the torsional vibrations in the drive line. The bandwidth of the signals depends on the digital filters used to remove measurement noise. The accuracy and the bandwidth of the ratio and rate of ratio change are given in Table 4.2.

Table 4.2. Measurement accuracy of CVT response.

	range	rms error	bandwidth
CVT ratio	0.445 ··· 2.25	0.003	20 Hz
CVT ratio change	$-1.5 \ldots 1.5\ s^{-1}$	$0.02\ s^{-1}$	10 Hz

4.2.3. Test-rig layout

The mechanical part of the test-rig contains two identical flywheels (Figure 4.1 and 4.2) which are coupled to the CVT. This yields a test-rig which is symmetrical with respect to the CVT. The test-rig has a high torsional resonance frequency, enabling the CVT response to be analyzed without drive line interference. The fairly large inertias assure smooth running of the drive line. Small rate of ratio changes represent the most critical operating conditions of the CVT in the hybrid drive line and, hence, require most attention during verification.

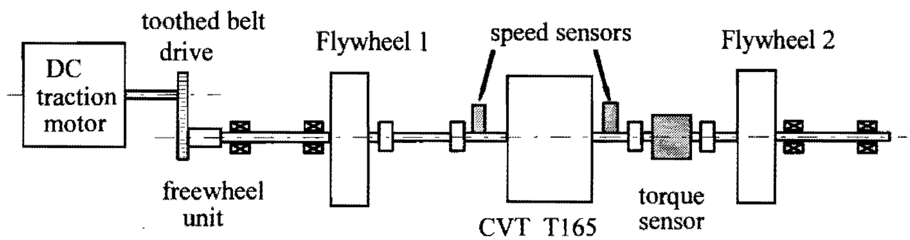

Figure 4.1. CVT test-rig layout of mechanical components.

A 12 kW electrical DC-motor is used to accelerate the drive line up to the operating speed via a toothed belt drive. Once the desired speed is achieved, the motor is stopped and automatically disconnected through a freewheel unit. Because the motor is shut off during the experiments, the DC motor characteristics are not relevant for the test-rig dynamic behaviour.

Table 4.3. CVT test-rig characteristics.

DC motor	12 kW
Flywheel 1 inertia	4.5 kgm^2
Flywheel 2 inertia	4.5 kgm^2
flywheels maximum operating speed	3000 rpm
torsional resonance frequency (i = 1.0)	15 Hz

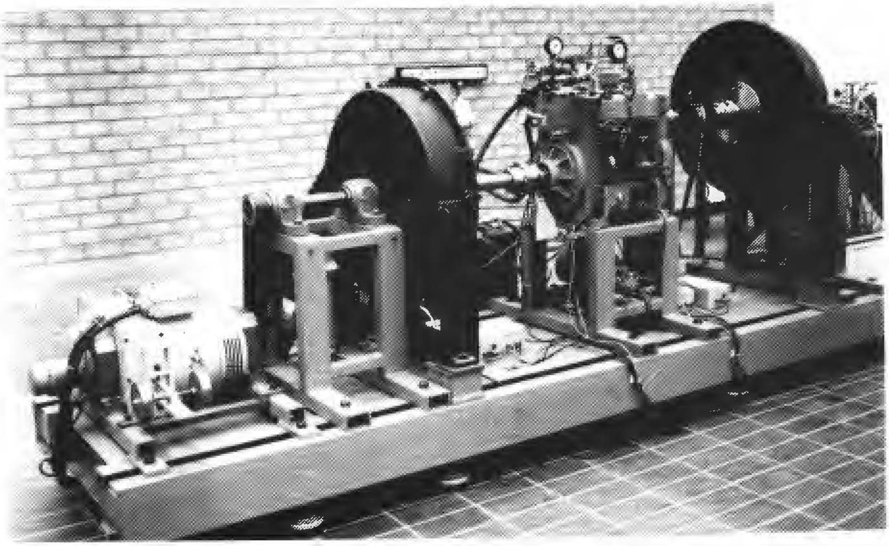

Figure 4.2. Photograph of CVT test-rig.

4.2.4. The CVT specifications

The CVT used is a Van Doorne Transmissie T165 (van der Veen, 1977) for industrial applications which was modified to have the same characteristics as the CVT used in the hybrid drive line. The internal hydraulic pump and valves were removed. External pumps and a reservoir were added. The primary hydraulic cylinder was modified in such a way that both cylinders have equal piston areas. These modifications yield a symmetrical CVT in both layout and response. The cylinders are activated by hydraulic servo-valves (Mannesmann Rexroth product description, 1989). The CVT properties are given in Table 4.4, and the geometrical details are given in Appendix C.

Table 4.4. T165 CVT characteristics.

maximum running speed	6000 rpm
maximum torque at minimum radius	100 Nm
ratio	$i = 0.445 \ldots 2.25$
ratio coverage	5.06

The transmission is protected against overload by a hydraulically actuated wet plate clutch. The hydraulic cylinder of the clutch in this test-rig has a fairly large volume compared to the cylinder of the starting clutch in the hybrid transmission. This results in slow dynamics of the clutch pressure controller in the test-rig. Therefore, accurate simulation of the hybrid transmission starting clutch, which is used to accelerate the vehicle from zero speed, can not be obtained. The slower clutch response does not influence the CVT performance nor does it interfere with the drive line controller verification, i.e. the clutch is closed during these experiments.

4.2.5. The hydraulic system

The hydraulic system (see Figure 4.3) incorporates a high pressure circuit, which provides the operating pressure for the CVT, and a low pressure circuit which provides the clutch pressure and an oil flow to the V-belt and to the clutch for lubrication and cooling. A circulating pump is used on the sump return line.

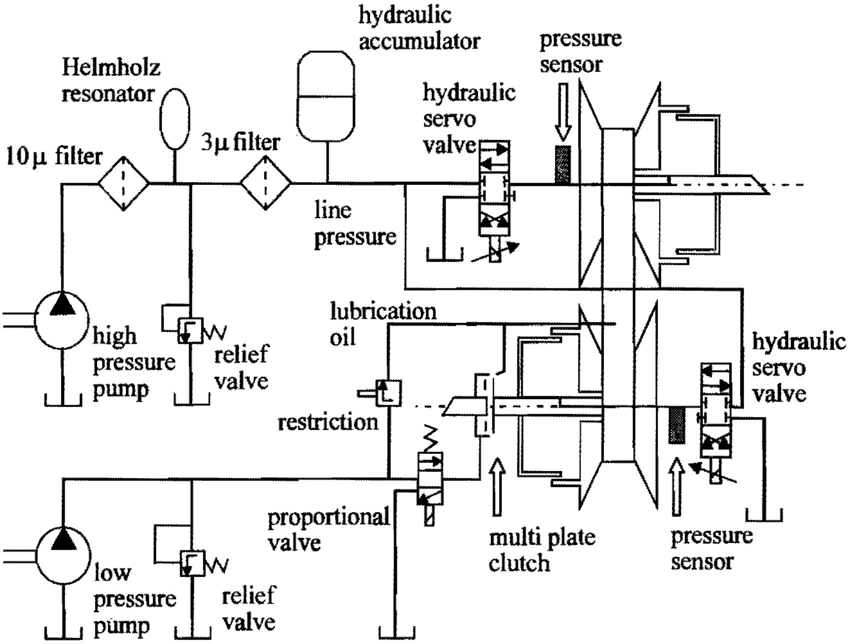

Figure 4.3. Hydraulic circuit of test-rig.

Incorporated in the high pressure circuit are a pump, filters, a Helmholz resonator, a relief valve and an accumulator. The Helmholz resonator eliminates high frequency pump flow pulsations (Stubbe, 1987). The relief valve limits the line pressure and the accumulator assures a nearly constant line pressure at the end of the line, independent of the flow requirements of the valves. The servo-valves at the T165 are identical to those in the EUT hybrid vehicle. The constant line pressure is set at 70 bar, which is an average value for the line pressure in the hybrid vehicle. Additional details of the hydraulic circuit are given in Appendix C.

Table 4.5. Electro hydraulic servo-valves.

flow capacity	20 litre/minute at 70 bar
minimum operating pressure	30 bar
bandwidth	100 Hz, at 1 litre/min flow

The electro hydraulic servo-valve contains an electrically activated pilot stage and a hydraulically activated main valve. The position of the main valve is measured electronically and a correction signal is applied to the pilot valve. The pilot valve adjusts the position of the main valve hydraulically. The valve requires only a small electrical signal. It uses hydraulic power to control the main valve. Therefore, a minimum line pressure is required to operate this type of valve. The relation between the flow Q through the valve, the pressure difference Δp across the valve and the voltage u applied to the pilot stage is:

$$Q = \text{constant}\, u\sqrt{\Delta p}. \tag{4.1}$$

The constant factor in this equation depends on the actual line pressure level and the valve electronics. Stubbe (1987) checked and modified these electronics in order to optimize the valves for pressure control. Due to this modification the valve characteristic has been changed and in this thesis the new valve characteristic is denoted by:

$$Q = V(\Delta p, u). \tag{4.2}$$

The flow capacity and bandwidth of the servo-valves are adequate for this application. The valves do not pose any limitations on the experiments. It should be noted that these valves are not well suited for production of commercial transmissions, because they are vulnerable and expensive.

4.3. Test-rig for drive line controller validation

4.3.1. Validation objectives

The drive line controller must provide a smooth and accurate response of the drive line output torque. This requires that the output torque response of the drive line is measured. Because of the low drive line resonance frequency, the response to sudden changes in operating conditions has to be evaluated. These changes represent an abrupt change in output torque or even a load reversal.

4.3.2. Measurement methods and signals

The drive line output torque is the main variable of interest. The output torque is measured with the aid of a torque sensor and the rotational speeds are measured with Hall-sensors, as described previously in Subsection 4.2.2. The signal accuracy (including signal conditioners and prefilters) are given in Table 4.6.

Table 4.6. Signal accuracy.

	range	abs. error	bandwidth
torque signal	- 200···200 Nm	1 Nm	25 Hz
speed signal	120...6000 rpm	3 rpm	20 Hz

4.3.3. Test-rig layout

The test-rig for the drive line controller was designed in such a way that its torsional resonance frequency approximates the resonance frequency of the hybrid drive line (Egberts, 1993). The 'low speed' mode of the hybrid drive line was chosen because it is most often used in (sub-)urban traffic. In Chapter 3 a controller design model for the 'low speed' mode of the hybrid drive line was derived, consisting of two inertias, a CVT and a torsional spring. This configuration has been realized on the test-rig. It incorporates the relevant dynamics which are required to validate the drive line controller. Furthermore, it also utilises the CVT in the correct operating region, i.e. the speed and torque combinations match those of the CVT in the hybrid drive line.

Flywheel 1 and Flywheel 2 represent the high speed flywheel and the equivalent vehicle inertia, respectively. The inertias were transformed to equivalent inertias at the primary CVT shaft and match the controller design model. The flexible shaft represents the combined drive shaft and tire compliance (Egberts, 1993). It was specifically designed for this purpose and made from poly-urethane. This flexible shaft has a slightly higher torsional stiffness than intended. Hence, the resonance frequency of the test-rig is somewhat higher than the estimated resonance frequency of the hybrid drive line (Egberts, 1993). This, however, does not hinder the verification of the drive line controller since this resonance frequency can be incorporated directly in the controller.

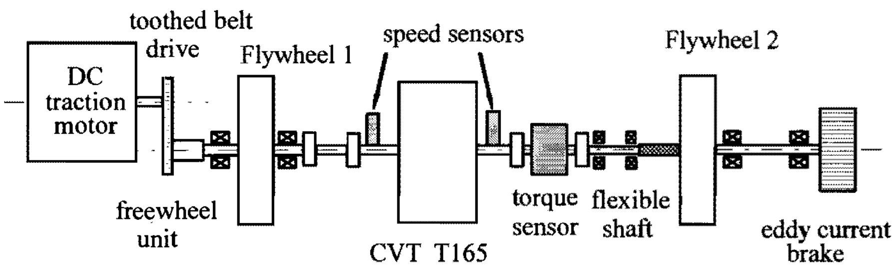

Figure 4.4. Drive line test-rig layout of mechanical components.

Again the 12 kW electrical DC-motor is used only to accelerate the drive line up to operating speed.

Table 4.7. Drive line test-rig characteristics.

DC motor	12 kW
Flywheel 1 inertia	25.1 kgm^2
Flywheel 2 inertia	1.32 kgm^2
stiffness of flexible shaft	232 Nm/rad
max operating speed Flywheel 1	2300 rpm
torsional resonance frequency (i = 1.0)	2.18 Hz

The rolling resistance and air drag are simulated by an air cooled eddy current brake. This brake is a commercially available retarder (Telma product description, 1985). A controlled current source is used to approximate the required road load characteristic of the vehicle (Overbeek, 1992).

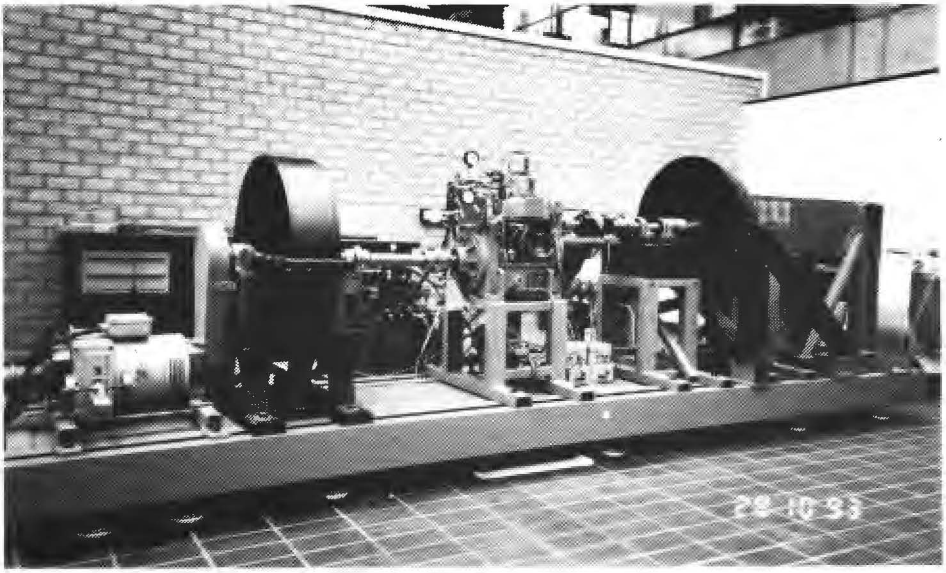

Figure 4.5. Drive line test-rig.

4.4. The electronic control system

The electronics used for the test-rig can be divided into three subsystems, the signal conditioning system, the data acquisition and control system, and the data analysis system. The first part is used for conditioning and prefiltering of the signals from the sensors. The signal conditioners convert the signals from the sensors to a level suitable for the data acquisition system. Prefilters are used to prevent aliasing during the A/D conversion. The discrete signals from the Hall-effect sensors are directly transmitted to the timers on the acquisition equipment.

The dedicated actuator electronics are an integral part of the servo-valves (Mannesmann Rexroth product description, 1989). Their input signals represent the desired position of the main valves. These desired positions are compared to the measured positions and a control current is applied to the valves.

The second part is the data acquisition and the on-line control system. Figure 4.5 shows the data acquisition set-up. The data acquisition system manufactured by dSpace (dSpace product description, 1992) is based on a digital signal micro-processor (DSP) and can perform on-line control tasks at high sampling rates. The hardware incorporates a main controller board with the DSP and a number of additional boards for input and output processing. A timer driven interrupt on the DSP activates the control algorithms at time intervals of 2 ms.

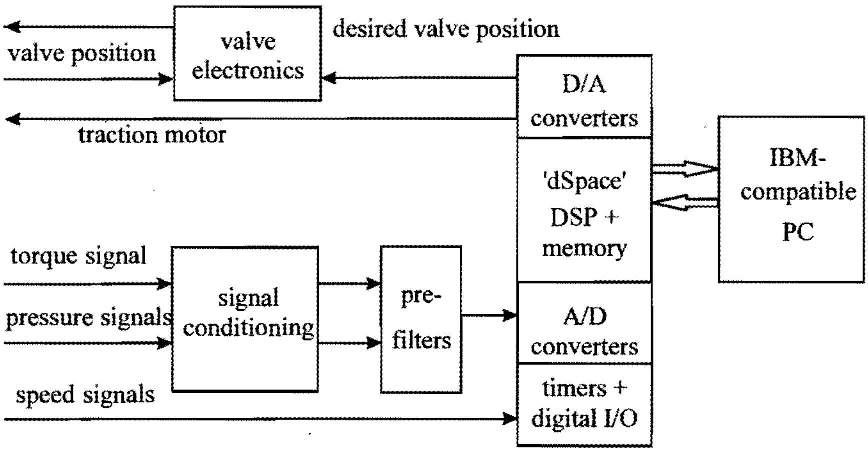

Figure 4.5. Data acquisition and control electronics.

The third part of the electronic system consists of an IBM-compatible PC which is used for control algorithm development, initialisation of the dSpace equipment and storage of the software. The available software for the data acquisition system enables fast implementation of control algorithms. The experiments can be monitored on-line on this PC. The test results are stored on a hard disc for off-line analysis.

Chapter 5

Continuously Variable Transmission in a flywheel-hybrid drive line

5.1. Introduction

The Continuously Variable Transmission (CVT) is one of the key elements in the hybrid drive line. Figure 5.1 shows a CVT of the so-called transmatic type with a metal V-belt, as used in this hybrid transmission. The CVT efficiency is one of the important factors defining the success of the flywheel-hybrid drive line (van der Graaf, 1987). It is one of the basic assumptions and not the subject of this thesis. In this chapter attention is focused on control of the CVT, because this is of major importance for the drive line control, and, hence, vehicle performance and attainable passenger comfort levels.

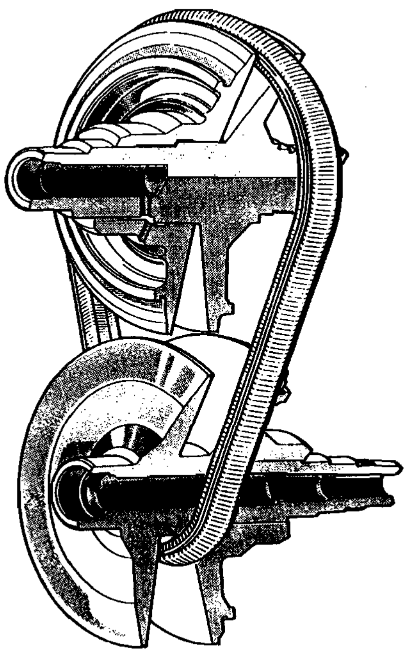

Figure 5.1. View on the CVT with a V-belt (courtesy of Van Doorne's Transmissie).

In Chapter 3, the rate of ratio change has been used to characterize the CVT behaviour in the hybrid drive line. In the present chapter, the function and construction of the CVT are discussed, and the CVT response is fine tuned for use in the hybrid drive line. In order to enable the design of control algorithms for the rate of CVT ratio change, a simple dynamic model is derived. With this model, the dynamic response is analyzed and appropriate control algorithms are proposed, implemented and verified by experiment. Finally, the closed loop bandwidth of the CVT rate of ratio change is discussed.

5.1.2. Function and layout

The CVT has two main functions in the hybrid drive line. The first is to transmit a torque from the input shaft to the output shaft, allowing these shafts to rotate with different and varying speeds. The second function is to either accelerate or decelerate the vehicle and the flywheel by means of varying the CVT ratio (see Chapter 2, Section 2).

In the EUT hybrid transmission a transmatic type CVT is used. This CVT consists of a metal belt composed of thin V-elements and strings, mounted between two V-shaped, adjustable pulleys. The CVT pulleys in the hybrid transmission have equal piston areas and, hence, the CVT is symmetrical. One of the conical sheaves of each pulley can move in axial direction (Figure 5.2). By means of an oil pressure in a hydraulic chamber, the belt is clamped between the sheaves of each pulley. The resulting tensile force in the strings, combined with a pushing force between the V-elements, allows the CVT to transmit a torque. Shifting of the sheaves in axial directions varies the running radius of the belt and, hence, varies the transmission ratio.

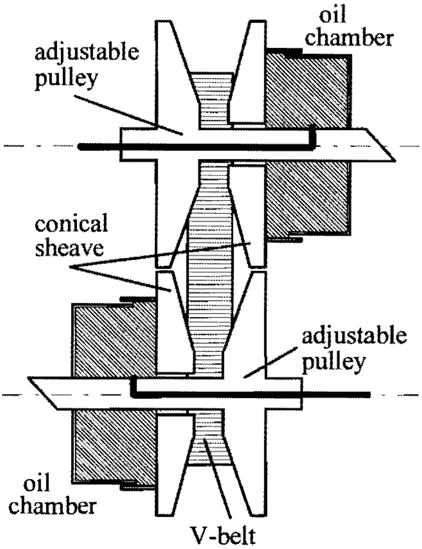

Figure 5.2. CVT schematic layout.

5.1.1. Definitions

In conventionally powered vehicles, the 'primary pulley' is defined as the pulley which is driven by the i.c. engine. The 'secondary pulley' is defined as the pulley at the output shaft of the transmission. In the hybrid drive line the same definition is used, thus the pulley which is mounted on the engine's side in the transmission and can be driven by the engine is called the 'primary pulley'. The other pulley of the CVT is called the 'secondary pulley'. This definition allows the pulleys to be uniquely identified in the hybrid transmission. This definition is independent from the power flow through the transmission or the specific mode of the drive line. As the power flow through this transmission is bi-directional, the driving pulley and driven pulley do not necessarily coincide with the physical primary and secondary pulley.

The terms 'primary pulley' and 'secondary pulley' are used when an explicit identification of the pulleys is required. The terms 'driving pulley' and 'driven pulley' are used if the power flow in the transmission is relevant. In these cases the pulleys are identified by the subscripts 1 and 2 for the driving, and the driven pulley, respectively. The CVT ratio i, as defined in Chapter 3, follows from the relation $\omega_s = i\ \omega_p$, where the lower indices s and p refer to the secondary, and the primary pulleys, respectively. The time derivative of this ratio is called the rate of ratio change.

5.1.3. CVT control in vehicles

For vehicles equipped with a CVT various control objectives can be identified:

- Controlling the rate of CVT ratio change. This allows the inertias to be accelerated or decelerated. It introduces a torque in the drive line. This type of control is essential for the hybrid vehicle and is discussed in this thesis.
- Keeping the CVT ratio at one specific operating point. This type of control is used if a single constant ratio is required. In the hybrid drive line this is used during mode shifts when clutches have to be synchronized. This type of control is briefly discussed in this thesis.
- Shifting the CVT ratio from one operating point to another operating point (so-called 'point to point control'). This is used during normal driving in a conventional vehicle, when the output power is controlled by varying the engine speed. In this case, the specific trajectory by which the new ratio is reached, is relevant for the driveability of the vehicle. It is also used in the hybrid vehicle when the 'engine' mode (see Section 2.2) is selected. The 'engine' mode is not considered in this thesis and, therefore, this type of CVT control is not discussed.

In order to obtain a certain required ratio, both the clamping pressure and the axial pulley sheave velocity have to be controlled. In conventionally, hydraulically, controlled CVT's in current productions vehicles (Röper, 1987; Sakai, 1990) the clamping pressure is applied to the secondary pulley. In these cases, ratio control is achieved through steering of the hydraulic flow in the primary pulley. During vehicle acceleration, an oil flow is directed into the oil chamber of the primary pulley. This guarantees an increase in primary pulley pressure and belt slip is prevented. During engine braking, when the vehicle decelerates, an oil flow is drained from the primary pulley cylinder. Belt slip is not critical in this case, since only small torques are transmitted. Most of the proposed electronically controlled CVT use the same principle (Abromeit, 1985; Falzoni, 1984; Gieles, 1989; Hirano et al., 1991; Namuri et al., 1990; Sakai, 1990). The electronic CVT control of Wade (1984) uses a different concept, in which both pulley pressures are controlled simultaneously. The pressure controllers are augmented by a ratio controller to achieve the desired ratio response.

In the hybrid drive line, high torques are transmitted, from flywheel to vehicle and vice versa. In order to prevent belt slip under all circumstances, pressure control is used on the driven pulley and an oil flow is directed into the driving pulley. Consequently, pressure control and flow steering on the pulleys must be switched during load reversal (Spijker et al., 1993a).

5.2. CVT modelling

In the discussion given in the present chapter, the CVT is isolated from the drive line and is considered as an independent component. The function and performance of the CVT in a hybrid drive line will be emphasized. The main objective is to obtain relations between the rate of CVT ratio change and the physical phenomena in the CVT. The models derived in this section are simple models which characterize the CVT and enable the CVT controller design. The metal V-belt is not considered in detail. Hendriks et al. (1988) provided a short overview on the application of metal V-belts in transmissions. Van Rooij and Schaerlaeckens (1992) gave a detailed analysis of V-belt forces and efficiencies in transmissions.

5.2.1. Geometrical and kinematic aspects

In order to obtain a desired rate of ratio change, a certain axial pulley sheave velocity is required. This velocity is proportional to the oil flow into the cylinder. The relations for the required flow can be derived from the ratio and the required rate of ratio change of the CVT.

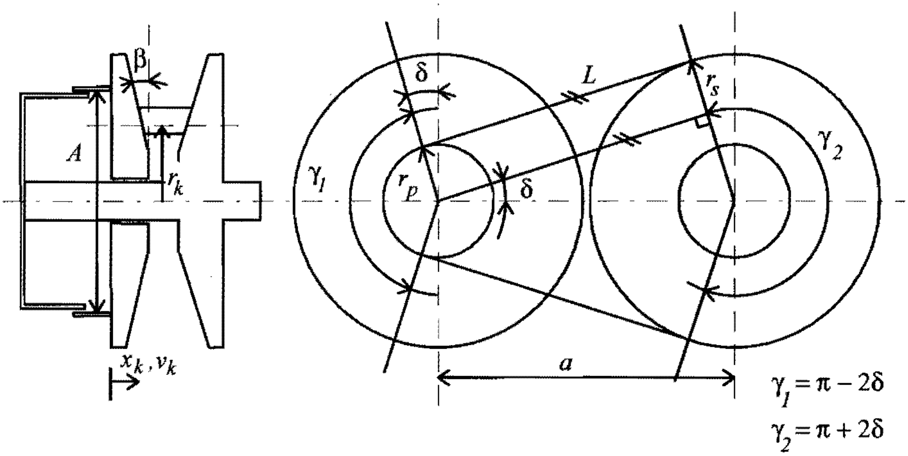

Figure 5.3. CVT geometry.

Several assumptions are made in order to derive the relation between the oil flow, the ratio and the rate of ratio change:

- The metal V-belt is a homogeneous endless metal belt with a rigid cross-section.
- The shafts and pulleys are rigid and the pulleys are perfectly aligned, spiral effects are not considered.
- Micro-slip between metal V-belt and pulleys is neglected.
- The centre distance a between input and output shaft and the length L of the belt are constant (see Figure 5.3).
- The belt on each of the pulleys forms an arc with constant radius.
- The hydraulic fluid is incompressible and the hydraulic cylinders are rigid.
- The top angle β is constant (see Figure 5.3).
- The oil leakages can be neglected.

With these assumptions it is possible to relate the running radii r_p and r_s on the primary, respectively on the secondary pulley to the CVT ratio i. Using the angle δ (see Figure 5.3) yields:

$$\begin{aligned} r_p &= i\, r_s, \\ (\pi-2\delta)r_p + (\pi+2\delta)r_s + 2a\cos\delta &= L, \\ r_s - r_p &= a\sin\delta. \end{aligned} \tag{5.1}$$

These equations form a set of three nonlinear algebraic relations with four unknown variables, r_p, r_s, i, and δ. If any of these variables is given, the other three can be obtained. After some algebraic manipulations, the set of equations can be rewritten as:

$$
\begin{aligned}
&(1-i)\cos\delta+\left[\left(\frac{\pi}{2}+\delta\right)+i\left(\frac{\pi}{2}-\delta\right)\right]\sin\delta=(1-i)\frac{L}{2a},\\
&\left[\left(\frac{\pi}{2}+\delta\right)+i\left(\frac{\pi}{2}-\delta\right)\right]r_s=a\left(\frac{L}{2a}-\cos\delta\right),\\
&r_p=i\,r_s\,.
\end{aligned}
\tag{5.2}
$$

The first nonlinear equation is used to determine δ as a function of i. With δ it is straightforward to determine r_p and r_s as a function of i, using the second and third equation. Röper (1987) suggested to linearize the equation for δ to approximate the desired relation for the angle δ and the CVT ratio i. This approach is not used in this thesis.

Each change of the running radius of the belt on a pulley results from a displacement of one of the sheaves of that pulley. The pulley sheave velocity v_k (see Figure 5.3) as a function of $\dot{r}_k$ is given by:

$$v_k=\dot{x}_k=2\tan\beta\,\dot{r}_k\,,\qquad k=p,s. \tag{5.3}$$

In turn, $\dot{r}_k$ is related to the rate of ratio change. From the earlier given relations it can be seen that:

$$
\begin{aligned}
&\left[\left(\frac{\pi}{2}+\delta\right)+i\left(\frac{\pi}{2}-\delta\right)\right]\dot{r}_p=\left(\frac{\pi}{2}+\delta\right)r_s\frac{di}{dt},\\
\text{and }&\left[\left(\frac{\pi}{2}+\delta\right)+i\left(\frac{\pi}{2}-\delta\right)\right]\dot{r}_s=-\left(\frac{\pi}{2}-\delta\right)r_s\frac{di}{dt}.
\end{aligned}
\tag{5.4}
$$

In an on-line algorithm (every sample interval during operation) for the control of the rate of change it is impractical to, first determine δ as a solution of the given nonlinear equation, then calculate r_s (and possibly r_p), and finally obtain $\dot{r}_p$ and $\dot{r}_s$. A more practical approach is to determine off-line (only once, before operation) a third order polynomial approximation for r_s as a function of i. Furthermore, the relations for $\dot{r}_p$ and $\dot{r}_s$ (given implicitly in Equation 5.4) are rewritten as:

$$\dot{r}_k=\rho_k\frac{di}{dt},\qquad k=p,s, \tag{5.5}$$

and for ρ_k as a function of i, polynomial approximations are determined off-line. The error caused by this polynomial approximation is an order of magnitude smaller than the error introduced by the assumptions used to derive these geometrical relations.

5.2.2. Oil flow requirements

The required oil flow to the hydraulic cylinder of a pulley is proportional to the axial sheave velocity of that pulley and to the piston area A of the hydraulic cylinder, i.e.:

$$Q_k = Av_k = 2A \tan\beta\, \rho_k \frac{di}{dt}, \qquad k = p,s. \tag{5.6}$$

This relation holds if:
- the deformation of the hydraulic cylinder is negligible,
- the oil is incompressible,
- the oil leakage is negligible.

It is noted that the Q_k can be rewritten as:

$$Q_k = f_k \frac{di}{dt}; \quad \text{with } f_k = 2A \tan\beta\, \rho_k; \qquad k = p,s; \tag{5.7}$$

where f_k is a function of the CVT ratio i. A graphical representation of the nonlinear function $f_k = f_k(i)$ is given in Figure 5.4.

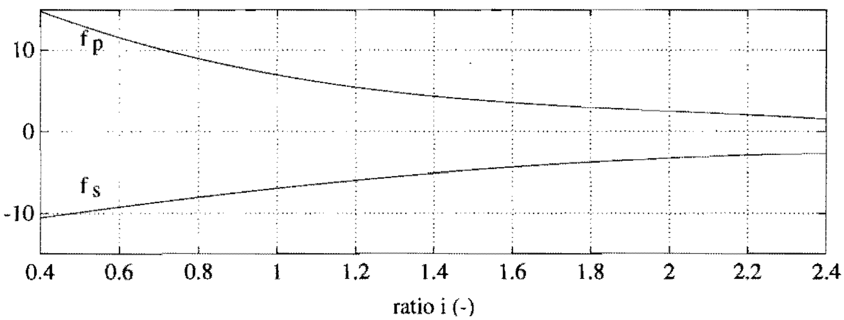

Figure 5.4. The function $f_{p,s}$ for the primary, respectively the secondary pulley.

Due to nonlinearities the required flows in the two pulleys are different and, hence, the flow Q_p must be directed into the primary pulley and Q_s must be directed into the secondary pulley. With Equation 5.7, the rate of CVT ratio change is expressed in an oil flow into the hydraulic cylinders. These relations (Equation 5.3 and 5.5) can be used to obtain the axial pulley velocity when a required rate of ratio change has to realized. Furthermore, a measured rate of change can be used to calculate the actual axial pulley velocity and can be used in a feedback loop.

5.2.3. Clamping forces

The clamping forces are required to prevent V-belt slip. Belt slip is not controlled directly. Its measurement is complicated and expensive, since it is a small quantity: it is approximately 1% of the belt velocity under nominal operating conditions (Becker, 1987). The required clamping pressures depend on the torques to be transmitted, the friction mechanisms and the geometry of the CVT. Several authors, Becker (1987), Gerbert (1984), Sun (1988), and van Rooij and Schaerlaeckens (1992) gave detailed descriptions of the forces on the pulley sheaves, the steel blocks and the metal strings of the metal V-belt. Becker (1987) and van Rooij and Schaerlaeckens (1992) also specified the forces in the V-belt at different transmission ratios for a mass produced, hydraulically controlled CVT. The models used by the above mentioned authors are very detailed and are not suitable for on-line use in control algorithms.

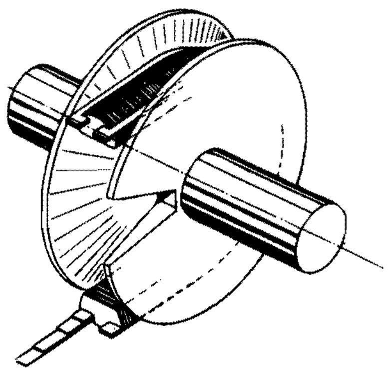

Figure 5.5. Detail of CVT pulley (van Rooij and Schaerlaeckens, 1992)

Slip can be avoided by applying sufficiently high clamping forces at the pulleys. The required clamping forces can be calculated from the contact forces between the belt and the sheaves, using a friction model for the belt-pulley contact. This calculation must be done on-line, to enable the use in a control algorithm. The result of this computation must be a setpoint for the clamping forces which are sufficiently high. On the other hand, because high pressures affect the efficiency and durability of the V-belt and pulleys, these pressures must not exceed this setpoint, that is, it also is a safe maximum level.

Röper (1987) describes the control of the Ford CTX-transmission using simple, but somewhat inaccurate, relations for the forces in the V-belt. Since they yield a usable upper bound for the required clamping force, their use is justified (Cadee, 1992). In this thesis, the relations between the transmitted torque and the minimal required clamping forces to prevent slip are derived on a similar basis.

The following assumptions and approximations are made:

- The metal V-belt is a homogenous endless belt with a rigid cross-section.
- The shafts and pulleys are rigid; the pulleys are perfectly aligned, and spiral effects are not considered .
- The radial velocity of the belt can be neglected.
- The friction between belt and pulleys can be modelled as Coulomb friction with a constant friction coefficient.

These assumptions can be used also for a CVT with a chain instead of a V-belt. Hence, the following analysis can be used also for chain type CVT's. Different types of chains were proposed by Dittrich (1990) and van Rooij (1991).

The relevant forces acting on the belt and the pulley are shown in Figure 5.6. The axial force F_{ax} due to the pressure p_{ax} is applied on the piston area A, so $F_{ax} = A\, p_{ax}$. The torque T is the result of the tensile force difference F_1 - F_2 at radius r. In order to derive the required clamping force, the contact area between the belt and the pulley is considered. In Figure 5.6 this is the circular part of the belt and the pulley at radius r between $\varphi = 0$ and $\varphi = \gamma$.

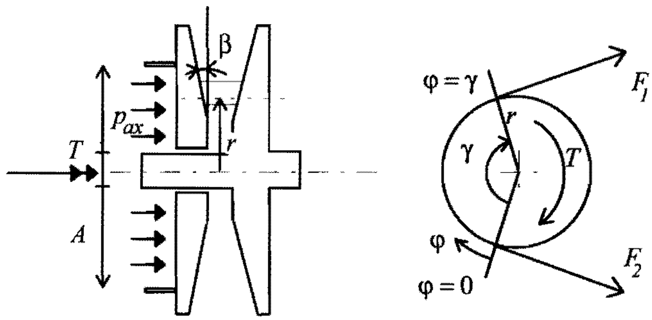

Figure 5.6. Forces acting on pulleys and V-belt.

The relevant forces in and on the belt are shown in Figure 5.7. The forces for this application are the tensile force $f(\varphi)$ in the belt and the forces due to the interactions between the pulley and the belt in the contact area. It is assumed that these interactions can be modelled by a force $q(\varphi)$ per unit length, perpendicular to the pulley, and a force $w(\varphi)$ per unit length in circumferential direction.

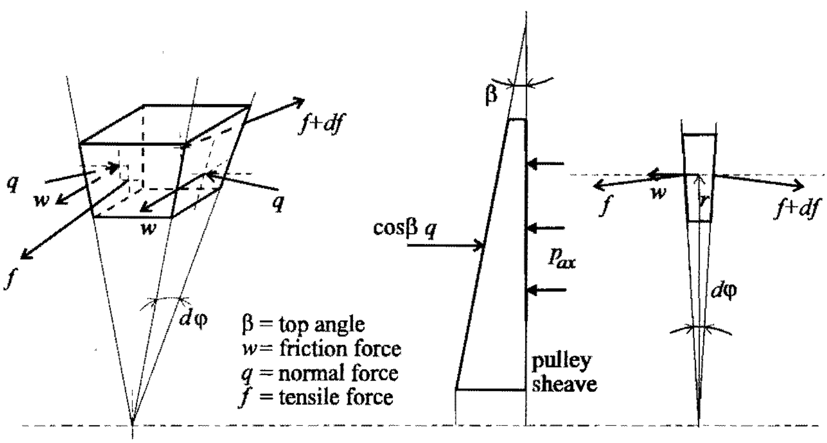

Figure 5.7. Forces acting on cut part of V-belt.

According to the principle 'action = - reaction' forces, exerted by the belt on the pulley, are represented by the normal force $q(\varphi)$ and the circumferential force $w(\varphi)$, both per unit length on each of the discs of the pulley (see Figure 5.7). The other force quantities on the pulley are the axial force $F_{ax} = A\, p_{ax}$ and the torque T. Ignoring the inertia terms due to the axial motions of the sheave, the relevant equilibrium equations for the pulley are:

$$
\begin{aligned}
&F_{ax_k} = Ap_k = \cos\beta\, r_k \int_{\varphi=0}^{\gamma_k} q_k(\varphi)d\varphi; \\
&w(\varphi) = \mu q(\varphi), \quad 0 < \varphi \leq \gamma_k, \\
&T_k = 2r_k^2 \int_{\varphi=0}^{\gamma_k} w(\varphi)d\varphi, \qquad k = p,s.
\end{aligned}
\tag{5.8}
$$

For a detailed analysis of the interactions between the belt and the pulley one would have to specify the relations between $w(\varphi)$ and $q(\varphi)$ in detail (see for instance Wang, 1991). However, the only result of interest here is the minimum pressure p_{min} that is required to prevent slip of the belt with respect to the pulley for a given torque T. For this pressure the belt is about to slip and, using a Coulomb friction model, the friction force $w(\varphi)$ is equal to $\mu q(\varphi)$ for all values of φ between 0 and γ_k. The Coulomb friction coefficient μ is assumed to be constant and substitution of:

$$
w(\varphi) = \mu q(\varphi), \qquad 0 < \varphi \leq \gamma_k, \tag{5.9}
$$

into Equation 5.8 results in:

$$
p_{k,\min} = \frac{\cos\beta\, T_k}{2\mu A\, r_k} \qquad k = p,s. \tag{5.10}
$$

Substitution of T_k yields $p_{k,min}$. Since a safety margin ('safe' > 1) is used in practice, the expression becomes:

$$
p_k = c_{safe} \frac{\cos\beta\, T_k}{2\mu A\, r_k}. \tag{5.11}
$$

For CVT pressure control normally a safety margin of $c_{safe} = 1.3$ is used. The safety margin depends on the designers judgement and the expected torsional vibrations.

5.3. Experiments and physical analysis

Dynamics of the hydraulic and mechanical components have not been taken into account in the models of the previous section. In order to obtain control laws for the clamping pressures and flow rates, the dynamic behaviour of the CVT with its hydraulic circuit for the hybrid transmission is analyzed. The main purpose is to obtain dynamic models which are suitable for control design. These models are obtained by a combination of experiments and physical modelling.

5.3.1. Hydraulics for the hybrid transmission

Since high drive line efficiency is one of the main objectives, special consideration has been given to the high pressure hydraulic circuit layout. Pumping losses are minimized by using a high pressure pump that delivers a moderate oil flow while short term high flow rates are delivered by an accumulator. The schematic diagram in Figure 5.8 contains only the most relevant components of the hydraulic circuit.

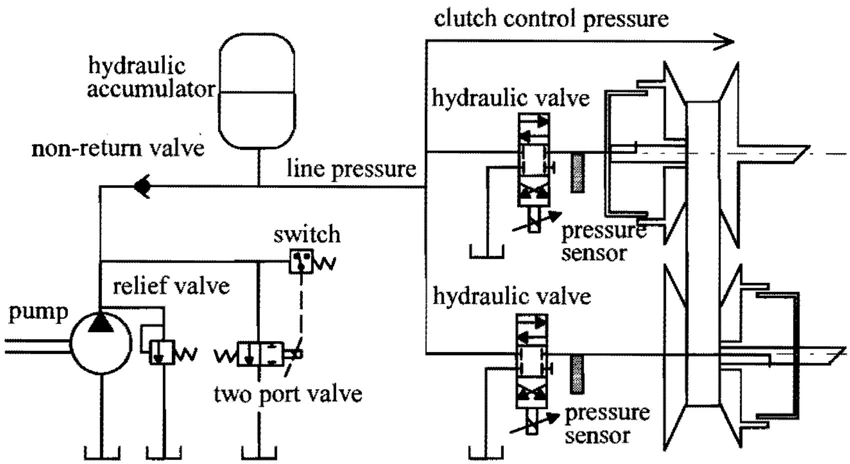

Figure 5.8. Main components of the hydraulic circuit for the CVT in the hybrid drive line.

The accumulator is charged by the pump flow. The circuit is controlled by a switch in combination with the two port valve to control the pump flow. When a pre-determined upper pressure limit is reached, the two port valve is opened and the pump flow is released into the tank. This is a standard application of a circuit that must maintain an operating pressure at the valves (Pinches and Ashby, 1988). The accumulator eliminates small pressure fluctuations. However, due to the on/off nature of the pump, the average pressure level is not constant but varies slowly. A relief valve is employed as a safety valve to protect the pump and the hydraulic circuit. Lubricating and cooling oil for the CVT, gears and clutches is delivered by a separate low pressure hydraulic pump.

5.3.2. Experiments

To arrive at a dynamic model of the hydraulic system, experiments were carried out on a test-rig to measure the CVT response (Section 4.2). Step functions were used for the inputs u_p and u_s of the servo-valves in the primary, respectively the secondary pulley, during the initial experiments (Spijker, 1993b). It took about one second for these pressures to monotonically converge to their final values. These final values depended on the CVT ratio and also on the temperature of the hydraulic fluid. Furthermore, variations in the input u_p of the valve of the primary pulley resulted in variations in the pressure p_s at secondary pulley and vice versa, except for zero rotational pulley speeds. In the latter case the pressure responses of the pulleys were almost independent of each other.

In a second series of experiments, the transfer functions from the input signal u_p of the valve at the primary pulley to the pressure p_p, and on the pressure p_s at the secondary pulley were obtained. A schematic diagram of the CVT with the measured quantities is shown in Figure 5.9.

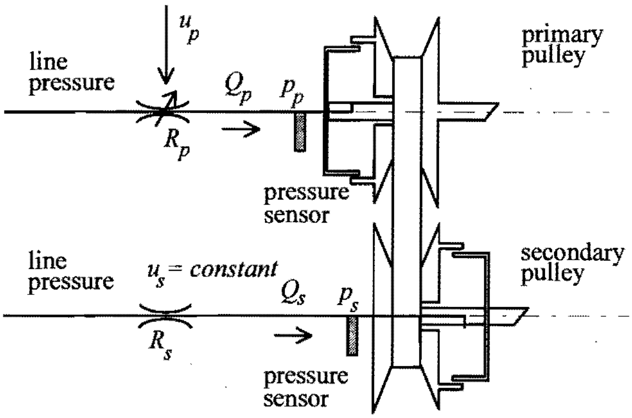

Figure 5.9. Measurement of the open-loop pressure response of the CVT hydraulic system.

The two variable restrictions R_p and R_s represent the proportional hydraulic valves (Viersma, 1980). Only restriction R_p is modulated by the signal u_p. The bandwidth of these proportional valves is sufficiently high (> 100 Hz) to permit this simplification. The quantities Q_p and Q_s represent the oil flows in the pipes from valve to oil chamber. Because the CVT is symmetrical both pulley models are identical. The hydraulic line pressure is assumed to be constant.

In the transmission, the CVT pulleys rotate at approximately 2000 rpm and operate with a pressure ranging from 5 bar up to 50 bar, and a CVT ratio which ranges from low ($i = 0.445$) to high ($i = 2.25$). The following operating conditions were selected during the experiments:

- Rotational speeds of approximately 700 rpm were used. This is below the nominal operating speed but guarantees save test-rig operation.
- An average pulley pressure of 10 bar.
- A CVT ratio of $i = 1$.

Because of small oil leakages, small positive values for u_p and u_s were required to obtain a constant 10 bar pressure. This was realized by applying constant signals u_p and u_s to the valves. A white noise signal was added to u_p. The pressures p_p and p_s of both pulleys were measured. The pressure signal p_p was characterized by a mean value of 10 bar and a variance of 2 bar. A Fast Fourier Transform (FFT) of the measured pulley pressures yields the open-loop pressure transfer functions from valve signal to pulley pressure.

$$H_1(s) = \frac{p_p(s)}{u_p(s)}, \quad H_2(s) = \frac{p_s(s)}{u_p(s)}, \tag{5.12}$$

where the variable s is the frequency in the Laplace domain.

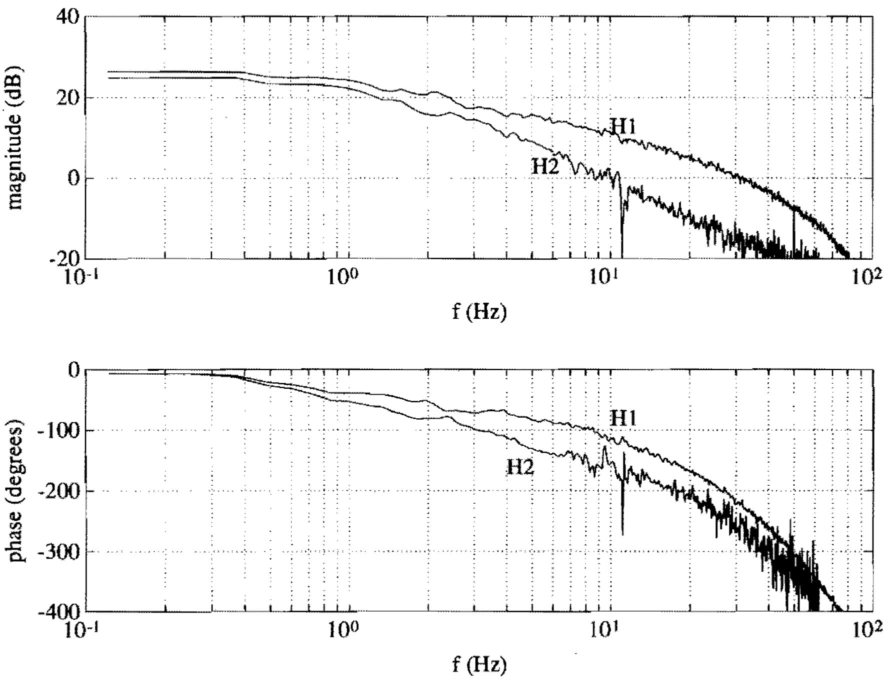

Figure 5.10. Bode plots of the transfer functions of the valve signal u_p to the pulley pressures p_p (H_1) and p_s (H_2).

The amplitude and phase of these transfer functions are shown in Figure 5.10. The CVT is symmetrical, and consequently, the transfer functions from secondary valve u_s to the pressures p_p and p_s are also known. Several observations can be made from these Bode plots. In the frequency range of interest, i.e. the range from 1 up to 20 Hz, the pressure responses for both pulleys show a decay of 20 dB/decade. The transfer functions have a small difference in amplitude in the lower frequency range (approximately 3 dB) while this difference increases to 15 dB at 20 Hz. This difference is probably caused by friction between V-belt and pulleys, since the friction tends to reduce the secondary pulley sheave movements. The 20 dB/decade decay can be modelled as a first order response. The phase lag of a first order system response equals 45° at the -3 dB value (or bandwidth) of the system. In this case, the phase plot shows a phase lag of 45° at 1.5 Hz. Hence, an open-loop bandwidth of 1.5 Hz is assumed for this first order pressure response.

The rotational pulley speed (700 rpm equals 11 rotations per second) can be noticed in the transfer function of H_2, i.e. the noise at 11 Hz. The pressure variations caused by the rotating pulleys are not correlated to the input signal and appear as noise in the transfer function.

The results of the two sets of experiments of this section, i.e. the step response and the measured transfer functions, are summarized below:

- The pressure response is independent of the rotational pulley speeds, with zero speed as the only exception.
- The open-loop pressure response can be modelled as a linear first order response and has a bandwidth of 1.5 Hz.
- The steady state gain depends on the pressure level and the temperature of the hydraulic fluid.
- The coupling between the pressure responses of both pulleys is small in the frequency range from 2 to 20 Hz. This indicates that the coupling between the pulley responses can be neglected.

Based on these response measurements a simple linear dynamic model is proposed to describe the pressure response of the hydraulic system of Figure 5.9. This simple first order model for the pressure response is given by:

$$\dot{p}_k = -a_p p_k + b_p u_k, \qquad a_p, b_p > 0 \text{ and } k = p,s. \tag{5.13}$$

In Equation 5.13, the variable p_k represents the pressure at the pulley and u_k represents the input signal for that particular pulley. This pressure model is valid for pressure variations at a given operating point. The pulley pressures are considered to be independent of each other. Therefore, only one input is required for this model.

5.3.3. Dynamic CVT control models

The pressure response model described above is only valid in a specific operating point. In order to analyze the applicability of the pressure response for the pulley sheave velocity model, a physical model is derived. For this application the oil flows are relevant and the nonlinear valve characteristic must be considered. The model consists of a variable restriction R_k representing the oil valve and a compliance C which represents the combined compliance of the hydraulic fluid and the oil chamber. The oil leakage is modelled by a restriction R_{leak}. The mass of the variable pulley sheave is neglected. The linearized model of a hydraulic cylinder of the CVT is shown in Figure 5.11. The numerical values of the parameters C, R_k and R_{leak} can be obtained from the physical parameters of the system. The combined compliance C is dominated by the compliance of the mechanical structure. The compliance of the hydraulic fluid can be neglected and, hence, the ratio dependence of the oil volume can be neglected. Therefore, the compliance is independent of the CVT ratio. The value R_k of the proportional valve depends strongly on the operating conditions of the valve. The parameter R_k was tuned to obtain a simulated pressure response that corresponds closely to the measured

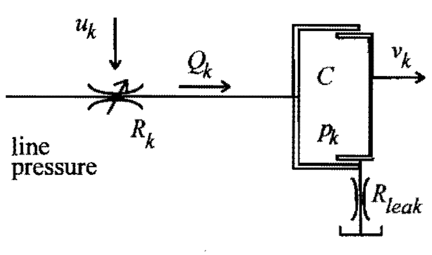

Figure 5.11. A linear model of one of the CVT's hydraulic cylinders.

response. The input signal u_k is proportional to the valve opening, linearized in the given operating point. The simulated transfer function is shown in Figure 5.12. For comparison, the measured transfer function H_1 is shown as well.

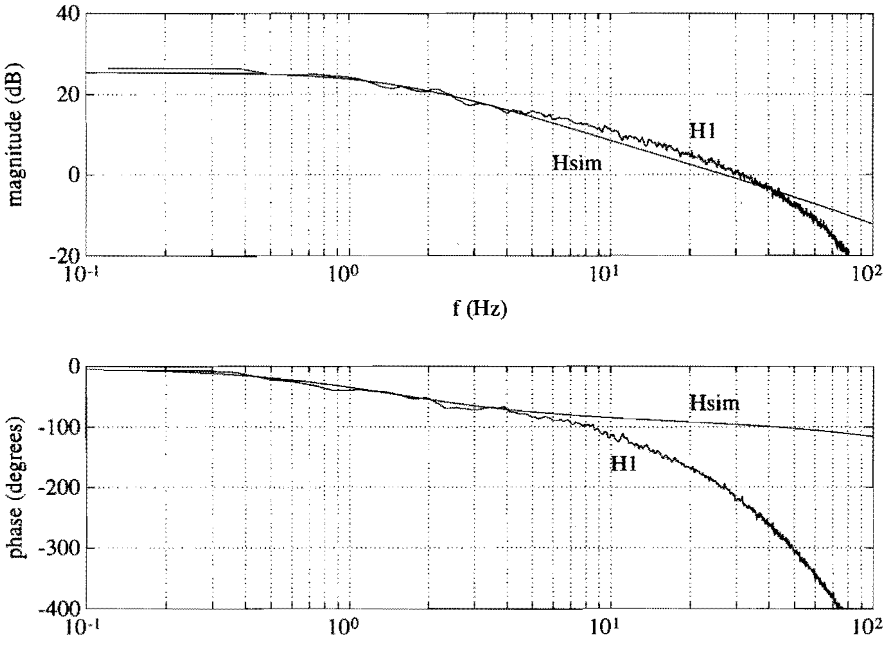

Figure 5.12. Measured and simulated pulley pressure transfer functions.

The pressure response depends strongly on the operating conditions, i.e. the pressure level and the oil temperature. The magnitude of the measured transfer function is approximated rather well and the phase lag is accurately modelled for the lower frequency range ($<$ 10 Hz). The effects of the phase lag at the higher frequency range ($>$ 10 Hz) are considered during the experimental verification. It is concluded that the first order pressure response can only be used at a given operating point. New operating conditions require new parameters for the model.

As a pulley sheave velocity is introduced by a pressure difference over the hydraulic cylinders, the transfer function of the pressure response can be used for the pulley sheave velocity model. In order to derive a mathematical model for the pulley sheave response, the following assumptions are made:

- The mass of the pulley sheaves and the V-belt can be neglected.
- Sheave velocity fluctuations of one pulley due to pressure fluctuations at the other pulley, and vice versa, are 'dampened' by friction between pulleys and V-belt and can be neglected. Consequently, the axial sheave velocity of one pulley can be controlled independently from the pressure in the other pulley.
- A pressure increase at a pulley sheave immediately causes an axial shift of the sheave.

- The oil leakage in the hydraulic cylinders is very small and can be neglected.
- The dynamic response of the pulley sheave velocity is independent of the CVT ratio.
- The pulley sheave velocity response due to a flow variation at the corresponding valve is directly related to the pressure response and, hence, has a similar bandwidth as the pressure response.
- A first order pulley sheave velocity model can be used for all operating conditions.

Therefore, a first order model for the open-loop pulley sheave velocity response is proposed:

$$\dot{v}_k = -a_q v_k + b_q Q_k, \qquad a_q, b_q > 0 \text{ and } k = p,s. \tag{5.14}$$

In this equation, the variable v_k represents the sheave velocity and Q_k represents the oil flow through the valve. For the pulley sheave velocity response the coupling between the pulleys is neglected, hence, only one input is required for this velocity model. The oil flow Q_k is the input variable of the model of Equation 5.14. Nevertheless, the valve opening is the physical quantity which must be controlled. In order to obtain the proper valve opening, the valve is modelled as a nonlinear static relation between the oil flow, the pressure difference Δp over the valve and the signal u, which is linear proportional to the valve opening (Subsection 4.2.5). The valve may, therefore, be represented by the following equation:

$$Q_k = V_q(\Delta p, u_k). \tag{5.15}$$

Because the pulley pressures can be measured, and, under the assumption that the pulley pressures vary slowly during normal operation, this valve characteristic can be used to control the valve opening.

5.4. CVT control

This section describes the design of controllers for the CVT. The control philosophy is discussed and the required CVT responses for use in the hybrid transmission are specified. The clamping pressure controller and the pulley sheave velocity controller are given. These controllers are integrated and the structure of the CVT rate of ratio change controller is presented. Finally, a CVT ratio controller is presented which is to be used during mode shifts of the transmission.

5.4.1. Desired CVT rate of ratio change response

The CVT, being the main component in the drive line, will dominate the dynamic behaviour of the entire drive line. Due to the low closed loop bandwidth of the drive line, a CVT rate of ratio change control with a large bandwidth will allow a separation of the drive line control and the CVT control. A bandwidth of 2.5 Hz for the drive line torque is considered to be sufficient (Section 2.5 and Subsection 6.6.6). A bandwidth of approximately 10 times the closed-loop drive line bandwidth, i.e. a rate of CVT ratio change bandwidth of 20 Hz, is considered to be sufficient to accomplish this separation.

The CVT ratio change bandwidth is defined as the frequency at which the amplitude of the realized rate of change is $\frac{1}{2}\sqrt{2}$ of the amplitude of the desired rate of change.

The required accuracy for the rate of ratio change can be derived from the required drive line torque accuracy. The relation between drive line torque and rate of ratio change can be obtained with the drive line control model introduced in Section 3.5. In this case, a constant output torque is assumed, and by using Equations 3.20 and 3.21 the relation for the rate of change can be approximated by:

$$T_{out} = \dot{\varphi}_{flw}\left(\frac{i^2}{\eta J_{flw}} + \frac{1}{J_{veh}}\right)^{-1}\frac{di}{dt}. \tag{5.16}$$

The specific operating conditions for the CVT in the hybrid transmission are summarized in Table 5.1. Substitution of these operating conditions in Equation 5.16 and assuming an order of magnitude of 5 Nm for the output shaft torque error yields an error of 0.02 s^{-1} for the rate of ratio change.

Table 5.1. Typical operating conditions.

rotational speed	$\dot{\varphi}_{flw} = 200$ rad/sec
ratio	$i = 1$
efficiency	$\eta = 0.95$
output shaft torque error	$T_{out} = 5$ Nm

The 20 Hz bandwidth for the CVT control must be realized by a pulley sheave velocity with a 20 Hz bandwidth. The corresponding clamping pressure must be applied to prevent belt slip. The bandwidth of the controlled clamping pressure must match the bandwidth of the rate of CVT ratio change, i.e. the ability to generate a torque in the transmission. Consequently, a bandwidth of 20 Hz for both clamping force and pulley sheave velocity control is chosen.

5.4.2. Mode shifts and the desired CVT ratio response

During shifts, from one operating mode of the hybrid drive line to another, control of the CVT ratio is required. During these mode shifts certain clutches have to be opened while others have to be closed. In order to obtain smooth and fast shifts, the ratio is controlled to synchronize rotational speeds of the coupling parts. This minimizes shocks, wear, and losses. These synchronising shifts are relatively small changes of the ratio. They have to be fast, within 0.5 seconds, and should be performed accurately (van Nijnatten, 1986).

5.4.3. Control philosophy

The expression 'CVT ratio change control' is used in this thesis for the control strategy of the entire CVT. The term 'axial pulley sheave velocity control' is used only when the control of the driving pulley is meant. This pulley sheave velocity is realized by flow steering, i.e. the desired oil flow is converted into an appropriate valve opening.

During CVT ratio change control, the driven pulley is under pressure control while the driving pulley is under flow steering. This is expressed by the following switching logic:

```
if (rate of CVT ratio change ≥ 0) then
        pressure control on secondary pulley
        if (primary pulley pressure ≥ necessary pulley pressure) then
                flow steering on primary pulley
        else    pressure control on primary pulley
else
        pressure control on primary pulley
        if (secondary pulley pressure ≥ necessary pulley pressure) then
                flow steering on secondary pulley
        else    pressure control on secondary pulley
end
```

The switching logic also includes monitoring of the driving pulley pressure, which is redundant during normal operation. As stated before, this concept prevents belt slip under all circumstances. The required bandwidth for both clamping pressure and pulley sheave velocity must be maintained under all operating conditions. These operating conditions are determined by the hydraulic fluid viscosity which is temperature dependent, the oil flow rates, and the pressure levels. The control of the CVT ratio change in the 'hybrid-mode' of the vehicle demands a low average flow rate, which must be applied to the primary pulley during a positive rate of ratio change and to the secondary pulley during a negative rate of ratio change.

In order to realize the required bandwidth of the clamping pressure, an adaptive controller is designed. This pressure controller is adapted on-line after comparison of the desired pressure response and the measured response. This allows the pressure controller to operate independently of the CVT ratio, the required oil flows, the oil temperature, and the pressure levels. Hence, it is independent of the CVT operating conditions.

The axial pulley sheave velocity is controlled by a linear control law. The control law specifies the required oil flow through the valve and yields a fast closed loop pulley sheave velocity controller. However, neither the actual axial pulley sheave velocity nor the flow through the valve can be measured. An adaptive control strategy, such as used for the pressure controller can, therefore, not be used. Hence, a somewhat different approach is proposed. The output of interest is the rate of CVT ratio change and this quantity is measured with a moderate accuracy. The obtained signal has a considerable noise level and low bandwidth (< 10 Hz.). In order to recover the actual axial pulley sheave velocity, the measured rate of change is combined with a dynamic sheave velocity model and integrated in a Kalman filter. This Kalman filter than yields a low noise estimate of the realized pulley sheave velocity. A significant uncertainty, which remains in this pulley sheave control concept, is the oil flow steering through the valve. The specified valve characteristic has a limited accuracy (5-10% error). Therefore, an adaptation of the flow steering is proposed to compensate for this valve uncertainty.

This adaptation is a rather slow process which guarantees that, eventually, the desired flow will be realized smoothly.

5.4.4. Pressure control

As discussed in Section 5.3, the driven pulley pressure p_2 is assumed to relate to the corresponding valve as expressed by:

$$\dot{p}_2 = -a_p p_2 + b_p u_2, \qquad a_p, b_p > 0. \tag{5.17}$$

The desired value $p_{2,set}$ of this pressure follows from Equation 5.11, where the torque T_2 and radius r_2 refer to this driven pulley. The proposed linear control law is:

$$u_2 = -k_p p_2 + m_p p_{2,set}. \tag{5.18}$$

In order to obtain appropriate behaviour under all operating conditions, i.e. the model parameters a_p and b_p depend on the operating conditions, the control parameters k_p and m_p are adapted on-line. To find suitable adaptation laws for k_p and m_p, such that stability is guaranteed, an appropriate Lyapunov function V is chosen (Åström and Wittenmark, 1989; Slotine and Li, 1991).

The desired pressure behaviour is specified by means of a reference model. Here a reference model of the same order and structure as the model in Equation 5.17 is used:

$$\dot{p}_r = -a_{pr} p_r + b_{pr} p_{2,set}, \qquad a_{pr} > 0, \quad a_{pr} = b_{pr}. \tag{5.19}$$

As the input to the reference model, the desired pressure $p_{2,set}$ is used. If $p_{2,set}$ is constant this guarantees that the reference pressure p_r converges to the desired value of $p_{2,set}$. In the actual implementation of the control law the parameter a_{pr} is chosen such that the bandwidth of the reference system equals 20 Hz. The difference between the reference pressure p_r and the actual pressure p_2 is denoted by e_p, so:

$$e_p = p_r - p_2. \tag{5.20}$$

If e_p converges to zero then p_2 converges to $p_{2,set}$. From Equations 5.17, 5.18 and 5.19 it is easily seen that:

$$\dot{e}_p = -a_{pr} e_p - \bar{a}_p p_2 + \bar{b}_p p_{2,set}, \tag{5.21}$$

where the parameter error coefficients $\bar{a}_p$ and $\bar{b}_p$ given by:

$$\bar{a}_p = a_{pr} - (a_p + b_p k_p); \quad \bar{b}_p = b_{pr} - b_p m_p. \tag{5.22}$$

In order to arrive at a proper adaptation law for the parameters k_p and m_p a candidate Lyapunov function V is defined by:

$$V = \tfrac{1}{2} e_p^2 + \tfrac{1}{2} \alpha \bar{a}_p^2 + \tfrac{1}{2} \beta \bar{b}_p^2, \quad \alpha > 0, \beta > 0, \tag{5.23}$$

which represents an accumulation of the pressure error and the assumed parameter errors. Differentiation of this relation with respect to time yields:

$$\dot{V} = -a_{pr} e_p^2 + \bar{a}_p (\alpha \dot{\bar{a}}_p - e_p p_2) + \bar{b}_p (\beta \dot{\bar{b}}_p + e_p p_{2,set}), \tag{5.24}$$

and therefore $\dot{V} < 0$ for each $e_p \neq 0$ if $\dot{\bar{a}}_p$ and $\dot{\bar{b}}_p$ satisfy:

$$\dot{\tilde{a}}_p = \frac{1}{\alpha} e_p p_2, \quad \dot{\tilde{b}}_p = -\frac{1}{\beta} e_p p_{2,set}. \tag{5.25}$$

If the model parameters a_p and b_p are constant or are slowly varying this results in the following adaptation law for the controller parameters:

$$\dot{k}_p = -\frac{1}{\alpha b_p} e_p p_2, \quad \dot{m}_p = \frac{1}{\beta b_p} e_p p_{2,set}. \tag{5.26}$$

With this adaptation law the equilibrium point $e_p = 0$ is globally asymptotically stable in the sense of Lyapunov (Åström and Wittenmark, 1989; Slotine and Li, 1991). The complete adaptive pressure control system is shown in Figure 5.13.

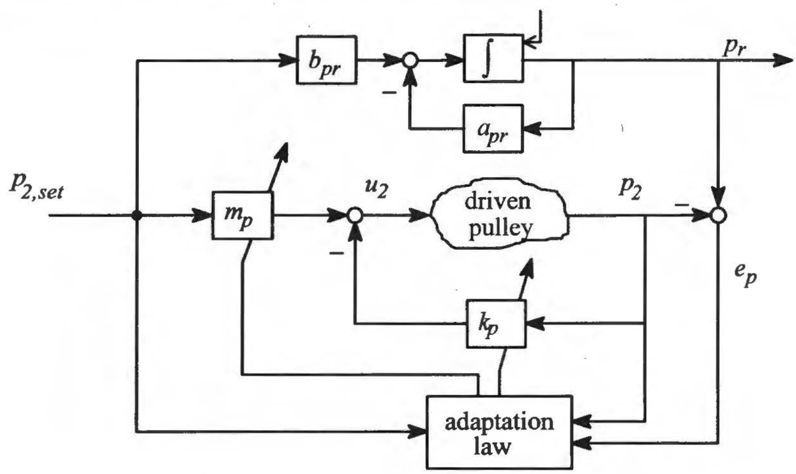

Figure 5.13. Structure of CVT adaptive pressure control.

The given adaptation laws are derived under the assumption that the structure of the model represented by Equation 5.17 is correct. This will not be the case in practice. As a consequence the controller performance can deteriorate. Precautions must be taken to avoid this. One of the major problems associated with adaptive control is parameter drift caused by insufficient information in the measured signal. In such cases, the parameter adaptation mechanism can not identify a correct set of parameters. In order to prevent parameter drift, the adaptation of k_p and m_p must be stopped when no significant information can be extracted from the measured pressure signal. This is the case during constant pressure, causing noise to be a dominant component in the signal. Therefore, the adaptation laws are modified, and a so-called 'dead zone' is included in these algorithms (Åström and Wittenmark, 1989; Slotine and Li, 1991).

$$\begin{aligned} &\text{if } |e_p| > \|\text{noise}\| \\ &\text{then } \dot{k}_p = -\frac{1}{\alpha b_p} e_p p_2; \quad \dot{m}_p = \frac{1}{\beta b_p} e_p p_{2,set} \\ &\text{else } \dot{k}_p = 0; \quad \dot{m}_p = 0. \end{aligned} \tag{5.27}$$

In order to implement the dead zone, an error bound must be defined. In this case twice the absolute error of the pressure sensor is used. This bound is based on experimental results, it proved to be very effective.

5.4.5. Pulley sheave velocity control

The rate of ratio change has to be a smooth function of time. Corruption with measurement noise of the input signal which must realize the desired rate of ratio change has to be prevented. Research by Elzinga (1987), Stubbe (1988), and Kok (1989) demonstrated this effect. They tried to control the rate of ratio change by simultaneous control of the pressures at both pulleys. The effect of measurement noise in the rate of ratio change limited the accuracy. Besides that, the complexity of the clamping pressure control algorithm was a serious problem. To avoid such algorithms, steering of the oil flow instead of the pressure is used. A required rate of ratio change is translated into a desired pulley sheave velocity and an oil flow is applied to the driving pulley. In order to reduce the noise of the measured rate of ratio change, a Kalman filter is employed. Furthermore, adaptive steering of the flow valve is introduced to minimize the flow error.

The driving pulley sheave velocity v_1 is related to the oil flow Q_1 through the valve by:

$$\dot{v}_1 = -a_q v_1 + b_q Q_1, \qquad a_q, b_q > 0. \tag{5.28}$$

After identifying the driving pulley as either the actual primary or secondary pulley, the desired velocity $v_{1,set}$ is obtained from Equation 5.3. For velocity control a simple lineair control law is proposed:

$$Q_1 = -k_q v_1 + m_q v_{1,set}. \tag{5.29}$$

The parameters k_q and m_q are used to obtain the desired closed-loop bandwidth of 20 Hz. The input Q represents the oil flow at the proportional valve. This flow is applied to the pulley chamber by an appropriate signal to the valve. For this purpose the valve characteristic expressed in Equation 5.15 is rewritten and the following valve control signal u_1 is obtained:

$$u_1 = d_q V_q^{-1}(\Delta p, Q_1). \tag{5.30}$$

Because the effects of the nonlinear valve characteristic, the temperature dependence of the hydraulic fluid and the neglected oil leakage flow are not known quantitatively, an adaptive parameter d_q must guarantee accurate steering of the oil flow. It is noted that $d_q = 1$ is used in the case that $u_1 = V_q^{-1}(\Delta p, Q_1)$ is an exact representation of the inverse valve characteristics. In order to obtain a suitable value for d_q as well as to guarantee stability of the combined feedback law and parameter adaptation, a reference model is defined. This reference model has the same structure as the velocity model in Equation 5.28 and is given by:.

$$\dot{v}_r = -a_{qr} v_r + b_{qr} v_{1,set}, \qquad a_{qr} > 0, \quad a_{qr} = b_{qr}. \tag{5.31}$$

With this reference model and the known model parameters a_q and b_q, the parameters k_q and m_q of the flow control law can be specified:

$$k_q = \frac{a_{qr} - a_q}{b_q}, \quad m_q = \frac{b_{qr}}{b_q}. \tag{5.32}$$

The error e_q between desired pulley velocity v_r and actual velocity v_1 is:

$$e_q = v_r - v_1. \tag{5.33}$$

The following Lyapunov function is proposed:

$$\begin{aligned} &V = \tfrac{1}{2} e_q^2 + \tfrac{1}{2} \gamma \bar{b}_q^2, \\ &with: \bar{b}_q = b_{qr} - b_q m_q (d_q V_q^{-1} V_q). \end{aligned} \tag{5.34}$$

This Lyapunov function contains the velocity error e_q and the parameter error $\bar{b}_q$. The compensation of the valve characteristics is included in this Lyapunov function by the factor $(d_q V_q^{-1} V_q)$. Differentiation of Equation 5.34 with respect to time and substitution of the Equations 5.28, 5.29, 5.31, and 5.33, yields the following expression for the time derivative of the Lyapunov function:

$$\dot{V} = -a_q e_q^2 + \bar{b}_q e_q v_{1,set} + \gamma \bar{b}_q \dot{\bar{b}}_q. \tag{5.35}$$

This derivative of the Lyapunov function is negative, for the following adaptation law:

$$\dot{d}_q = \frac{1}{\gamma} e_q v_{1,set}, \qquad \gamma > 0, \tag{5.36}$$

where γ denotes the adaptation speed. Because the adaptation of the parameter d_q should not respond to measurement noise, a low adaptation speed is chosen. The pulley sheave velocity control structure is given in Figure 5.14.

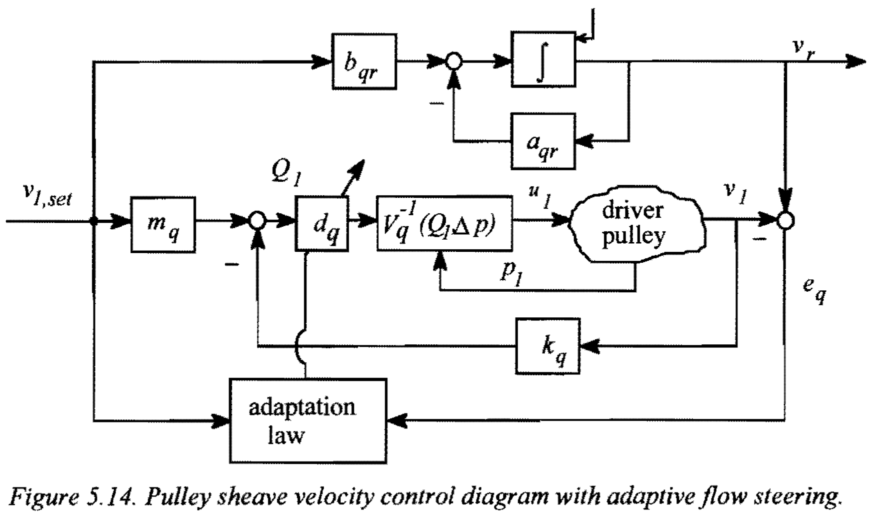

Figure 5.14. Pulley sheave velocity control diagram with adaptive flow steering.

The adaptation law can be simplified. The reference model is only used in the adaptation law of the valve steering, and the adaptation is slow compared to the flow dynamics. This allows the signal v_r to be replaced by the reference input signal $v_{I,set}$. Compared to the adaptation speed, the signal v_r follows $v_{I,set}$ instantaneously. The resulting modification of the adaptation law is given Figure 5.15.

A pulley sheave velocity signal v_I is used in the feedback law and in the adaptation law to form the error signal e_v. This signal can not be measured in a direct manner but must be derived from the CVT ratio change and subsequently substituted in Equation 5.3. The rate of ratio change can be obtained by differentiating the measured CVT ratio (Spijker et al., 1992). In order to reduce the remaining noise, a Kalman filter is used. This filter yields optimal estimates of the oil flow, given the model accuracy and measurement signal accuracy (Grewal and Andrews, 1993). The estimator is designed independently of the control law. This separation has been shown to be valid for linear systems only (Kwakernaak and Sivan, 1972). In this case, where the adaptation is a slow process, it is reasonable to assume that this separation still holds. The estimator uses the measured signal to form an error signal e_v which is used to obtain estimates of v_I with a minimum of noise.

$$\dot{\hat{v}}_I = -\hat{a}_q \hat{v}_I + \hat{b}_q Q_I - l_q e_v, \qquad e_v = v_I - \hat{v}_I. \tag{5.37}$$

The flow Q_I is the input of the model. This flow is realized by means of the known valve characteristic and the adaptation parameter d_q and, hence, it is assumed to be accurately realized. The velocity control diagram, including the estimation, is given Figure 5.15.

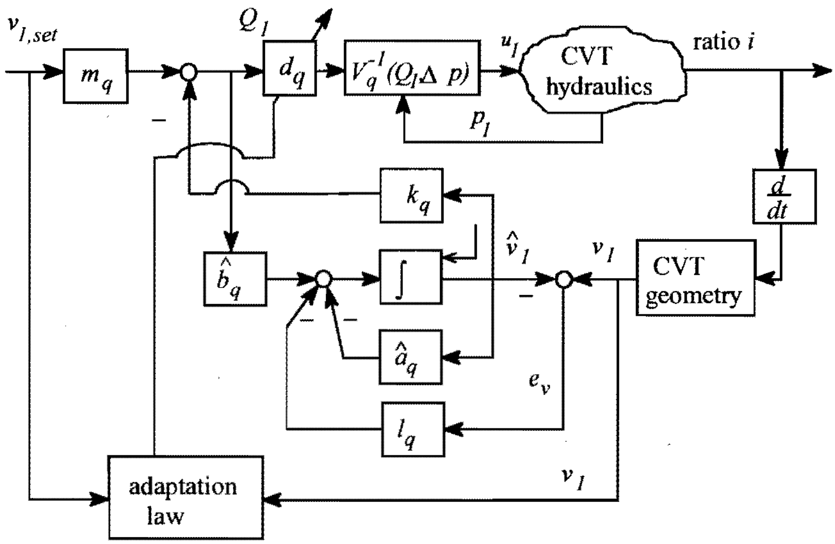

Figure 5.15. Sheave velocity control diagram.

5.4.6. CVT ratio change control

The previously derived pressure and sheave velocity control algorithms can be integrated. During CVT ratio change control, the driven pulley is under pressure control and the driving pulley is under flow steering. After determining which pulley is driving and which is being driven, the proper signals can be directed to the control algorithms and hydraulic valves, as shown in Figure 5.16.

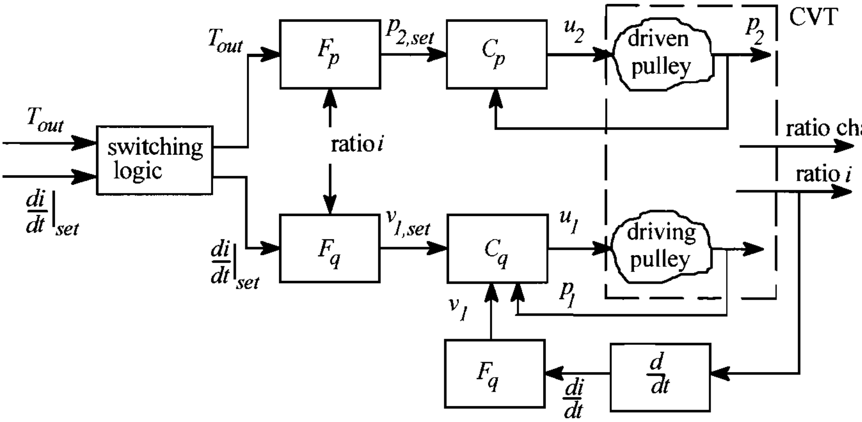

Figure 5.16. CVT ratio change control flow diagram.

As shown in this diagram, the torque T_{out}, consisting of i.c. engine torque and inertia torque, is translated into a minimum pressure level represented by the function F_p, and given in Equation 5.11. This pressure is controlled at the driven pulley by the control law of Equation 5.18 and the adaptation laws of Equation 5.27, summarized by the function C_p. The desired rate of change is used to calculate the required sheave velocity, denoted by F_q, and has been derived in Equation 5.3. The required flow is obtained by using the known hydraulic valve characteristic and is applied to the driving pulley. The flow control laws of Equations 5.29 and 5.36 are summarized in C_q. In order to adjust the oil flow, the obtained rate of ratio change is translated into a pulley sheave velocity by F_q, and used in the adaptation of the flow steering.

5.4.7. Mode shifts and CVT ratio control

The ratio control is used during mode shifts in the hybrid drive line. During these shifts no torque is transferred by the CVT. In this case, the expressions driving and driven pulley do not uniquely identify the pulleys, therefore, the expressions primary and secondary pulley will be used. The previously derived pressure control law can be applied directly to the secondary pulley while for $p_{2,set}$ a minimum operating pressure level is used. The sheave velocity control is applied to the primary pulley. A diagram of this ratio control is shown in Figure 5.17. The CVT operates in a specified operating interval with small flow rates and nearly constant pressures. Because the measurement signals are not persistently exciting (Åström and Wittenmark, 1989), parameter drifting may occur. Therefore, the parameter adaptation is switched off. This is of no consequence for the CVT ratio control. The CVT ratio is the output of interest, hence, small rate of ratio change errors can be tolerated.

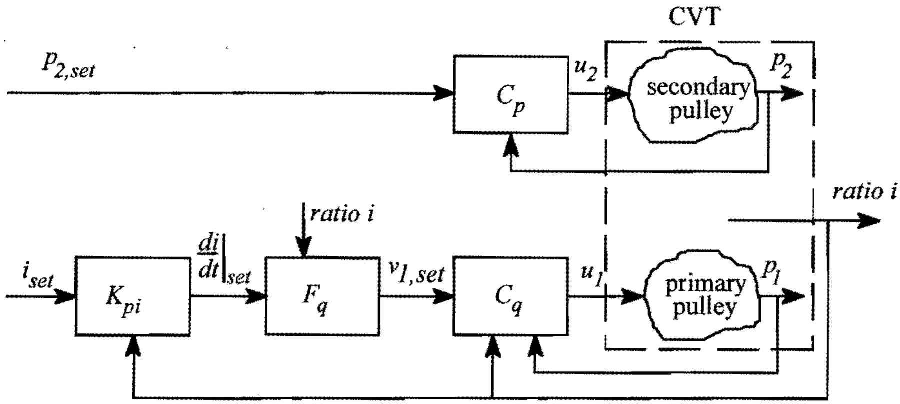

Figure 5.17. CVT ratio control flow diagram.

During mode shifts, only the CVT ratio is of interest, not the exact shifting trajectory. For this type of control problem, a straight forward PD-type control law is sufficient (Slotine and Li, 1991). Hence, a trajectory is obtained by:

$$\frac{di}{dt} = K_{pi}(i_{set} - i) \qquad K_{pi} > 0, \tag{5.38}$$

where K_{pi} is a proportionality constant and used to obtain the desired ratio. For this specific application, the new setpoint should be reached within 0.5 seconds.

5.5. Experimental verification

The experimental verification of the CVT response is focused on the application of the CVT in the hybrid vehicle. First, the response of the clamping pressure is analyzed. This response must be fast and accurate over the entire operating range of the CVT. Second, the CVT response on the desired rate of CVT ratio change is analyzed.

Experimental verification was carried out on the test-rig, which was described in Section 4.2. In order to collect significant measurement results, a proper selection of test signals and operating conditions is rather important. The operating conditions should not only be representative for use in the actual vehicle, but must also allow the evaluation of specific performance characteristics of the CVT.

5.5.1. Selection of test signals

The torque and speed characteristics of the hybrid vehicle determine the rotational speed and torques of the CVT on a test-rig. Additionally, steady state driving at low vehicle speed requires accurate and low output torques. Torques with such low levels are obtained by a small CVT rate of ratio change. Therefore, small rates of ratio change must be achieved with small errors. Additionally, small rates of ratio change allow the observation of nonlinear valve characteristics. Hence, small rates of change are to be used for CVT ratio change control verification.

Measurement of the pressure is carried out by pressure sensors positioned as close as possible to the hydraulic cylinders. These signals can be used directly. A low-pass prefilter with a cut-off frequency of 125 Hz is employed to prevent aliasing during the A/D conversion.

Measurement of the rate of change is more difficult. The signal is derived from the measured CVT ratio by its differentiation with respect to time. This yields a signal which is corrupted by noise. Removing the noise by a low pass filter also removes essential information of the CVT performance, as it only yields the low frequency component of the rate of ratio change (Spijker et al. 1992). Since the rate of change is proportional to the drive line torque, the rate of ratio change can be derived from the measured output torque and rotational speed (Section 3.5, Equations 3.20 and 3.21). Unfortunately, the torque signal also incorporates the drive line dynamics, i.e. the resonance frequency of the drive line. It is measured in the complete drive line system. Therefore, the pressure signals are used to obtain the dynamic rate of CVT ratio change response. The pressure ratio of both pulley pressures determines the response of the variable pulley sheaves. Any increase or decrease of the pulley pressure immediately results in a pulley sheave displacement because of the low pulley sheave masses.

5.5.2. Pressure control

The pressure controller was experimentally verified on the test-rig. The CVT ratio was changed from low to high by steering an oil flow into the primary pulley cylinder while the secondary pulley was under pressure control. Flywheel 2 was accelerated and, consequently, Flywheel 1 was decelerated (see also Figure 4.1). The input signal, i.e. the desired pressure, was a block shaped signal which operates in the pressure range from 15 to 25 bar.

Experimental results of the adaptive pressure control algorithms are shown in Figure 5.18. Shortly after $t = 1$ second, the adaptation algorithms were activated and appropriate parameters were found for the pressure controller. The pressure error between reference model and measured pressure is minimized. The adaptation rate is high. The parameter change is relatively fast when compared to the pressure response. The parameters change significantly when a new operating point is selected. The pressure response strongly depends on the actual pressure level. It is noted that the parameters do not converge to constant values for a constant pressure. This is caused by the CVT ratio dependence of the pressure response. A slow increase of the parameters can be noticed during the CVT ratio change, from $t = 1$ to $t = 14$ seconds. The pressure step response shows a smooth transition from the old pressure level to the new level.

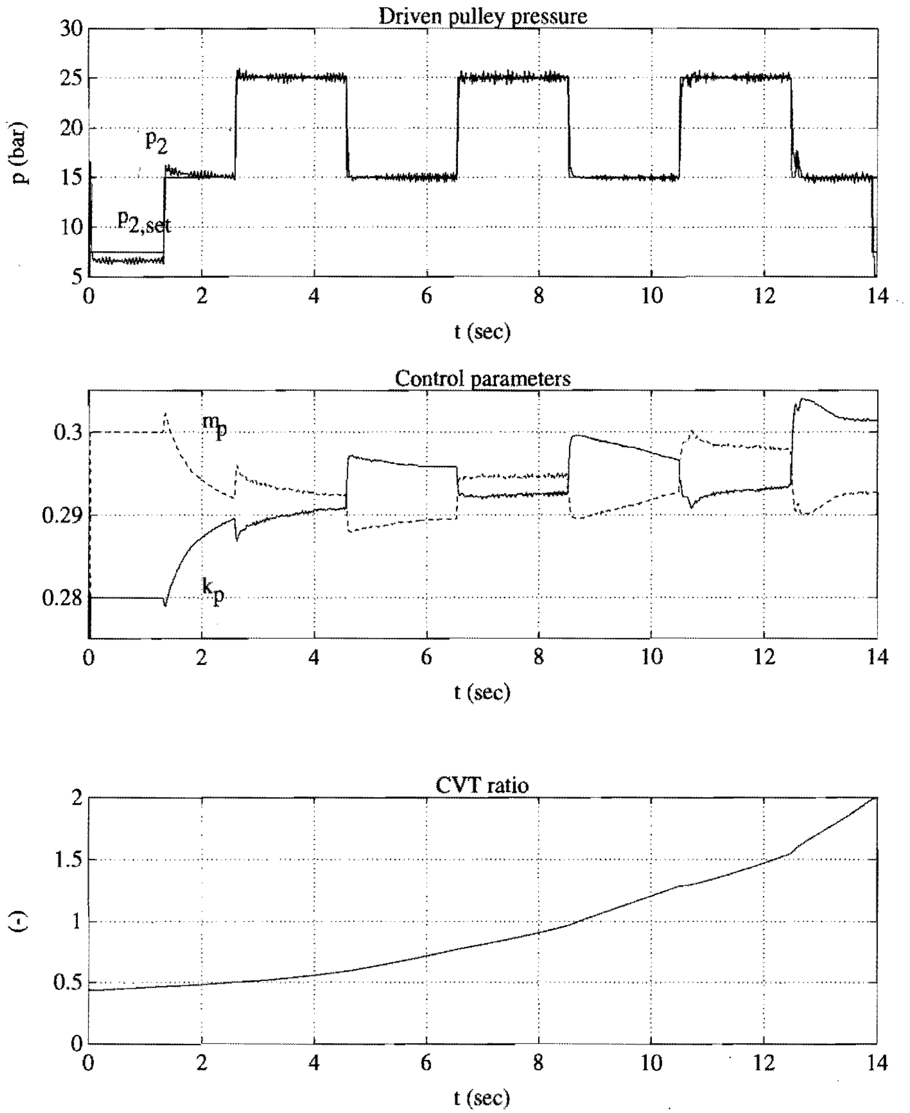

Figure 5.18. Experimental results of the driven pulley pressure response. The adaptation of the controller parameter starts shortly after t = 1 sec.

The pressure response is accurate over the entire operating range. Therefore, the proposed pressure controller suits its purpose well. The pressure response is shown on a magnified time scale in Figure 5.19. The step response does not show the first order response which was assumed earlier in Subsection 5.3.2. This corresponds to the phase lag which was coarsely modelled for the higher frequency range (> 10 Hz in Figure 5.12).

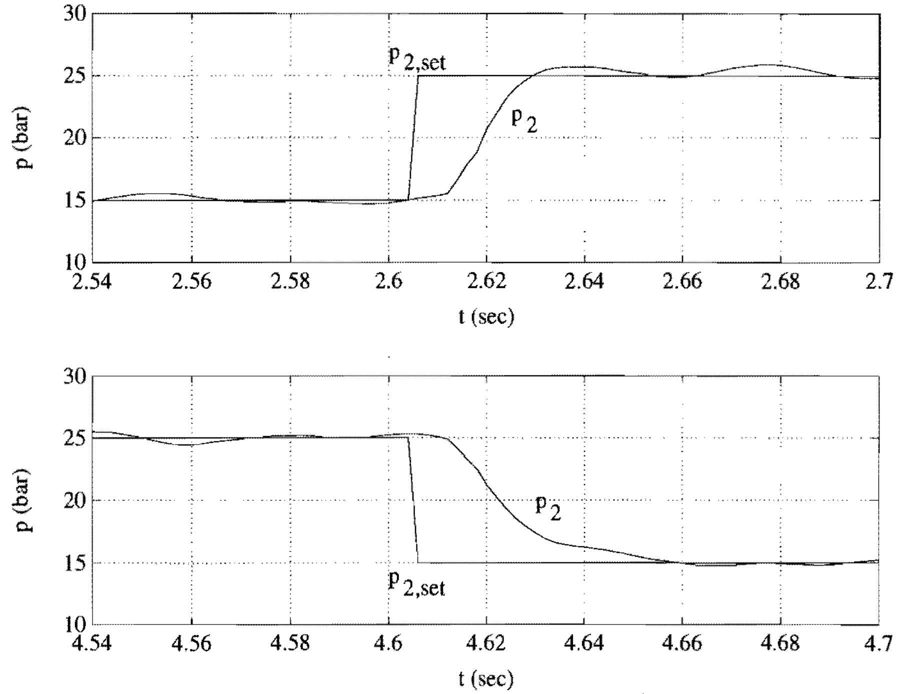

Figure 5.19. Pressure step response on a magnified time scale. Shown is a pressure increase and a pressure decrease.

However, the rise time of the pulley pressure closely approaches the rise time of the reference model and is sufficiently fast (where the rise time is defined as the time required to reach 90% of the target pressure). The pulley pressure has a rise time of approximately 0.02 seconds. The target pressure is reached with a rather small overshoot. The noise or pressure ripple which is visible in Figures 5.18 and 5.19 is thought to correspond to the tilting of the rotating pulleys. The rotating pulleys have a small axial motion which induces small pressure perturbations. Hence, the rotating frequency of the pulleys corresponds to the frequency of the pressure ripple.

5.5.3. Rate of ratio change

A repetitive input signal was chosen for the desired rate of ratio change which allows step response evaluation during a CVT ratio change from low to high. The flywheels, connected through the CVT, were accelerated up to 2000 rpm, followed by a change of the CVT ratio from low to high. During this action the oil flow was directed into the primary pulley, while the secondary pulley was under pressure control. The desired rate of ratio change was the input signal to the controller. The CVT ratio and the rate of ratio change were the measured output signals. The desired rate of change, the resulting rate of change, and the CVT ratio are shown in Figure 5.20.

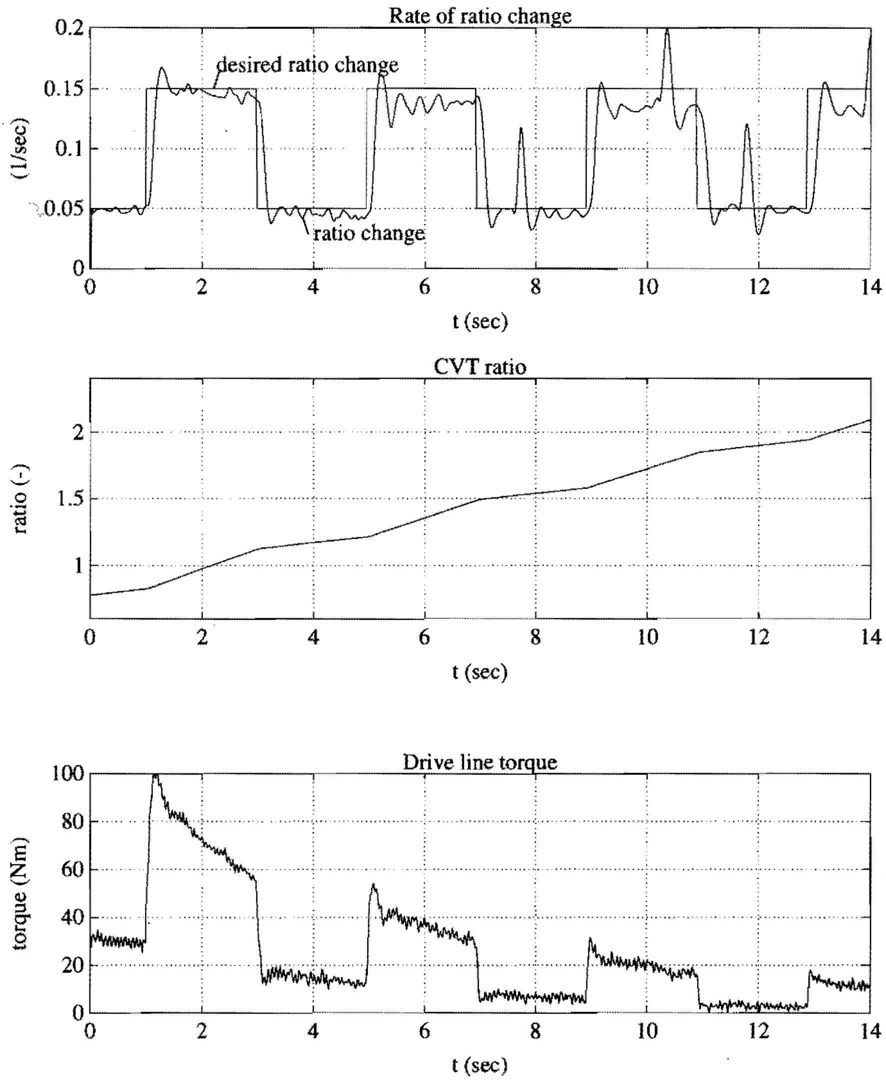

Figure 5.20. The desired (block shaped) and measured rates of ratio change.

The desired rate of ratio change yields a step response at different CVT ratios and is achieved by different flow rates and corresponding valve orifices. The average rate of change of 0.1 s^{-1} allows the entire range of ratios to be covered in 14 seconds. Figure 5.20 shows a rate of change with an error of 0.02 s^{-1} over the entire range. The occasional peaks occurring in the rate of ratio change do not cause peaks in the measured torque. Hence, they are caused by measurement errors and are to be considered as random noise. The adaptation of the flow steering guarantees an accurate response over the entire CVT ratio range.

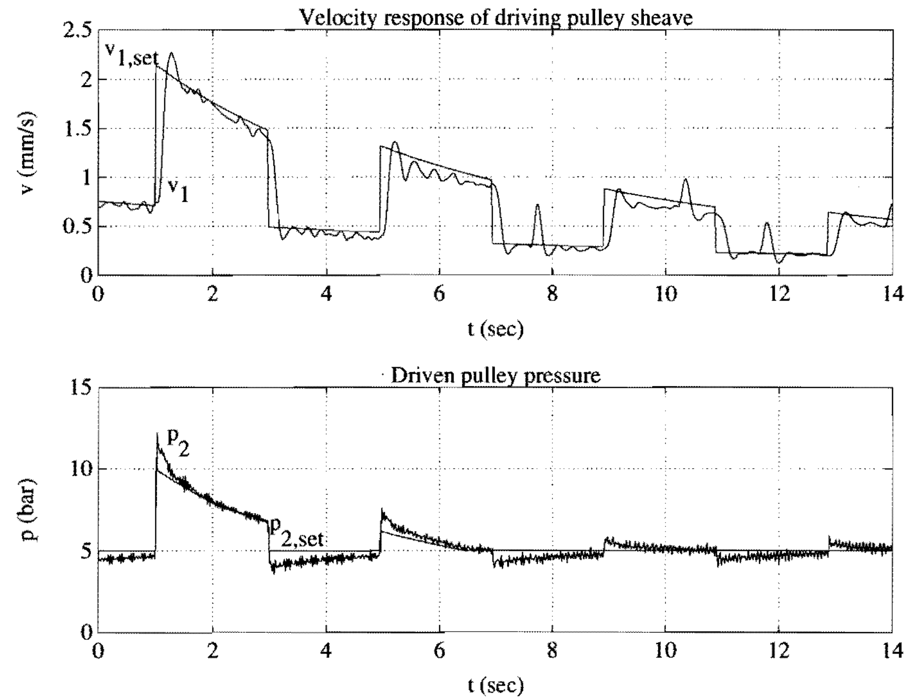

Figure 5.21. The desired and measured velocity response on the driving pulley and the required and measured clamping pressure responses on the driven pulley. These velocities and pressures correspond to the rate of ratio change shown in Figure 5.20.

The measured rate of change has a substantial noise level and contributes to considerable noise in the approximated axial pulley sheave velocity (see Figure 5.21). The minimally required secondary pulley pressure and the actually measured pressure are shown in Figure 5.21. The dynamic pressure response is fast, indicating that the pressure controller functions properly. After a step input of the rate of change, a steady state pressure error of 0.5 bar remains, representing the dead zone which is included in the adaptation laws to prevent parameter drifting.

The pressure ratio is given in Figure 5.22. A step response at a magnified time scale is analyzed. The pressures show a small ripple, which is caused by tilting of the rotating pulleys. The rotational frequency of the pulleys is reflected in the frequencies of the pressure fluctuations. The pressure ratio shows limited overshoot and a small rise time, indicating that the required bandwidth has been obtained. This plot also shows that the clamping pressure on the secondary pulley reaches its new value within 0.03 seconds. Moreover, the observed time delay in the driven pulley pressure response of Figure 5.22 does not deteriorate the controller performance and shows that the pressure controller suits this application.

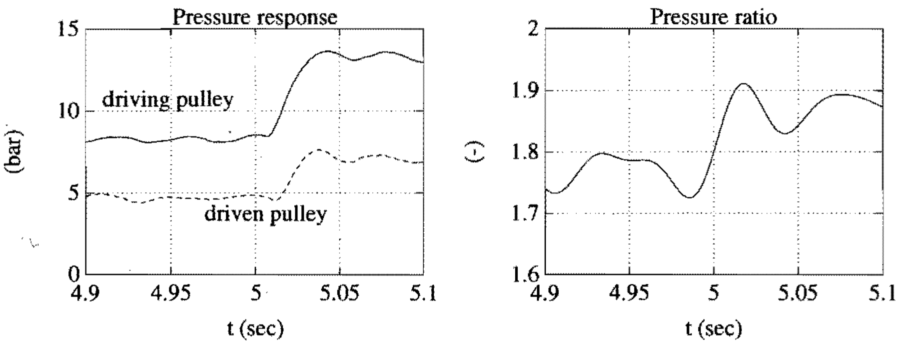

Figure 5.22. The measured pulley pressures and the corresponding pressure ratio due to a step input of the CVT ratio change at t = 5.00 sec.

5.5.4. CVT ratio control for mode shifts

Control of the CVT ratio is used during mode shifts of the drive line. For these shifts only a small change in the ratio has to be accomplished. In order to verify the ratio controller, a shift from CVT ratio $i = 0.50$ to $i = 0.55$ is analyzed. The results, shown in Figure 5.23, indicate that smooth shifts which have an accuracy of $i = 0.003$ can be achieved within 0.4 seconds for upwards shifts and in 1.0 seconds for downward shifts.

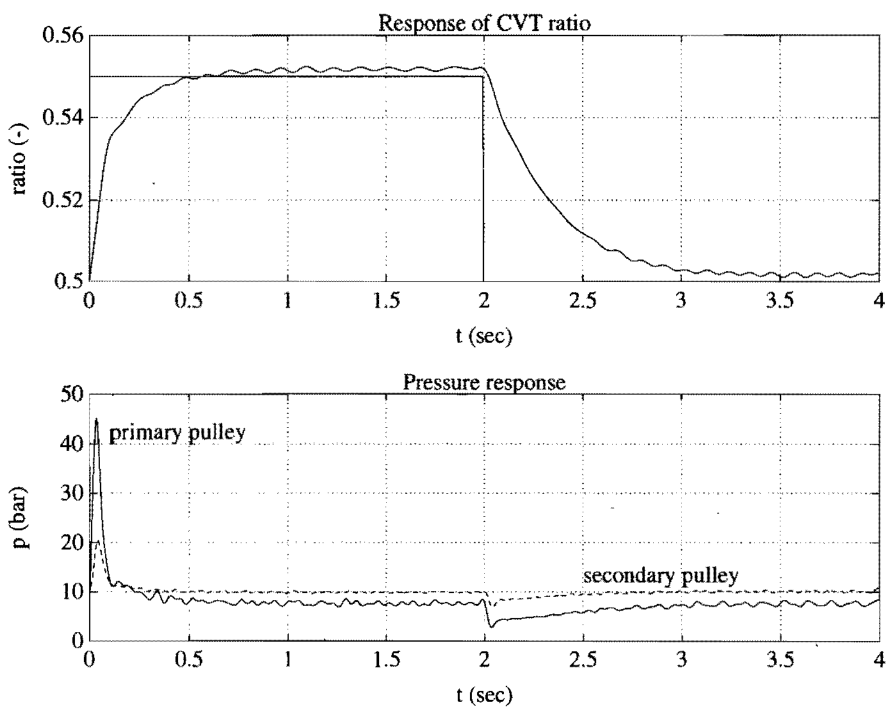

Figure 5.23. Step response of CVT ratio control, to be used during mode shifts.

The pulley pressures show a substantial increase of the driving pulley pressure during the ratio step at t = 0.0 seconds. This is in sharp contrast to the pressures during the ratio step at t = 2.0 seconds. As a result the CVT ratio response is slower. This originates from the specific pressure dependence of the flow through the valve on the primary pulley. Decreasing the response time of the CVT is only possible by increasing the oil flow from the primary pulley. For this, a larger pressure difference over the valve is required. Another option, which decreases the response time during a ratio decrease, is to switch the flow steering from the primary to the secondary pulley. In this case, the pressure difference over the secondary valve is considerable and high flow rates can be achieved. Consequently, the CVT ratio response can be made equally fast for ratio increases and decreases.

The steady state error of $i = 0.003$ corresponds to a rotational speed error of 6 rpm at 2000 rpm shaft speed. These small speed errors are eliminated smoothly by closing the appropriate clutches. Furthermore, by simultaneously closing the clutches and controlling the CVT ratio, a smooth and fast mode shift can be achieved.

5.6. Discussion

The results obtained with the rate of CVT ratio change controller and the CVT ratio controller have been evaluated with respect to operating conditions as can be found in the hybrid vehicle. The specific operating conditions of the hybrid drive line require a different control strategy compared to a CVT in vehicles with conventional drive lines.

During normal operation the required rate of change is within the -1 to 1 s^{-1} range. The error is 0.02 s^{-1} and is independent of the required oil flow and pressures and, hence, independent of the CVT operating conditions. This error in the rate of ratio change is sufficiently small for use in the hybrid drive line. The dynamic response of the CVT is essential for the performance of the drive line controller. The experimental results, given in Figure 5.20, show that both desired rate of ratio change and the corresponding clamping pressure are obtained. A small time delay of 0.01 second can be noticed. Because of the fast rise time of the responses, this time delay is considered to be acceptable.

The pressure controller component in the CVT controller can be modified. The modification should enable the fast pressure increase (20 Hz bandwidth) combined with a slow pressure decrease (0.5 Hz bandwidth). This feature ensures smooth running of the transmission and is used for the experiments in Chapter 7.

The dynamic response of the rate of ratio change is independent of the physical quantities which are being controlled, i.e. pressures and oil flows. This first order response with a 20 Hz bandwidth is independent of transmitted torque, CVT ratio, and rotational speed, i.e. the operating conditions of the CVT. The CVT is reduced to an independent component in the hybrid drive line.

The CVT controller basically consists of two separate single-input single-output (SISO) controllers, one for the pressure and one for the axial pulley sheave velocity. Integration of both controllers in one multiple-input multiple-output (MIMO) controller could be advantageous. It can enhance the response time of the CVT because the interaction between the pulley chambers can be used. For instance, an increase in flow at the driving pulley can be compensated directly at the driven pulley. This type of control strategy might be required when less expensive, pulse width modulated, hydraulic valves with a slower response are to be used.

The CVT in a hybrid drive line continuously changes its transmission ratio. Bonthron (1985) showed that the mechanical efficiency of the CVT is mainly determined by the transmitted torque and the clamping pressures. A change of CVT ratio influences the hydraulic losses but not this mechanical efficiency. Because the pressures are kept on a minimum level, the mechanical efficiency of the CVT in the hybrid drive line is high under all operating conditions.

Both the CVT efficiency and its durability depend on the clamping pressures. In order to obtain a high efficiency the clamping pressures must be low. In the CVT control strategy the clamping pressures are kept on a minimal level. The safe minimal level must guarantee belt operation without slip. Because the CVT torque is known, the required clamping pressures are also known, and, hence belt slip is prevented. This indicates that both requirements can be met, i.e. low pressure levels and maintaining safe pressure levels.

Chapter 6

Drive line controller design

6.1. Introduction

The present chapter discusses the controller for the 'low speed' hybrid mode. Since the resonance frequency is below the closed-loop bandwidth, and frequent engine start-up and stop transients occur in this mode, this is the most crucial mode to control.

The design of the drive line controller is divided into a number of stages. In the first stage the desired drive line response is specified by means of a desired bandwidth and accuracy. The next stage involves a feedback linearization procedure to linearize the input-output relations of the drive line model. The linearization enables the use of a linear controller. The third stage concentrates on the design of the linear control law, and the last stage involves the evaluation of the controller. This is achieved by numerical simulations where the extended drive line simulation model is used. The experimental verification is discussed in Chapter 7.

6.2. Controller design

Closed-loop drive line control is not new in automotive applications. Drive line control originates from areas where steering was insufficient. Examples of such applications are engine-transmission management, anti-lock braking and traction control. Engine-transmission control is used in vehicles equipped with conventional automatic gearboxes. The shifts of these stepped gearboxes are accompanied by a transient change in the output torque of the drive line. Closed-loop control of this torque should enhance passengers comfort levels in these vehicles (Moskwa and Hedrick, 1990). Engine-transmission management of vehicles equipped with CVT's, which have fluent torque shift changes, is aimed at obtaining vehicle driveability and low fuel consumption. For these vehicles output power steering is used. These CVT based drive lines are, up to now, not closed-loop controlled.

The closed-loop output torque controller of the hybrid vehicle has to take into account the special drive line characteristics such as the use of a CVT to accelerate or decelerate the vehicle, and the relatively low torsional resonance frequency (Spijker et al., 1993). Output torque steering can not be used since changing the CVT ratio may lead to excitation of the resonance frequency. The torsional vibration around this frequency would be sustained.

Sweet et al. (1978) proposed an optimal control strategy for the dynamic behaviour of a flywheel-hybrid vehicle drive line. They derived a controller which minimizes drive line losses. In order to obtain such a controller, a considerable effort has to be made. Van Kemenade (1992) showed that a similar controller can be designed for the EUT hybrid drive line. However, in order to minimize the drive line losses a complicated set of nonlinear differential equations has to be solved. The advantages of such an optimal controller do not justify the use of the complex optimisation algorithms which are required for the on-line control in a vehicle. Therefore, this option is not pursued. A different philosophy is followed, which is discussed in the following subsection.

6.2.1. Control philosophy

The mathematical model of the hybrid drive line in the 'low speed' hybrid mode, as derived in Chapter 3, consists of a set of nonlinear (differential) equations:

$$\begin{aligned} \dot{x} &= f(x,w) + g(x,u), \\ y &= h(x), \\ \text{with: } w^T &= \begin{bmatrix} T_{engine} & T_{ext} \end{bmatrix}. \end{aligned} \tag{6.1}$$

The state vector x represents the torsional deformation (x_1), its time derivative (x_2), the CVT ratio (x_3) and the flywheel speed (x_4). The input u represents the rate of CVT ratio change, the output y is the output torque and the disturbance w consists of the known engine torque T_{engine} and the unknown external torque T_{ext}.

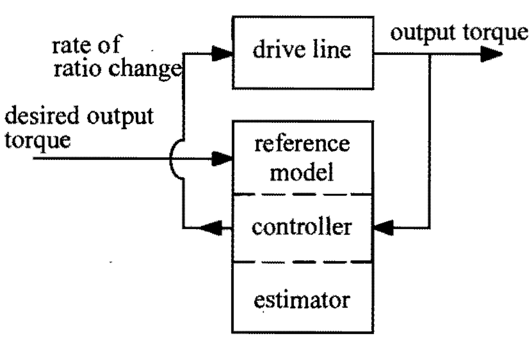

Figure 6.1. Control strategy for the hybrid drive line output torque.

The control strategy which is proposed for the hybrid drive line is shown in Figure 6.1. The desired drive line response is specified by means of a reference model. In the presence of noise and modelling errors, a reference model yields a more robust control system. The controller consists of two parts. The first part is a feedback linearization to compensate for the nonlinearities in the drive line. The second part is a linear control law to reduce the error between the measured output torque and the desired (reference) output torque. The estimator (or observer) provides the states of the system with very low noise levels. It also provides estimates of the state variables which are not measured. The output of the controller is the required rate of ratio change for the CVT. Since the closed-loop bandwidth of the CVT is significantly higher than the closed-loop bandwidth of the drive line, the CVT dynamics are not considered. The CVT controller has been discussed in Section 5.4.

6.2.2. Control objectives

In order to realize the vehicle performance specifications of Section 2.5, these specifications have to be restated in torque response requirements. The specifications are given in terms of desired vehicle and output torque behaviour (Table 6.1).

Table 6.1. Desired vehicle behaviour.

Steady state torque error	10%.
Maximum vehicle acceleration ripple	0.08 ms^{-2},
and equivalent output torque ripple	4 Nm.
Time required to reach 90% of the target value	0.2 - 0.3 s.

These response requirements are specified in the time domain. By using the step response of a linear second order system, the equivalent specifications for the frequency domain (Table 6.2) can easily be obtained (Franklin and Powell, 1980).

Table 6.2. Closed-loop drive line specifications.

Closed loop bandwidth	2.5 Hz.
Relative damping	0.9 .

These specifications in the frequency domain are used for the design of the controller. The accelerator pedal position, as selected by the driver, is considered a measure for the desired output torque. For instance, when the driver presses the pedal 50% down, he requires half of the maximum available output torque. It should be noted that the maximum allowable torque of the transmission depends on the CVT torque capacity. This is caused by the maximum allowable stress in the endless metal strings of the V-belt (Van Doorne's Transmissie). It results in a maximum allowable torque depending on the CVT ratio. Exceeding this maximum torque reduces the CVT life span. This capacity limit should be taken into account when the desired output torque is determined.

6.2.3. Feedback linearization

Feedback linearization involves a transformation of the input u to a new input v, such that the relation between the output y and the new input v is linear. A practical description of this method has been given by Slotine and Li (1991) whereas a more fundamental, mathematically oriented, approach has been presented by Isidori (1989). The basic idea is to differentiate the output equation $y = h(x)$ with respect to time and to replace $\dot{x}$ in the obtained relation by $f(x,w) + g(x,u)$. This results in a relation of the form $\dot{y} = h_1(x,w,u)$. If the right hand side does not explicitly depend on the input u, then the new "output" equation is once more differentiated with respect to time and the system equation is used again to eliminate $\dot{x}$. The process is repeated until an explicit relation between the time derivatives of the output y and the input u is obtained. The number of differentiations, required to obtain this explicit relation, is called the relative degree r of the system. If the relative degree is smaller than the order n of the system then the so-called internal dynamics of order $n-r$ occur.

In the output equations, as given in Section 3.5, the torsional damping of the drive line is taken into account. As a consequence, the relative degree is equal to one. This gives rise to some difficulties in the design of a control law for the hybrid drive line. In practice, the torsional damping of the drive line is small and may be neglected in the relation for the output torque y. The new output equation then becomes:

$$y = k_t x_1, \tag{6.2}$$

where only the torsional stiffness k_t is used and the associated relative degree equals 2. Hence, the order of the associated zero-dynamics is $n-r=4-2=2$. Differentiation of the new output equation and elimination of $\dot{x}$ with the system equation results after some calculations in:

$$\begin{aligned} \dot{y} &= k_t \dot{x}_1, \\ \ddot{y} &= -\alpha + \beta u, \end{aligned} \tag{6.3}$$

where α and β are given by:

$$\alpha = \frac{k_t}{J_{flw}}[(k_t x_1 + b_t x_2)\left(\frac{x_3^2}{\eta} + \frac{J_{flw}}{J_{veh}}\right) + b_{flw} x_3 x_4^2 \ldots$$

$$- x_3 T_{engine} - \frac{b_{veh}}{J_{veh}}(x_3 x_4 - x_2)^2 - \frac{T_{ext}}{J_{veh}}], \tag{6.4}$$

$$\beta = k_t x_4.$$

Therefore, the following transformation of the original input u to a new input v,

$$u = \frac{\alpha + v}{\beta}, \tag{6.5}$$

yields a linear relation between the second time derivative of the output y and the new input v:

$$\ddot{y} = v. \tag{6.6}$$

This result can be written in conventional state space form if new state variables z_1 and z_2 are introduced, defined by the coordinate transformations $z_1 = y = k_t x_1$ and $z_2 = \dot{y} = k_t x_2$ respectively. However, in order to comply with literature these new variables are renamed x_1 and x_2:

$$\begin{aligned} \begin{bmatrix} \dot{x}_1 \\ \dot{x}_2 \end{bmatrix} &= \begin{bmatrix} 0 & 1 \\ 0 & 0 \end{bmatrix} \begin{bmatrix} x_1 \\ x_2 \end{bmatrix} + \begin{bmatrix} 0 \\ 1 \end{bmatrix} v, \\ y &= \begin{bmatrix} 1 & 0 \end{bmatrix} \begin{bmatrix} x_1 \\ x_2 \end{bmatrix}. \end{aligned} \tag{6.7}$$

The associated internal dynamics represent a subsystem that does not contribute to the output y. It is given by:

$$\begin{bmatrix} \dot{x}_3 \\ \dot{x}_4 \end{bmatrix} = \begin{bmatrix} \dfrac{\alpha + v}{\beta} \\ \dfrac{1}{J_{flw}} \left(-b_{flw} x_4^2 - \dfrac{x_3}{\eta}(x_1 + \dfrac{b_t}{k_t} x_2) + T_{engine} \right) \end{bmatrix}. \tag{6.8}$$

Although this subsystem does not contribute to the output y, it must be analyzed in some detail with respect to stability (Slotine and Li, 1991).

The engine torque T_{engine} and the external torque T_{ext} are required in order to obtain the correct transformation. The engine torque can be obtained with a high degree of accuracy. The external torque is unknown and, hence, it can not be used. This torque usually is constant or slowly varying compared to the drive line dynamics. It is neglected in the transformation. Therefore, any errors due to this external torque must be compensated for by the closed loop controller. The transient engine torque can be obtained by using engine rotational speed, inlet manifold pressure, air-fuel ratio, and known engine characteristics (van den Berg, 1993; Dalmayer, 1986; Hendricks and Sörenson, 1990; Schols, 1985; Schols, 1986). Dalmaijer measured the characteristics of the i.c. engine used in the hybrid drive line. The steady state engine torque can be estimated accurately from throttle angle, inlet manifold pressure and engine rotational speed. The transient torque response proved to be complicated and less accurate. Hendricks and Sörenson (1990) presented a relatively simple nonlinear mean engine torque model. Once the parameters of this engine model are obtained from steady state measurements, the model is able to describe the transient torque response. Van den Berg (1993) fitted this nonlinear model on the engine, used in the EUT vehicle, by using the measurements of Dalmaijer. He showed that the dynamic response could be estimated conveniently and accurately with the nonlinear engine model.

6.2.4. Design of controller

A linear control law for the input v can be used to obtain the desired output torque. A reference model is used to specify the desired response. The reference model is defined by:

$$\begin{aligned} \dot{x}_r &= \begin{bmatrix} 0 & 1 \\ -\omega_n^2 & -2\xi\omega_n \end{bmatrix} x_r + \begin{bmatrix} 0 \\ \omega_n^2 \end{bmatrix} r, \\ y_r &= \begin{bmatrix} 1 & 0 \end{bmatrix} x_r . \end{aligned} \tag{6.9}$$

The natural frequency ω_n^2 and the relative damping ξ are used to specify the desired response. The reference input r represents the desired output torque level which is derived from the accelerator position. The following PD-type control law is chosen:

$$v = \dot{x}_{r2} - K_d(x_2 - x_{r2}) - K_p(x_1 - x_{r1}). \tag{6.10}$$

Substitution of Equation 6.10 into the nonlinear feedback law of Equation 6.5 yields a relation for the original input u, i.e. for the rate of change of the CVT ratio (Figure 6.2). The error $e = x_1 - x_{r1}$, satisfies the differential equation:

$$\ddot{e} + K_d\dot{e} + K_p e = 0. \qquad (6.11)$$

The bandwidth of these error dynamics is determined by the controller parameters K_d and K_p. These parameters can be chosen to satisfy additional constraints (Slotine, 1991). For the hybrid drive line, the unmodelled dynamics originating in the engine unit's support, should not be excited (Hendrikx, 1992). The lowest frequency of these unmodelled dynamics is approximately 8 Hz. This constrains the error dynamics bandwidth to approximately 4 Hz.

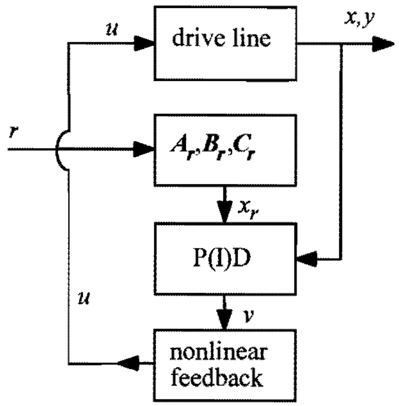

Figure 6.2. Structure of the drive line controller.

In order to prevent overloading of the CVT, a torque limiter must be included in the controller. Therefore, the control law of Equation 6.10 has been extended with an integral term, to be activated only when CVT overloading occurs. The extended law is given in Equation 6.12.

$$v = \begin{cases} \dot{x}_{r2} - K_d\dot{e} - K_p e, & x_{1min} \le x_1 \le x_{1max} \\ \dot{x}_{r2} - K_d\dot{e} - K_p e - K_i \int e\,dt, & x_1 < x_{1min} \vee x_1 > x_{1max} \end{cases} \qquad (6.12)$$

This integral part enables accurate model following of the drive line. The error e between desired torque y_r and realized torque y is eliminated for constant torques. Hence, the output torque is accurately controlled. It should be noted that this controller does only respond to fairly slow disturbances (< 2 Hz). A safety margin is introduced in the CVT clamping pressure (Subsection 5.2.3) in order to deal with higher frequency disturbances.

6.2.5. Stability and robustness

Stability of the linearized subsystem of Equation 6.6 with the control law of Equation 6.10 is guaranteed as long as K_p and K_d are positive. Stability of the original system is guaranteed if the nonlinear internal dynamics subsystem, expressed in Equation 6.8, is stable (Slotine and Li, 1991).

The internal dynamics can be analyzed by considering the zero-dynamics, i.e. the internal dynamics when the output y stays at zero. Then $x_1 = y = 0$ and $x_2 = \dot{y} = 0$ and the zero-dynamics are given by:

$$\begin{bmatrix} \dot{x}_3 \\ \dot{x}_4 \end{bmatrix} = \frac{1}{J_{flw}} \begin{bmatrix} \frac{1}{k_t x_4}\left((b_{flw} - b_{veh})x_3 x_4^2 + x_3 T_{engine} - T_{ext}\right) \\ -b_{flw} x_4^2 + T_{engine} \end{bmatrix}. \tag{6.13}$$

Because the ratio x_3 and the flywheel speed x_4 are always positive, the stability of this system depends entirely on the sign of the top entry between brackets at the right-hand side of the above Equation:

$$(b_{flw} - b_{veh})x_3 x_4^2 + x_3 T_{engine} - T_{ext},$$

$$x_4 > 0, \text{ and } x_{4,\min} < x_4 < x_{4,\max}.$$

In this subsystem the engine torque T_{engine} and the external torque T_{ext} are unknown and, hence, stability cannot be proven. By assuming a zero external torque and zero engine torque, the sign of the above given expression is determined by the sign of:

$$(b_{flw} - b_{veh}).$$

This expression can physically be interpreted as an increase or a decrease in the CVT ratio depending on the air drag of flywheel and vehicle. The air drag of the flywheel is smaller than the vehicle air drag, thus the CVT ratio has to be decreased in order to maintain zero output torque. This decreasing CVT ratio is an inherent property of the drive line and does not imply stability. Therefore, proof of the stability of the internal dynamics is not straightforward. In this thesis it is assumed that the internal dynamics are stable and this assumption is verified by means of numerical simulations.

The ability to cope with modelling errors and disturbances characterizes the robustness of the closed-loop system. The modelling errors result from simplifications, from unmodelled and unknown influences on the system. For instance, a variation in vehicle mass due to a large number of passengers can change the behaviour of the closed-loop system. In the present chapter two extreme conditions are considered. In Subsection 6.3.2 the response to an external torque is analyzed while in Subsection 6.3.3, wheel spin on a slippery road surface is considered. By means of simulations the drive line response is analyzed. Satisfactory drive line behaviour in these cases is considered as an indication of good robustness of the controller.

6.2.6. State estimation

Unfortunately, not all variables used in the feedback and control law can be measured. Therefore, estimates for these variables have to be extracted from measurements. Available signals are the drive line torque, the CVT ratio and the flywheel rotational speed. Measurement noise is reduced by an estimation algorithm which includes a low pass filter for the measured signals (Grewal and Andrews, 1993). Other signals, as for instance rotational pulley speeds or output drive shaft speed, do not contain new or additional information. Consequently, they are not used in the estimation algorithm.

Various techniques for nonlinear state estimation are available. Misawa and Hedrick (1989) gave a comprehensive overview. They denoted that use of these estimators does not give any guarantee for the stability of the controller in a closed-loop. More research is needed on this subject.

Here, a straightforward approach is employed. The estimator is designed independently from the controller (Kwakernaak and Sivan, 1972). Because the system is well defined and most states can be measured, the control model is used in combination with a constant gain feedback matrix. This results in an estimator which reduces measurement noise and provides an estimate for the time derivative of the drive line torque (x_2), which is not measured (see Figure 6.3). In order to obtain state estimates $\hat{x}$, the nonlinear model of Equation 6.1 is used.

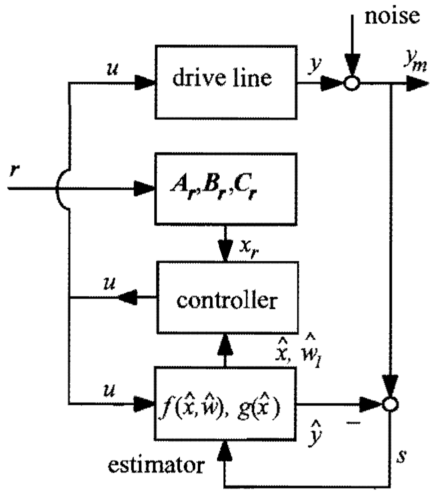

Figure 6.3. Estimation of the drive line state variables.

The estimates are updated in order to minimize the estimation error $s = \hat{y} - y_m$, where $\hat{y}$ is a model based prediction of the output and y_m represents the measured output:

$$\begin{aligned} \dot{\hat{x}} &= f(\hat{x},\hat{w}) + g(\hat{x},u) - \boldsymbol{K}s, \\ \hat{y} &= h(\hat{x}). \end{aligned} \tag{6.14}$$

To obtain the so-called steady-state Kalman gain matrix $\boldsymbol{K}$, a linearized drive line model (Subsection 3.3.2) is used. Estimates of modelling errors and of the maximum external torque T_{ext} are used to obtain an optimal $\boldsymbol{K}$. The output torque is obtained from a torque sensor in the secondary CVT shaft. The flywheel speed and CVT ratio are obtained by rotational speed measurements.

The torque sensor is vulnerable and relatively expensive. An alternative is to use the flywheel speed to estimate the output torque. Any increase or decrease in flywheel speed is due to the combination of drive line torque and engine torque. Since the engine torque can be estimated, the drive line torque can be obtained. However, because of the nonlinear characteristics of the hybrid drive line, estimation of the output torque based on speed measurements only is not straightforward.

Masmoudi and Hedrick (1992) presented a nonlinear shaft torque observer by using a so-called 'sliding mode' observer. Using only the speed measurements they obtained a torque estimate. Their observer is similar to the one presented in this thesis. It consists of a nonlinear drive line model and a constant gain Kalman feedback matrix. The observer is extended by switching terms to obtain the sliding mode observer. Such an observer should be able to provide torque estimates for the hybrid vehicle using speed measurements only.

6.3. Simulations

In order to analyze the properties of the hybrid drive line with the proposed controller, several numerical simulations have been carried out. In these simulations the torque response and the vehicle driveability are analyzed. The simulation model, as presented in Section 3.5, is used to evaluate the controller.

In the simulation model the higher drive line resonance frequencies as well as the tire-road interaction have been incorporated (Custers, 1992). The measured torque, the CVT ratio and the flywheel speed are contaminated by measurement noise and sensor inaccuracies (see Figure 6.4). This is simulated by adding white noise to the signals from the simulation model. The noise has a rms value which corresponds to the measurement errors (cf. Subsection 4.3.2). The friction force between the tires and the road is modelled explicitly in order to simulate driving on a slippery road. The disturbances are the engine torque and an external torque due to hill climbing. The CVT response has been modelled as a first order response with a 20 Hz bandwidth, as proposed in Section 5.6. These models have been implemented in ACSL (1986), a software package for continuous time simulation.

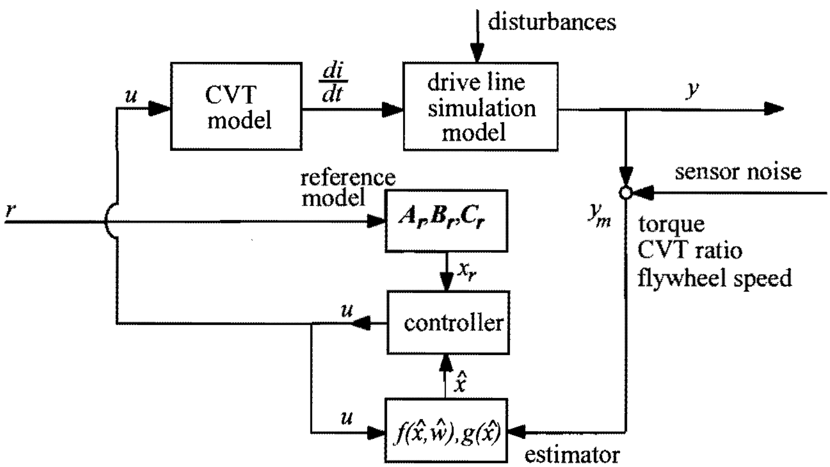

Figure 6.4. Block diagram showing the interconnection of the submodels used for the simulations.

In order to analyze the drive line response under representative driving conditions, a vehicle acceleration and deceleration cycle is used. This allows the vehicle response to be analyzed at different CVT ratios and vehicle speeds. After assessing the nominal drive line response, i.e. the response during normal driving conditions, a single disturbance phenomenon, for instance hill climbing or an engine on-off transient, is applied to the vehicle. Because identical drive cycles are used, the response to the disturbance can be compared to the nominal response.

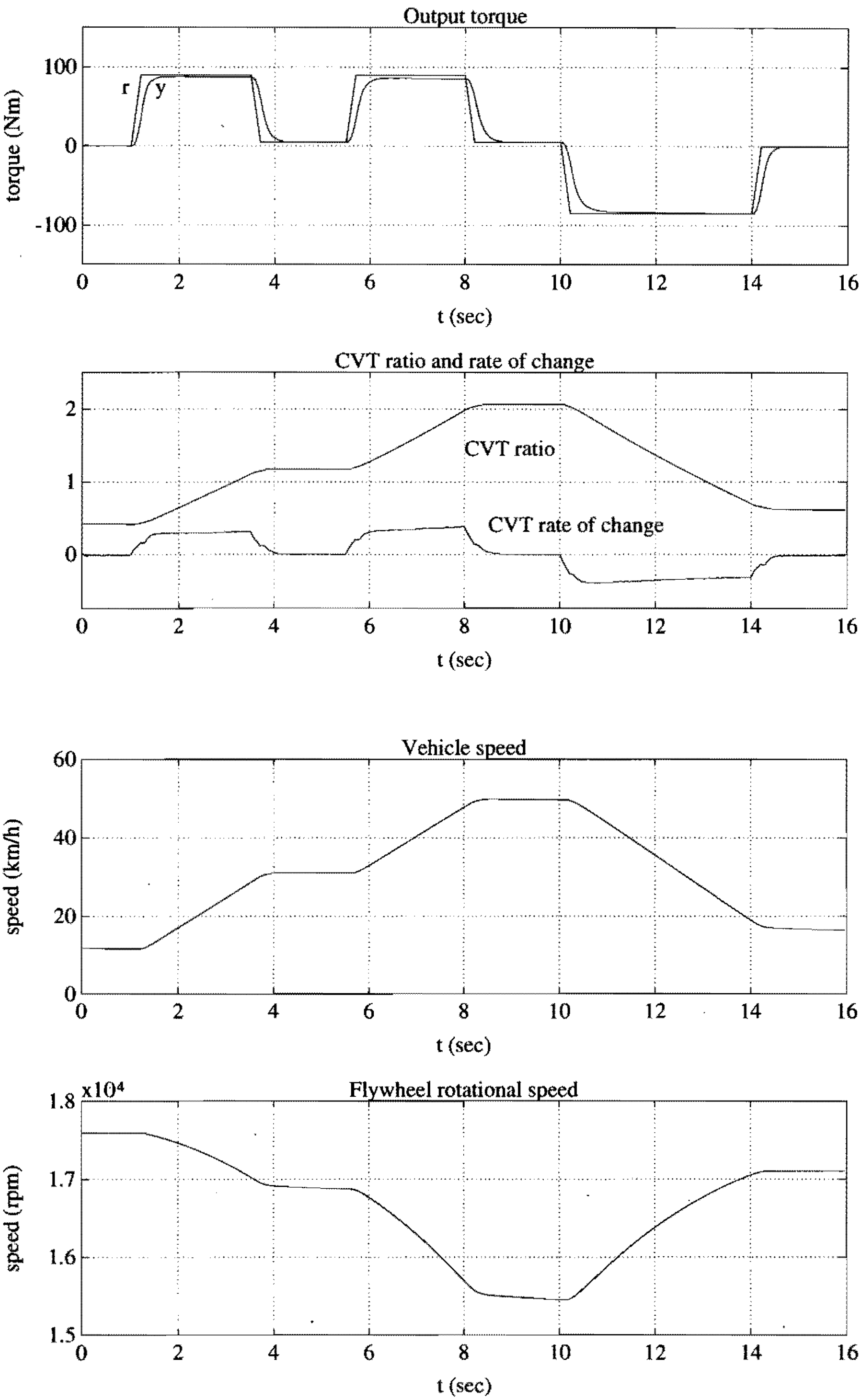

Figure 6.5. Simulation of the vehicle acceleration and deceleration cycle.

6.3.1. Vehicle acceleration and dynamic response

In Figure 6.5 a vehicle acceleration and deceleration cycle is shown. During this cycle, the output torque response can be analyzed at different CVT ratios and at different torques. The cycle used here allows the vehicle to accelerate up to approximately 55 km/h, which corresponds to the maximum speed in the 'low speed' hybrid mode. The deceleration represents braking and recuperation of the vehicle's kinetic energy in the flywheel.

The simulations in Figure 6.5 show that the dynamic response of the drive line can be controlled with the proposed controller. The obtained output torque shows no overshoot and no ripple, indicating that passengers in the vehicle perceive a constant acceleration and, hence, a high level of comfort. Furthermore, the response is independent of the CVT ratio and the desired output torque can simply be specified by the reference input r.

6.3.2. Engine start-up transients and CVT overload protection

Another phenomenon which occurs in the hybrid drive line is starting and stopping of the i.c. engine. The response of the output torque to such a cycle is shown in Figure 6.6. Because the engine output torque T_{engine} cannot be measured in the actual drive line, an estimate must be made. A maximum estimation error of 30Nm in T_{engine} during the start-up transient is assumed for this simulation. The plots show a decrease in the rate of change of the CVT ratio and a nearly constant output torque. This demonstrates that passengers in the vehicle do not notice the engine start-up transient, and that high comfort levels can be maintained.

When an external torque T_{ext} (for instance due to hill climbing) is applied to the vehicle, the output torque increases significantly ([b] in Figure 6.7, for t = 4 to t = 5.5 seconds). The road load variations are not entirely compensated by the controller. The increased drive line torque indicates that the vehicle acceleration is maintained during hill climbing and, hence, a good vehicle driveability is obtained. As the desired output torque increases ([a] in Figure 6.7, for instance during the interval t = 2 to t = 3.5 seconds), CVT overloading may occur when its maximum torque capacity is exceeded. Therefore, an integral (I) action has been added to the controller (Subsection 6.2.4) which ensures that the error between desired torque and realized torque vanishes. This integral part is only activated when a maximum bound in the output torque is exceeded. Simulations, as shown in Figure 6.7, confirm the effectiveness of these modifications. CVT overloading is avoided while driveability is maintained. Here, for these simulations, the bounds T_{min} and T_{max} for the CVT overload protection are set arbitrarily at constant values of -100 Nm and 100 Nm respectively. These constant bounds are chosen in order to clarify the simulations results.

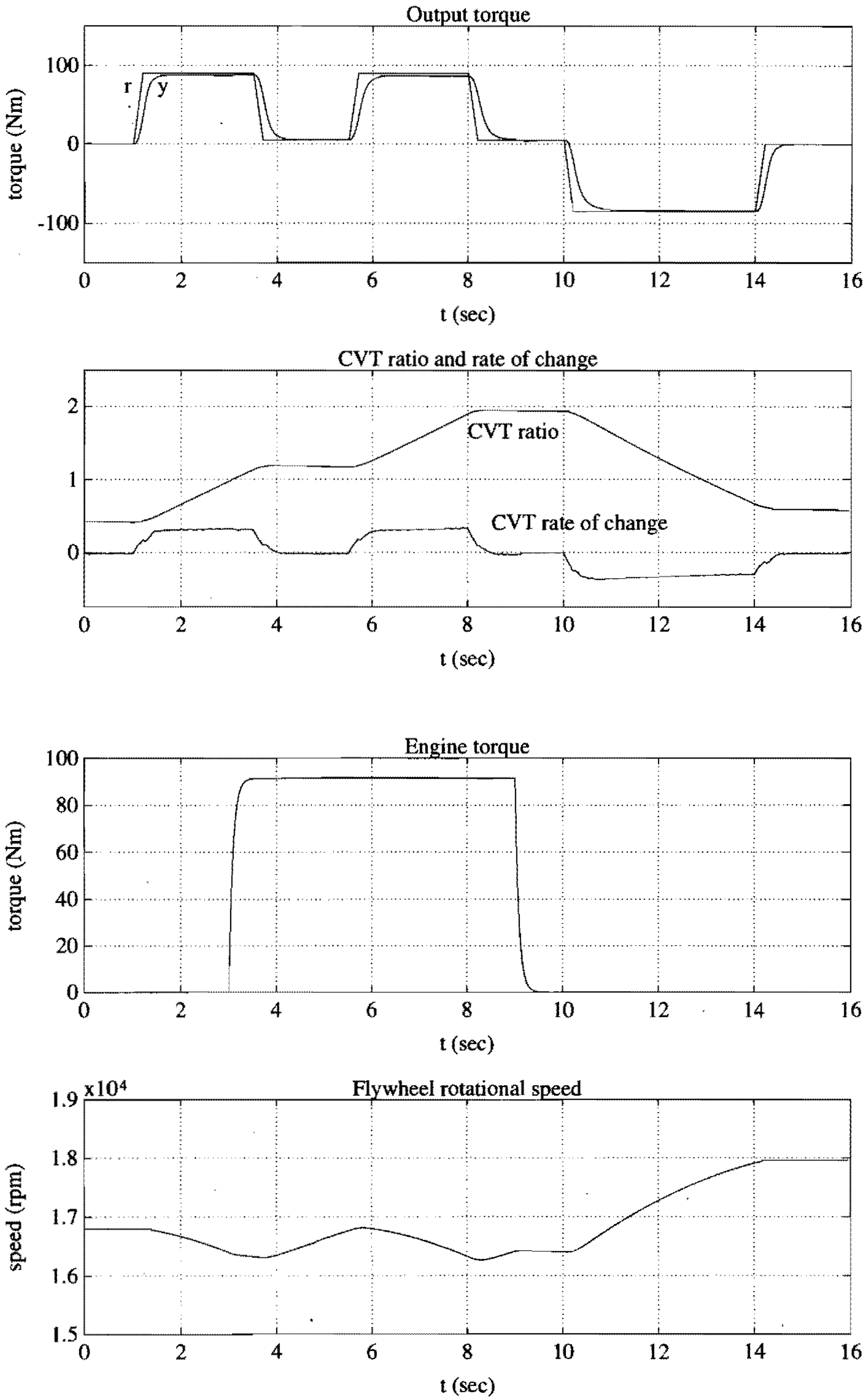

Figure 6.6. Simulation of an engine start and stop cycle.

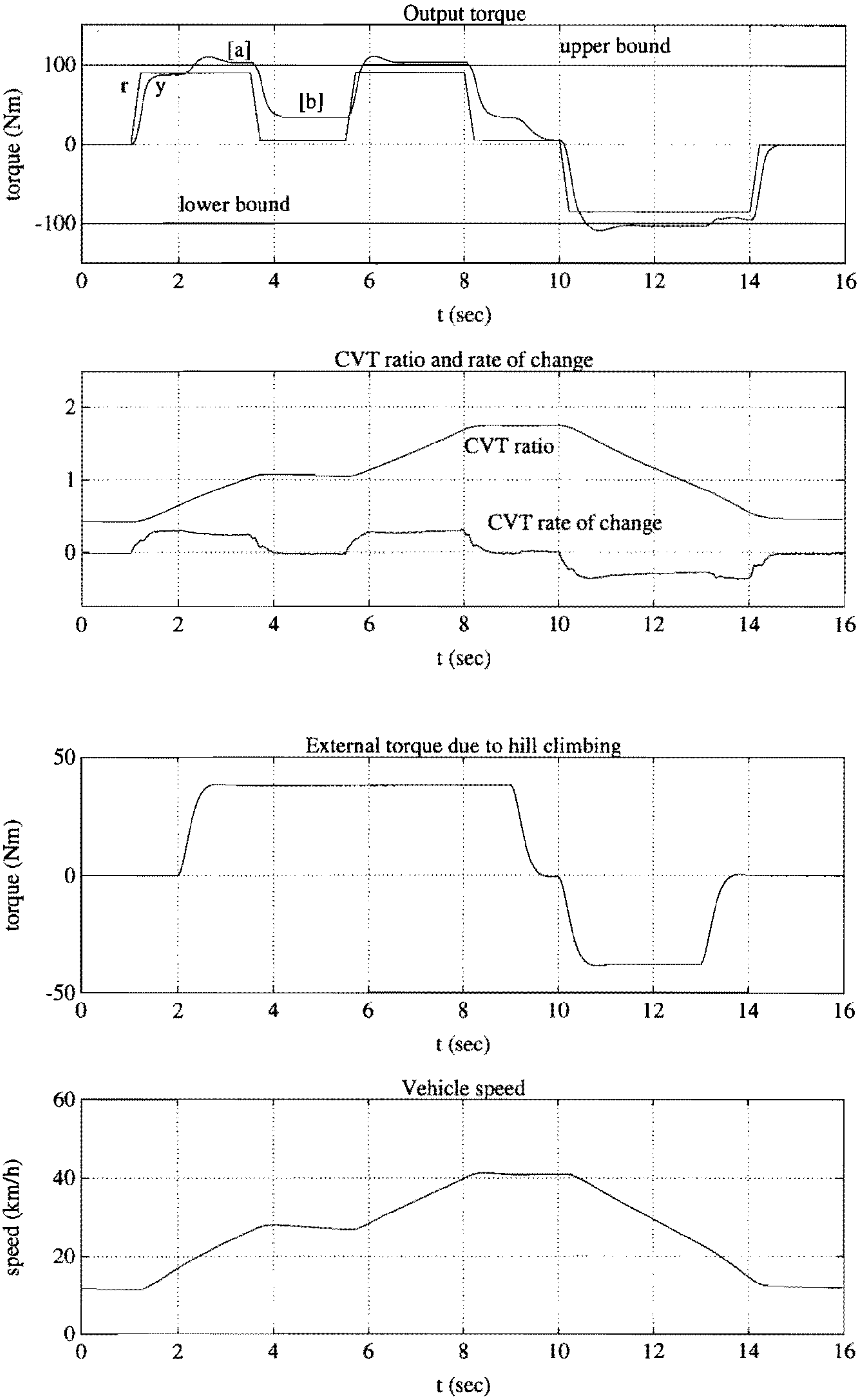

Figure 6.7. Simulation of hill climbing (equivalent torque at secondary CVT shaft) and CVT overload protection due to the integrator action.

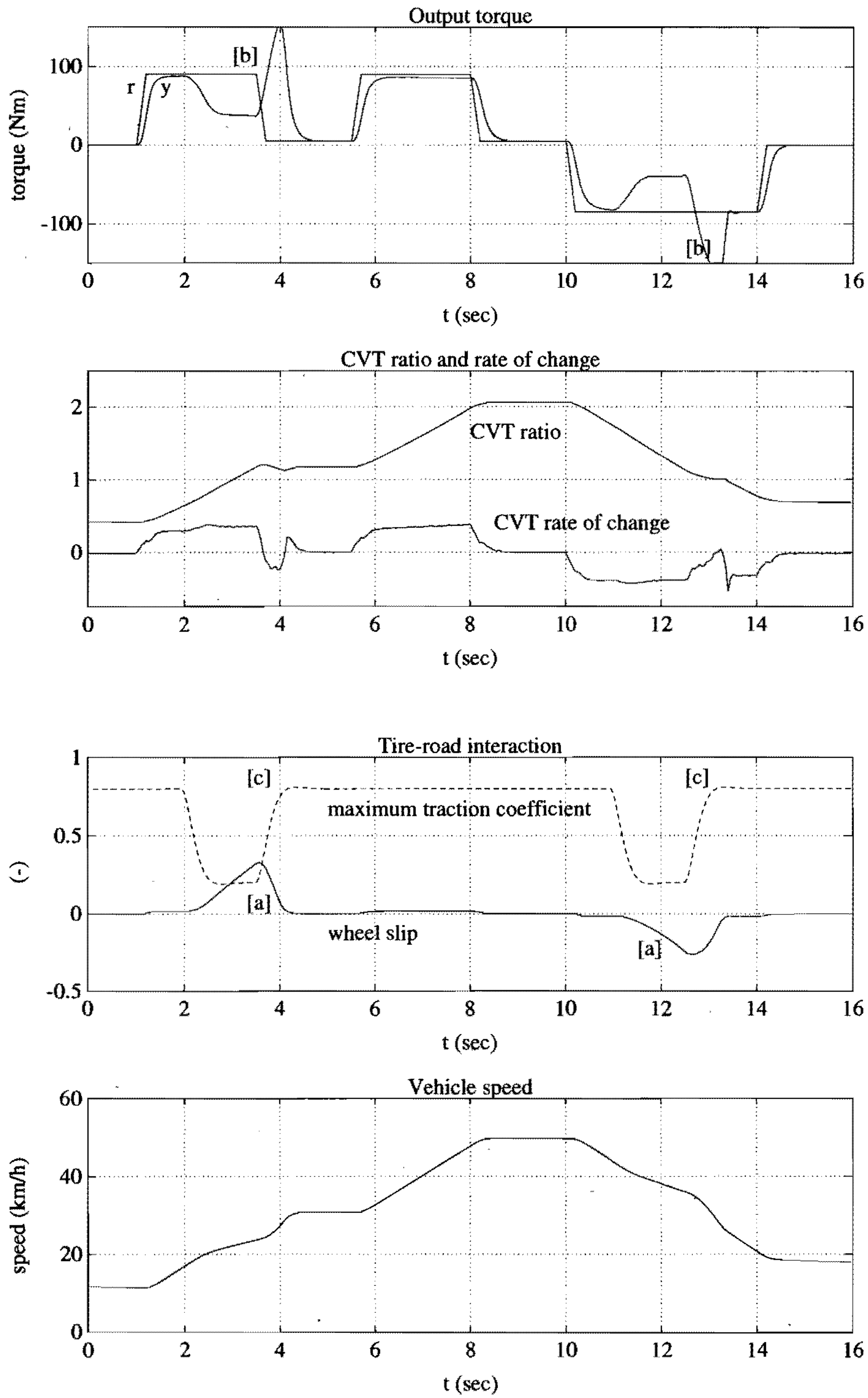

Figure 6.8. Simulation of the vehicle behaviour when driving on a slippery road.

6.3.3. Stability and robustness of the closed-loop

The simulation results shown previously have demonstrated the robustness of the closed-loop controller. For instance the tire-road interaction does not significantly influence the performance of the controlled system. Furthermore, the increased output torque due to the hill climbing allows the vehicle speed to be maintained.

One of the critical factors in the closed-loop stability is driving on a slippery surface. During wheel spin the vehicle dynamic behaviour is changed significantly. Simulation results of the vehicle driving on a slippery surface are shown in Figure 6.8. In this simulation an identical desired output torque trajectory has been used as in the other simulations. The maximum friction coefficient has been lowered intermittently to simulate driving on a slippery surface. The simulation results show the output torque response and the wheel slip caused by this low friction coefficient. Several conclusions can be drawn from these simulations:

- Closed-loop stability is maintained. The controller attempts to provide the desired output torque.
- Internal stability of the simulation model is not maintained. The significant wheel slip [a] indicates that the wheel speed increases without a sufficient increase in vehicle speed. When the wheels recover traction, the vehicle speed and flywheel speed are synchronized by adjusting the CVT ratio, i.e. the rotational wheel speed is adapted to the vehicle speed.
- When traction is regained [c], the fast increase in output torque [b] causes overloading of the CVT. The torque limiter is not sufficiently fast to prevent this overloading.
- Wheel spin is limited, not because of the controller but due to the mechanical link between flywheel and wheels.
- In order to prevent wheel slip, the control law should be extended to incorporate traction control. The maximum wheel spin should be limited.

These simulations shown in Figure 6.8 represent an extreme situation. Under normal conditions the hybrid vehicle can be used without reservation.

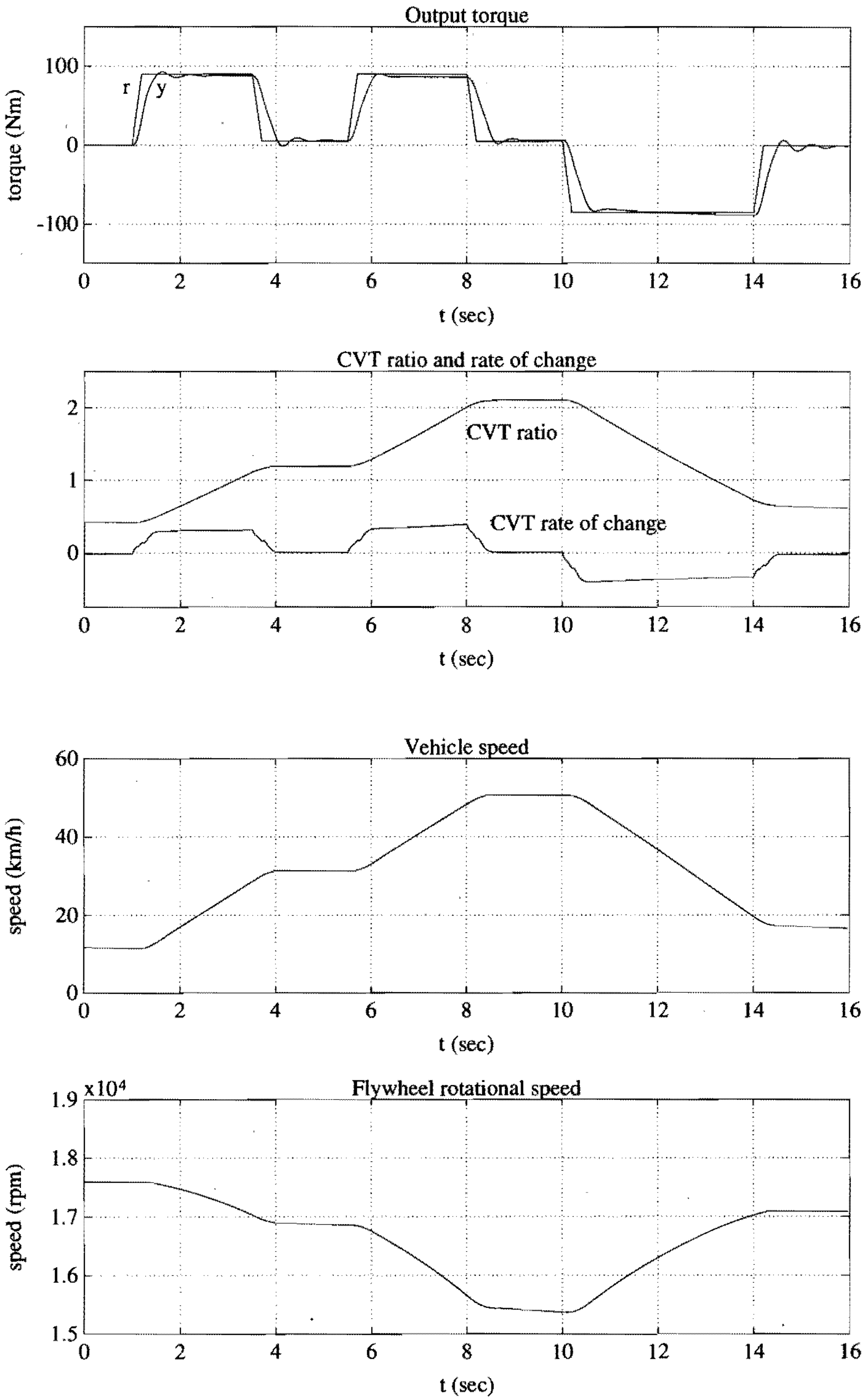

Figure 6.9. Simulation of the closed-loop drive line controller, with output torque estimation on speed measurements only.

6.3.4. Output torque estimation by speed measurements

Other simulation results are shown in Figure 6.9. This simulation shows the drive line response if only the speed measurements are used to estimate the drive line output torque. This is a relevant item because of the costs and vulnerability of the torque sensor.

The Kalman gain matrix has been adjusted to use the speed measurements only. This simulation shows that the drive line can be controlled smoothly. It implies that the torque estimation is sufficiently accurate. Unfortunately, the estimation algorithm is not robust. The torque estimation becomes unstable when large disturbances are encountered. For instance the algorithm fails during hill climbing. Misawa and Hedrick (1989) already mentioned that stability of the closed-loop, with a nonlinear estimator, could not be guaranteed.

6.3.5. Practical implementation of the controller

Implementation of this controller in computer software is straightforward. The availability of low cost, fast, onboard computer hardware enables economic implementation. The high sampling rates of the available hardware allow the nonlinear control algorithms to be discretized, using an explicit Euler integration scheme. This allows the continuous time algorithms, with the corresponding parameters, to be used.

6.4. Discussion

The control algorithm presented for an i.c. engine-flywheel hybrid drive line performs well during numerical simulations. The controller delivers high passenger comfort levels and good driveability. The nonlinearities have been identified and have been compensated for by using a feedback linearization. The PD-type control law is sufficient for a hybrid drive line controller and an I-action has been added to prevent CVT overloading. The simulations show stability of the system, even if operating with large disturbances.

The 'high speed' mode can be controlled by an equivalent controller. A controller for this mode is not given in this thesis, but can be designed similarly.

Topics which have to be considered for series production and operation of flywheel-hybrid vehicles have been identified. The output torque should be obtained from speed measurements only. This requires a more reliable estimation algorithm. Traction control must be considered in order to guarantee stability. These items are topics for future research.

Chapter 7

Experimental verification

7.1. Introduction

The previously designed drive line controller is experimentally verified. The main purpose is to analyze the influence of the CVT on the dynamic behaviour of the drive line, and to verify the drive line controller's performance. The experiments have been carried out on a test-rig. Results obtained on the test-rig are characteristic for the hybrid vehicle. Therefore, algorithms which are developed and verified on the test-rig, can be used and implemented in the hybrid vehicle.

7.2. CVT model verification

A test-rig, described in Section 4.3, has been designed such that its dynamics match the torsional behaviour of the hybrid drive line (Egberts, 1993). This implies that the inertias of the flywheels match those of the simple, reduced, model of the hybrid drive line. The flexible shaft between the CVT and Flywheel 2, representing the torsional stiffnesses of the drive shaft and the tires of the vehicle, has been realized by means of an especially designed poly-urethane shaft. The dynamic behaviour was identified by Egberts (1993).

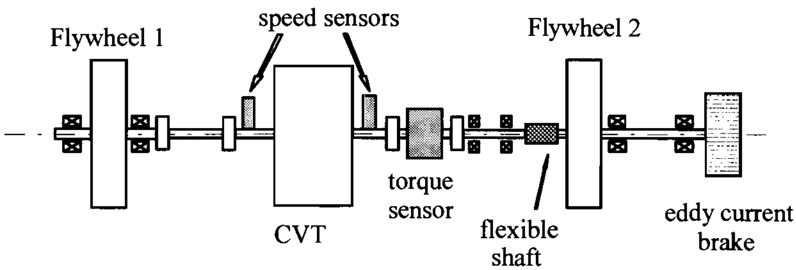

Figure 7.1. Drive line test-rig (see also Figure 4.4).

7.2.1. Objectives

The objective of this experimental verification is to analyze the influence of the CVT on the torsional behaviour of a drive line. In Section 3.3.1, the CVT was described with only two parameters, viz. only by a ratio and a constant efficiency. The validity of this approach is experimentally verified.

7.2.2. Selection of experiments

To determine the resonance frequency and the torsional damping of the open-loop drive line, the dynamic behaviour is studied with a set of simple experiments. This set of experiments is carried out at zero rotational speed. The drive line is excited by a torque pulse and the response is measured by the torque sensor. The second set of experiments is used to analyze the influence of the CVT torque on the open-loop torsional behaviour. These experiments are carried out at operating speed. By means of a step input of the required rate of the CVT ratio change, a torque is generated in the drive line. This torque response is recorded.

7.2.3. Experimental results

The CVT ratio was held at 'low' for the first experiment and at 'high' for the second experiment. This was accomplished by applying a pressure of 35 bar at the pulley with the belt situated at the largest radius and a 10 bar pressure on the other pulley. The drive line was excited by a torque pulse and the torque response was recorded. The results are shown in Figure 7.2.

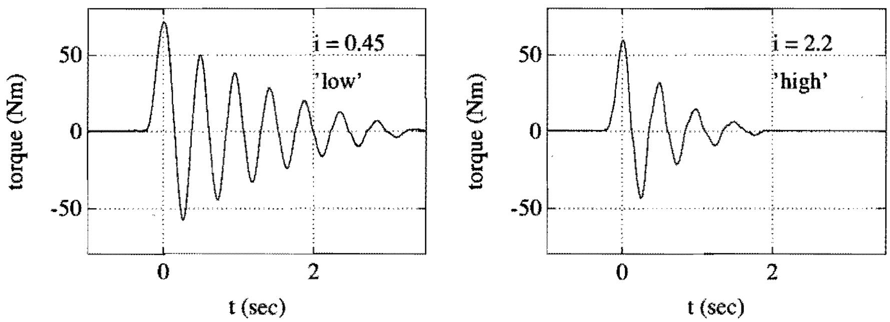

Figure 7.2. Measured open-loop response of the torsional behaviour of the drive line at zero rotational speed.

Egberts (1993) analyzed the torsional behaviour of the Flywheel 2 - flexible shaft subsystem. His results corresponded quite well with the measured responses for the drive line, with a CVT in 'low', shown in Figure 7.2. The nonlinear effects due to the poly-urethane shaft are very small and can be neglected. Therefore, it is concluded that this measured response represents the inherent drive line torsional behaviour. The response for a CVT at 'high' shows large damping. Furthermore, strong nonlinear effects occur during load reversal, specially play can be noticed. Hence, it is concluded that the increase in torsional damping and the nonlinear effects are caused entirely by the CVT.

A similar set of experiments was carried out at operating speed. In this case the drive line was excited by a step in the rate of CVT ratio change. The torque response at low load is shown in Figure 7.3, it is the result of a small rate of ratio change. The step input was applied at t = 0 seconds. At that specific moment the CVT ratio equals 0.5 and slowly increases for t > 0.

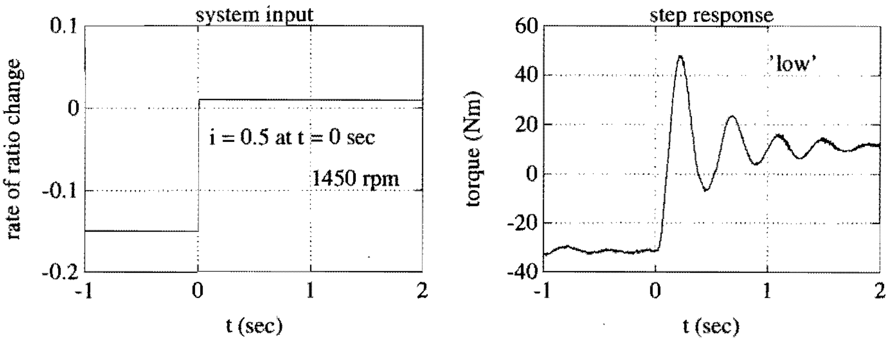

Figure 7.3. Measured step response of drive line torque at operating speed and at low load.

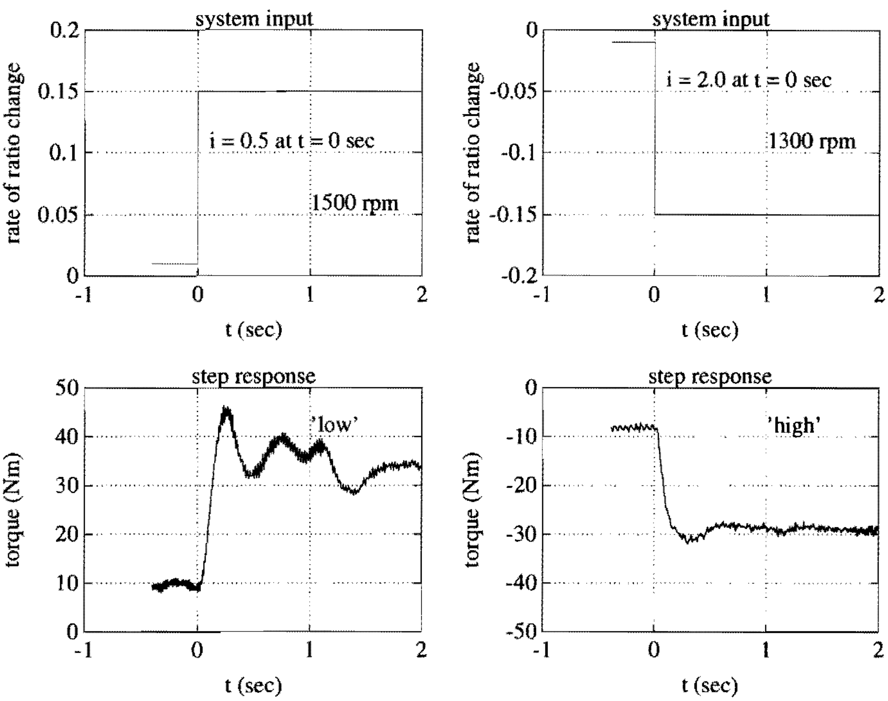

Figure 7.4. Measured step responses at operating speed and with a torque due to the CVT ratio change.

The measured responses at higher torques without load reversal are shown in Figure 7.4. The plots show a step input at t = 0 seconds of the rate of ratio change and the corresponding torque response. The responses at higher torques are significantly different from the previously measured responses. The torsional vibration is suppressed to a remarkable degree and results in a smooth torque response. The responses of Figure 7.4 indicate a strong dependence of the damping on the specific operating conditions of the CVT.

Several explanations can be given for the dependence of the torsional damping on the CVT ratio. Two important effects are mentioned here. The first is the friction between the V-belt and the pulley. This motion is dominant at the pulley with the smallest running radius. Hence, it depends on the CVT ratio. The second effect is the transferred energy through the CVT. For a CVT operating in 'low', the mass of Flywheel 1 is relatively large and this flywheel does not participate significantly in the vibration (see the vibration modes in Figure 7.5). Since the motion of the CVT pulleys corresponds to that of Flywheel 1, the energy is exchanged between the torsional spring and Flywheel 2 and only a small amount of energy is dissipated by friction in the CVT.

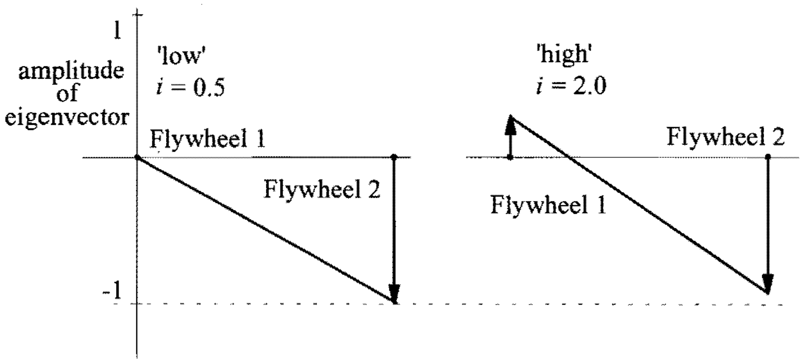

Figure 7.5. The vibration modes for the lowest resonance frequency at different CVT ratios (normalised so that the maximum value of the eigenvector equals 1).

For a CVT operating in 'high', the energy is transferred between the torsional spring and both flywheels. In this case the CVT dissipates a significant amount of energy and the vibration dies out quickly. A phenomenon that occurs specifically at load reversal is the motion of the V-belt relative to the pulleys. The deflection of shafts and pulley sheaves causes a deviation of the circular motion of the V-belt which depends on the torque and the pulley pressures (Gerbert, 1984). Furthermore, the play between the thin steel plates causes the pulleys to rotate over a small angle with respect to each other at load reversal (Gerbert, 1983 and 1984). It causes a discontinuity in the drive line torque. If the torque is measured on the secondary CVT shaft, the play is most significant for a CVT operating at ratios $i > 1$. The accumulation of these effects causes the CVT to perform as a mechanism with play. Hence, it introduces nonlinear effects at load reversal.

It must be concluded that the CVT ratio alone is not sufficient to characterize the CVT behaviour in a drive line. The presence of the CVT has a significant influence on the damping of the torsional vibration. The ratio and torque dependence of the torsional damping is due to the friction mechanisms in the V-belt/pulley contact.

The influence of the CVT on the torsional damping has been identified only qualitatively. In order to use this information in the drive line controller, the damping must be identified quantitatively. Incorporating this information will certainly improve the drive line model accuracy and the controller performance. For the controller verification in the next section, the torsional damping is represented by a constant average value.

7.3. Controller verification

7.3.1. Verification objectives

The torque response of the closed-loop controlled 'low speed' hybrid mode as presented in Chapter 6 has been experimentally verified. The torque responses for small output torques represent the most critical operating conditions. Hence, they require special attention during the verification.

7.3.2. The test signals

The test signals must excite the drive line resonance frequency, use the entire range of the CVT, and allow load reversals to be analyzed. Therefore, the demanded output torque is a sequence of subsequent steps. This introduces higher frequencies into the drive line, and it allows the entire CVT range to be used. Load reversal is analyzed by using small values for the demanded output torques when the sign of the output torque is changed. The sequence of steps for the demanded torque represents an extreme situation. A human driver can not move the accelerator pedal in an abrupt way; the time it takes to move the pedal position from minimum to maximum takes at least 0.2 sec. Therefore, the response of the hybrid vehicle will be much smoother.

The torque levels during the experimental verification are lower than during the numerical simulations because of the limited torque capacity of the multi-plate clutch in the test-rig. Another practical limitation is the necessity to operate the test-rig at rotational speeds lower than used in the hybrid vehicle. This is due to vibrations in the test-rig frame. Therefore, the operating speed of Flywheel 1 was limited to 1500 rpm. Because this speed is used in the nonlinear feedback component of the control law, it does not limit the validity of the torque response verification.

7.3.3. The torque response

The drive line controller was adjusted to take into account the identified properties of the test-rig, i.e. the resonance frequency and damping (see Table 7.1). Because the torsional damping strongly depends on the specific values of the torque and the CVT ratio, a particular operating point was chosen. The value for the torsional damping was chosen to match the response at low torques. This yields a good response during load reversal and at low torque. The relative damping is an estimate and is used for the entire range of ratios and torque levels, i.e. independent of the CVT operating conditions.

Table 7.1. The identified test-rig properties (CVT ratio i = 1, T_{out} = 30Nm).

resonance frequency	2.1 Hz
relative damping	0.3

The desired closed loop response of the controlled system is specified by means of the controller reference model, and the controller performance is specified by the error dynamics (Chapter 6). The controller specifications are given in Table 7.2.

Table 7.2. The drive line controller specifications.

	controller reference model
bandwidth	2.5 Hz
relative damping	1.0
	controller error dynamics
bandwidth	3.5 Hz
relative damping	0.9

Initial torque response measurements indicated that considerable errors occurred in the estimates of the state variables which were caused by model errors. Therefore, the state estimator has been changed such that the measured torque signal is not used in the estimation algorithm, and only the CVT ratio and flywheel speed are used. The filtering in the Kalman estimation algorithm reduces the measurement noise and also yields an estimate of the time derivative of the output torque. The measured torque signal is used directly in the control algorithms, see Figure 7.6.

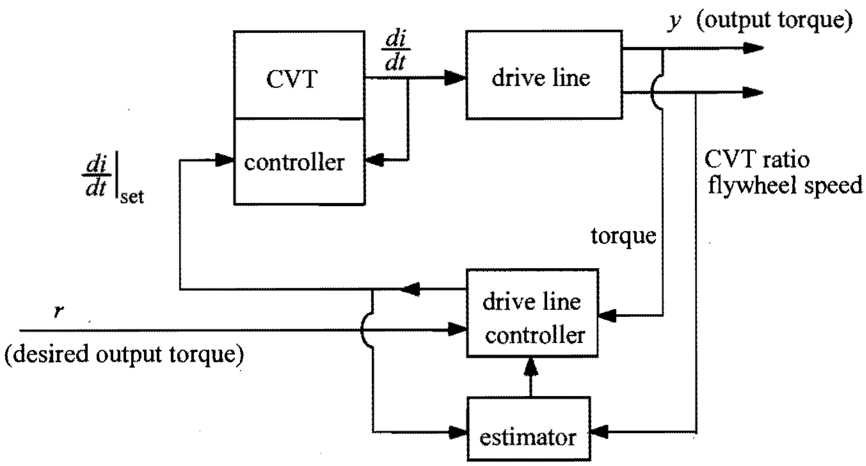

Figure 7.6. The control flow diagram of the hybrid drive line.

The measured torque response is shown in Figure 7.7.

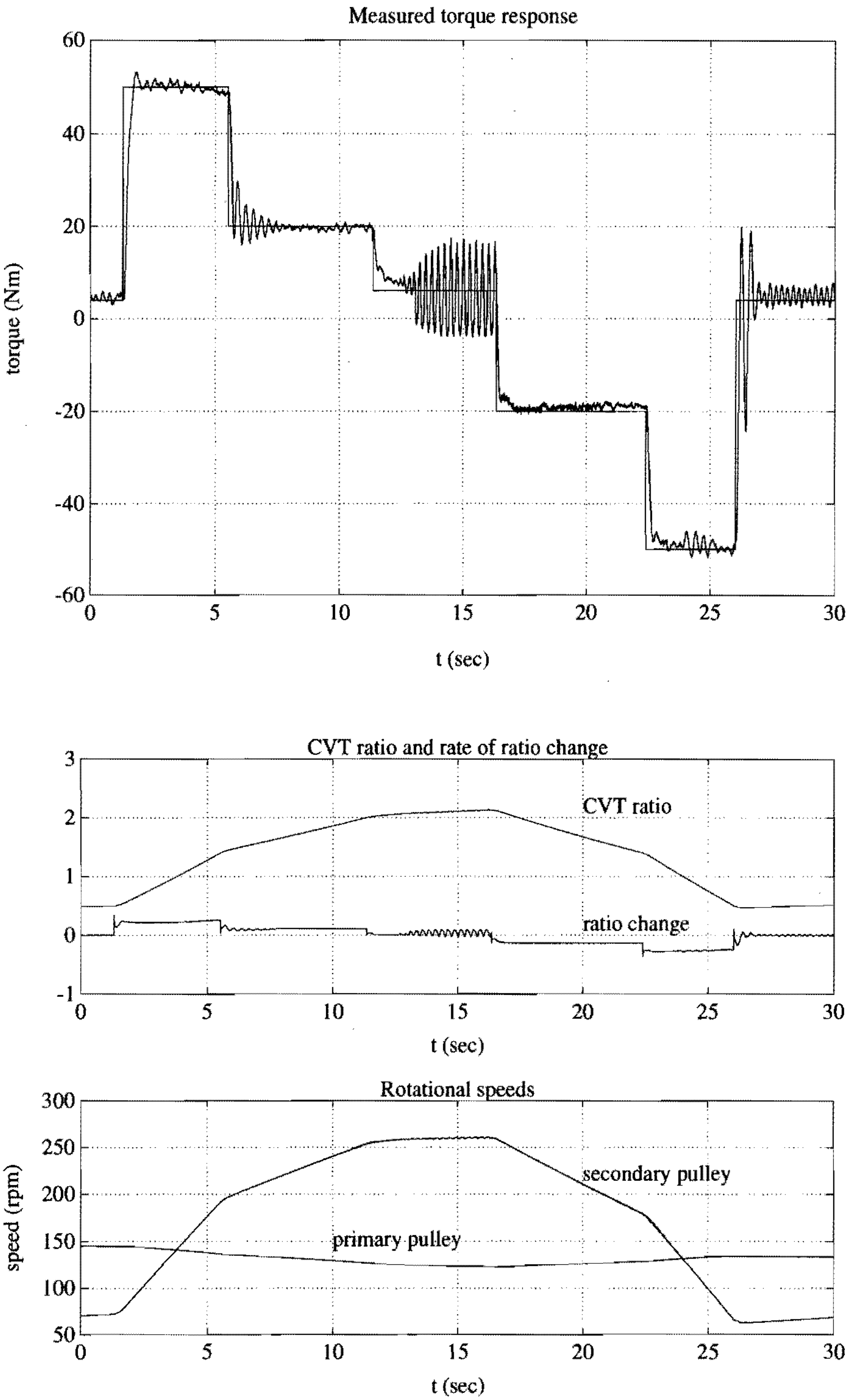

Figure 7.7. The drive line torque response.

The output torque is accurate at high torque levels, independent of the CVT ratio. However, the responses occurring at small torques and during load reversal are unacceptable. For small torques a torsional vibration is induced which is not suppressed by the controller. The vibrations are probably caused by an accumulation of errors, originating from the neglected response of the CVT hydraulics, the small torsional damping at low torque, and the play in the CVT during load reversal. The controller overcompensates each time at load reversal, and hence, the vibrations are maintained. In order to suppress the torsional vibration at low torque levels one might want to modify the mechanical construction by reducing the play and increasing the torsional damping. This appears to be impossible because the phenomena are inherent to the V-belt and the CVT. Another option is to modify the drive line controller and to include the CVT (hydraulic) response, the nonlinear damping characteristics, and the CVT belt play in the controller. A large effort is needed to model these phenomena accurately for all conceivable operating conditions. The resulting drive line controller would become very complex and this option has not been pursued. Therefore, another approach is chosen. The drive line controller is modified to avoid the excitation of the torsional vibration at low torque levels. This modification is relatively simple and straightforward. The modification is elaborated and the experimental results are shown in the next section.

7.3.4. The modified controller

The modification of the drive line controller as discussed above must ensure good driveability and prevent the occurrence of torsional vibrations. This can be achieved by modification of the controller reference model and of the error dynamics. The damping of the reference model is increased when operating at low torques, which in effect, decreases the bandwidth of the drive line. Additionally the bandwidth of the error dynamics, which determine the controller performance, is reduced below the resonance frequency of the drive line. The penalty for this is a somewhat slower torque response and an increased steady state error. Because this modification is used only at lower torques, the driver will probably not notice a difference. The controller modification is summarised in Table 7.3

Table 7.3. The modified drive line controller specifications.

	high torque (abs(T_{set}) > 20) and increase of abs(T_{set})	low torque (abs(T_{set}) $\leq$ 20) or decrease of abs(T_{set})
	reference model:	
bandwidth	2.5 Hz	2.5 Hz
relative damping	1.0	2.0
	error dynamics:	
bandwidth	3.5 Hz	1.5 Hz
relative damping	0.9	0.9

The torque response obtained with the modified controller is shown in Figure 7.8.

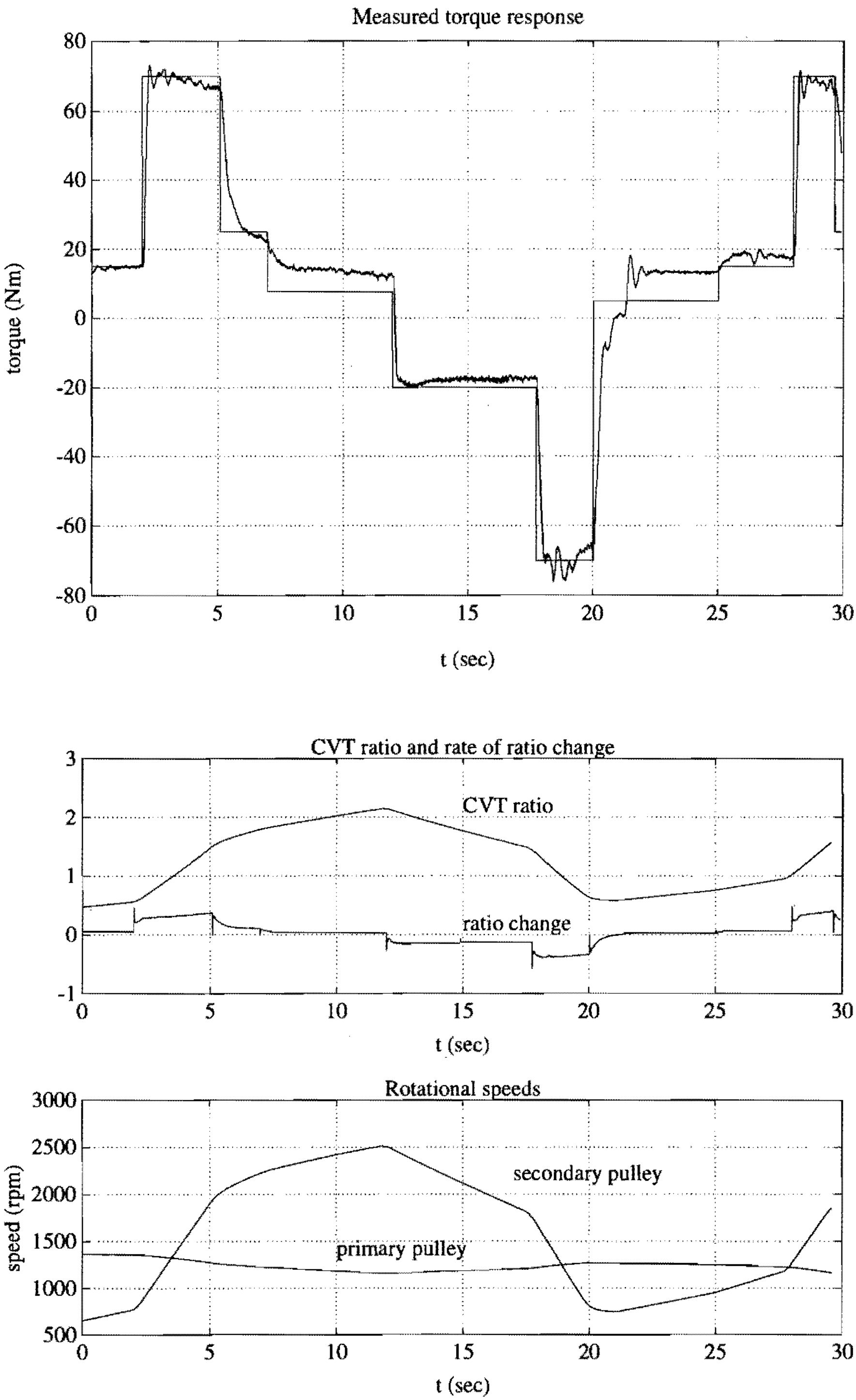

Figure 7.8. The torque response after modification of the controller.

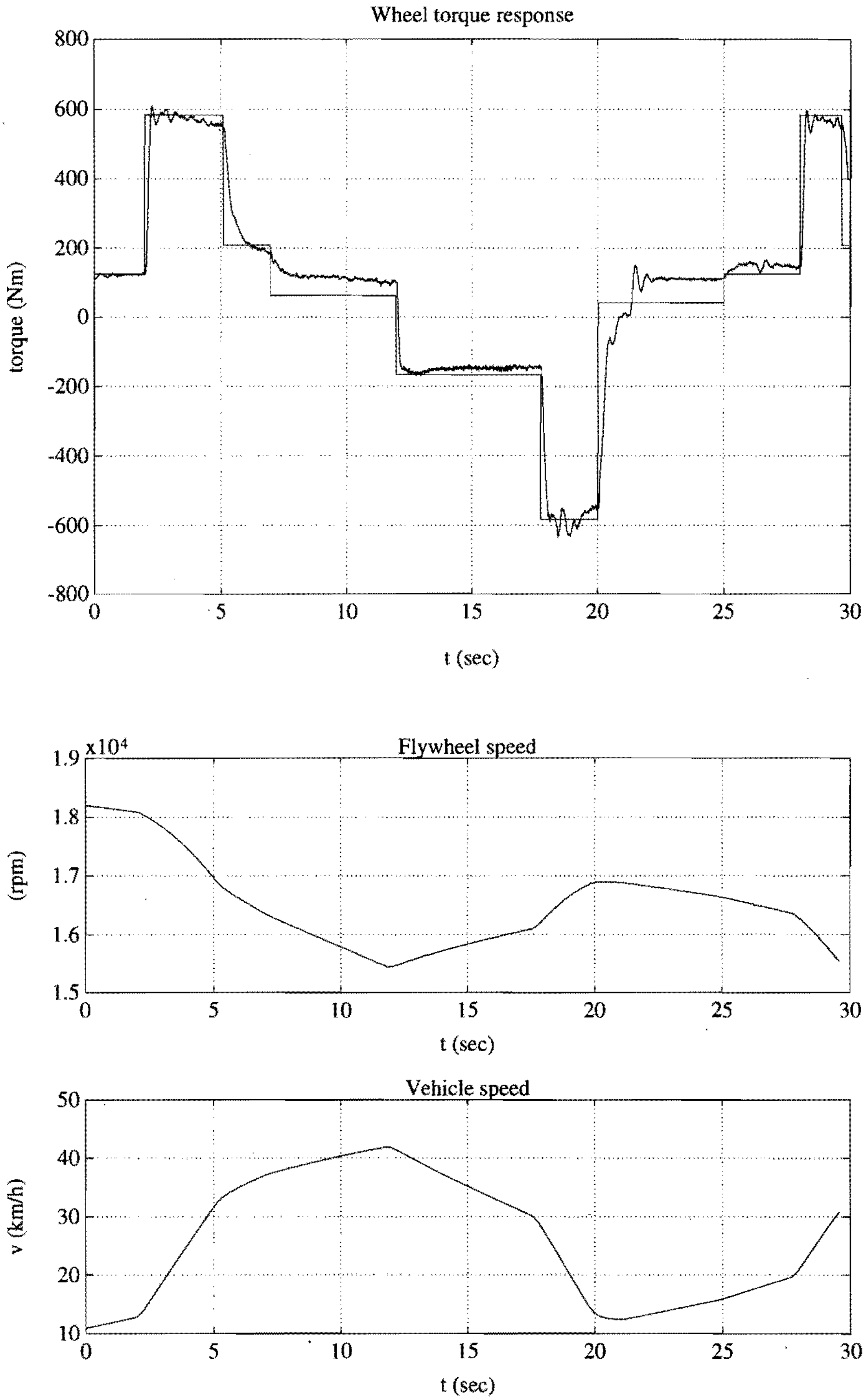

Figure 7.9. The experimental results translated into wheel torque, flywheel rotational speed and vehicle speed.

The oscillations at low torque levels have been eliminated but an increased steady state error between desired torque and obtained output torque can be noticed. This steady state error is acceptable because the vehicle's driver does probably not notice this error. The proposed modification of the drive line controller meets its purpose. In the hybrid vehicle the interpretation of the accelerator position must be based on a strategy which prevents oscillations at small output torques. A zero accelerator pedal position must be interpreted as an engine brake torque. This avoids very small torques (torques below the rolling resistance) and also avoids repeated load reversals. An additional effect is that the driver perceives a vehicle response as if he is driving in a conventionally powered vehicle.

For small torques (see Figure 7.8) the torque error is significant. This is mainly due to modelling errors and to errors in the CVT response. The controller is not able to compensate for these errors due to the limited error dynamics bandwidth. In Figure 7.9 the test rig measurement results are represented as wheel torque, flywheel speed, and vehicle speed. The torque response on a magnified time scale is shown in Figure 7.10.

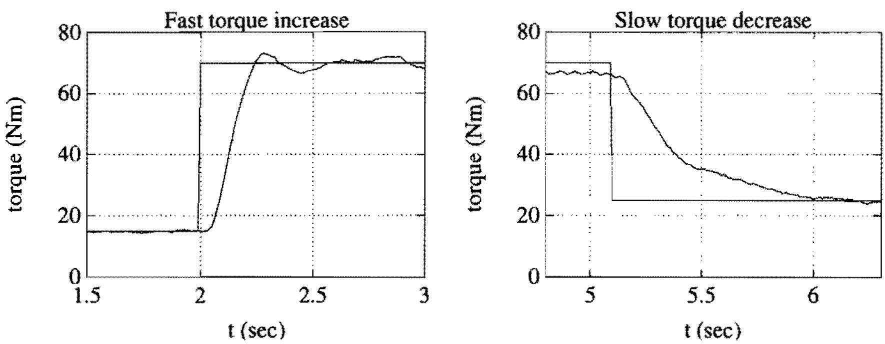

Figure 7.10. The torque response on a magnified scale.

This desired torque level is reached within 0.2 - 0.3 seconds, as was specified. The overshoot is 5%, which is higher than specified but within the absolute torque error bound of 4 Nm which is required to maintain high passengers comfort levels. The torque decrease is slower and is due to the controller modification. It is noted that this modification does not degrade the traffic safety. Since braking is considered as a negative torque, it has the same fast response, i.e. within 0.2 - 0.3 seconds.

7.3.5. The torque response using speed measurements only

In order to analyze the feasibility of a drive line controller without the explicit use of a torque sensor, the speed measurements are used in combination with a Kalman filter to obtain estimates of the actual drive line torque. The Kalman filter feedback has been obtained by specifying the sensor noise and the expected modelling errors for the hybrid drive line.

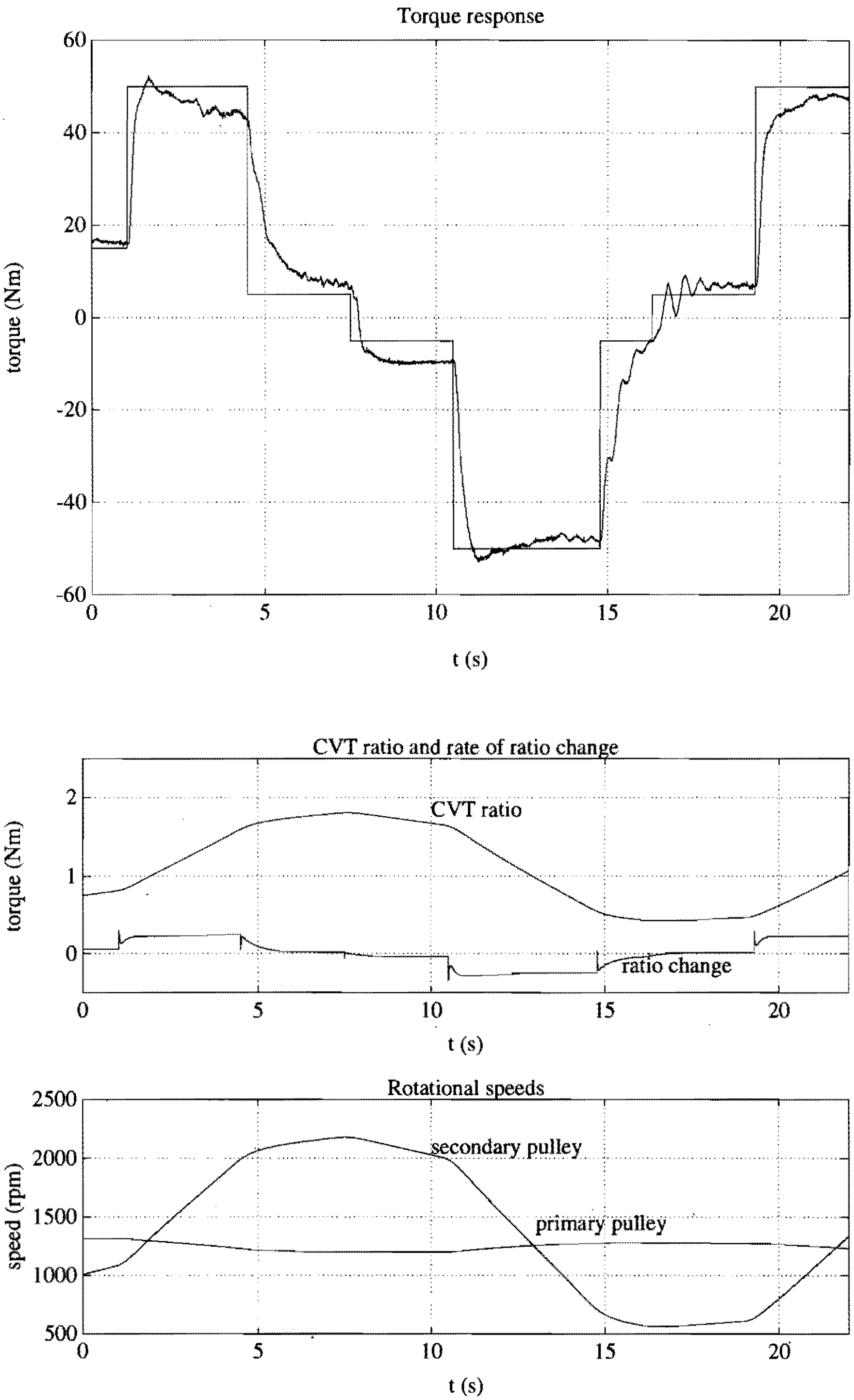

Figure 7.11. The measured torque response when speed measurements only are used for drive line torque control.

The normal load-road resistance has been simulated during this experiment. The torque response has been recorded and is shown in Figure 7.11. The desired response is obtained with an adequate accuracy. Only small oscillations occur during load reversal and at low torques. The origin of the steady state error, which strongly depends on the CVT ratio, can be traced back to the error in the CVT rate of ratio change, shown in Figure 7.12.

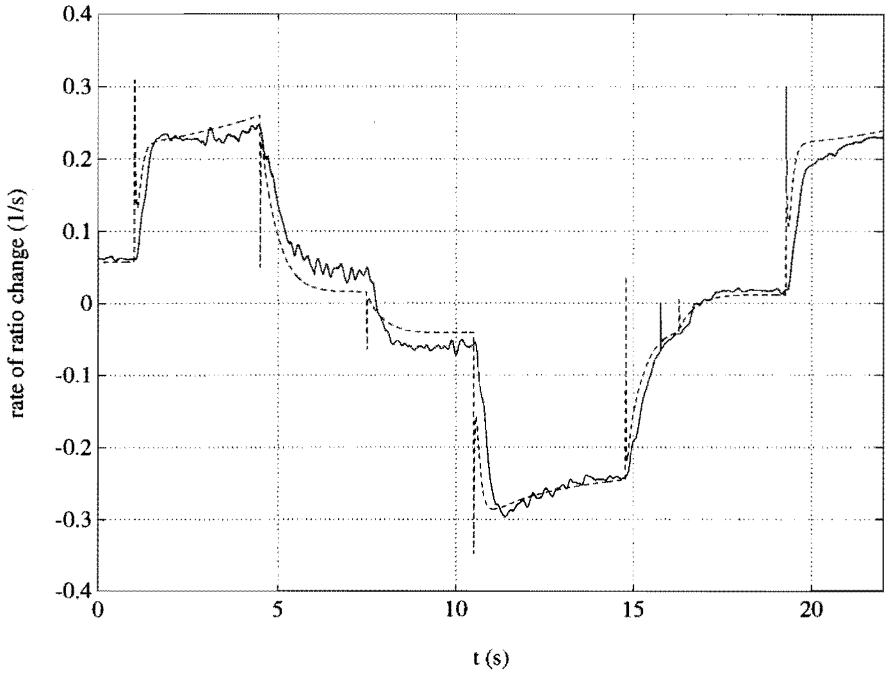

Figure 7.12. The measured (solid line) and desired (dashed line) rate of CVT ratio change corresponding to the drive line response of Figure 7.11.

Increasing the CVT rate of ratio change accuracy decreases the drive line torque error. The CVT rate of ratio change error originates from inaccuracies is the flow steering into the driving pulley. The adaptation mechanism in the pulley sheave velocity controller is too slow to guarantee a good response at rapid changes in the CVT operating conditions. Therefore, a more accurate flow steering could certainly enhance the accuracy of the CVT rate of ratio change considerably. A more accurate rate of ratio change would be sufficient to guarantee proper operation of the complete drive line.

Sudden changes in the demanded output torque are noticed as sharp peaks in the desired rate of ratio change (Figure 7.12). These peaks are required to obtain a fast response of the drive line. However, in order to obtain a smooth running of the transmission, these sharp peaks should be removed.

7.4. Discussion

The experimental results have shown that the basic concept, to separate the CVT controller and the drive line controller, yields a satisfying output torque response. The output torque response is fast and its accuracy allows the control concept to be used in the hybrid vehicle. The smooth response enables high passenger comfort levels and good vehicle driveability. The important results of the experimental verification are summarized:

- The torsional damping of the hybrid drive line is a function of the CVT ratio and torque. The play and nonlinearities, which are inherent to the CVT, are qualitatively identified. Further research is required to quantitatively determine the CVT characteristics.
- The measured torque responses show that a simple dynamic model of the hybrid drive line (see Chapter 3) is sufficient for the closed-loop output torque control. Furthermore, the simple CVT submodel in this drive line model is sufficient.
- The play of the metal V-belt can be dominant in the drive line response for small torques. A simple adjustment of the control law is sufficient to avoid oscillations in the output torque. This results in a slightly slower response which will hardly be noticed by the driver.
- The output torque control based on speed measurements is very promising. The output torque can be controlled smoothly. The output torque accuracy can be increased by improvements in the CVT controller. Further research should be carried out on estimation algorithms, and the stability of the closed-loop system should be considered.

The control law has been modified for torques below 20 Nm to avoid oscillations caused by, for instance, play in the V-belt. This modification is for both positive and negative torques. However, the play in the belt depends on the tensile forces in the belt and the pushing force between the V-elements. These forces both depend on the CVT ratio and on the torque (and are different for positive and negative torque). Therefore, further research should be carried out on the influence of the CVT (and V-belt) on the drive line behaviour for small torques.

Although the obtained results are satisfactory and can be used to control the hybrid vehicle, further improvements in accuracy and passenger comfort levels are still possible. In order to improve the torque response, several options are available.

- Increasing the accuracy of the drive line control model, especially with respect to the influence of the CVT on the torsional damping in the drive line. Including this item in the controller should enhance the controller performance.
- Optimization of the CVT rate of ratio change response. Errors in the CVT rate of ratio change immediately result in torque errors in the drive line. An accurate rate of CVT ratio change should be sufficient to control the drive line without the necessity of an explicit output torque measurement and, therefore, without torque sensor.
- Integration of the CVT controller and the drive line controller. This option allows the complete system to be controlled by a single control algorithm. In this case the CVT rate of ratio change is not separately controlled but incorporated in the drive

line model. An advantage of this approach is that a low bandwidth of the CVT rate of ratio change is sufficient. In that case, the higher frequencies (> 5 Hz) are avoided and very smooth running of the transmission can be expected. In addition, the errors in the rate of ratio change can be compensated for directly in the drive line controller. The major disadvantage of this last option is the increased complexity and the loss of the modularity of CVT controller and drive line controller.

Chapter 8

Concluding remarks and recommendations

8.1. Overview of the research

The basic idea of the flywheel-hybrid drive line, as discussed in this thesis, is to transfer energy between the flywheel and the vehicle. The choice for this type of hybrid system has important implications for the driveability of the vehicle. This system is significantly different from conventional vehicle drive lines in two aspects. First, by means of accelerating or decelerating the flywheel, an output torque can be generated. This is realized by changing the CVT ratio. Second, the resonance frequency of the drive line is below the closed-loop bandwidth of the controlled drive line. In order to obtain high passenger comfort levels and good driveability, the output torque of the drive line has to be controlled smoothly and accurately.

Drive line modelling and model reduction
A controller design model has been obtained by reduction of an extensive physical model of the drive line. Two model reduction techniques have been considered and their applicability for the hybrid drive line has been analyzed. The numerical reduction technique (balanced truncation) yields reduced models which closely match the response of the original model in the lower frequency range. However, because only linear (or linearized) models can be reduced, the resulting models do not contain the CVT ratio explicitly. The reduction technique based on modal analysis enables the CVT ratio to be incorporated and has been used in this thesis.

The reduced model for the drive line contains the flywheel inertia, the equivalent vehicle inertia, the CVT ratio and the torsional stiffness and damping of the drive line. This model relates the output torque to the flywheel rotational speed and the rate of CVT ratio change. This simple model has been used for the design of the drive line controller.

CVT control
The rate of CVT ratio change is realized by a CVT controller. The rate of ratio change is obtained by an axial pulley sheave velocity of the driving pulley. The clamping pressure, required to prevent belt slip, is applied to the driven pulley. The power flow in the hybrid drive line determines which pulley is driving and which is driven. The CVT

controller is fast and realizes the desired rate of ratio change, independent from the drive line operating conditions.

Dynamic CVT models for the pulley sheave velocity controller and the pressure controller have been obtained by experiments on a test-rig. These experiments showed that simple models can be used, and that the pulleys can be controlled independently.

The rate of ratio change is kinematically related to the axial velocity of the pulley sheave of the driving pulley and, hence, the desired rate of ratio change can be converted into a desired sheave velocity. The realized CVT output, i.e. the rate of ratio change, is determined from measurements of the rotational pulley speeds, using differentiation combined with low pass filtering. Here, a compromise has been found between signal bandwidth and accuracy. A Kalman estimation algorithm is employed to further reduce the influence of measurement noise. The estimated rate of ratio change is converted into a pulley sheave velocity and is used in a linear control law for the oil flow. The oil flow is realized by means of a servo-hydraulic valve, using a nonlinear valve characteristic. A slow adaptation mechanism is used to ensure that the required rate of change is obtained.

The pressure controller is based on a linear model that can be used in one specific operating point. In order to control the pressure under varying pressure levels, varying oil temperature and different flow rates, an adaptive control law is used.

Drive line control

In the drive line controller model, the CVT is characterized by two quantities, i.e. a ratio and a constant efficiency. The vehicle driver's commands are translated into a desired output torque. This output torque has to be realized by the drive line controller. The controller determines the rate of CVT ratio change which is required to accelerate the vehicle and to decelerate the flywheel and, hence, introduces a torque in the drive line.

This controller has been designed to compensate for the nonlinear drive line dynamics, vehicle air drag and rolling resistance. Because the i.c. engine operates in an on/off mode, the transient changes in the engine torque have to be taken into account. In order to obtain states which are not measured, a steady state Kalman filter is used. This filter uses the nonlinear drive line model and a constant feedback matrix.

The drive line controller uses a reference model to generate the desired output torque trajectory. Feedback linearization compensates for the nonlinearities of the drive line and a PD-type control law is used to track the desired torque trajectory. The PD law yields good vehicle driveability. However, in case of large variations in vehicle load, the output torque can not be controlled accurately and a considerable steady state error occurs. In order to protect the CVT from overloading, the control law is augmented by an integral (I)-action. This I-action is active only when an upper torque limit is reached and eliminates the steady state error and prevents CVT overloading.

The designed controller has been tuned by means of numerical simulations and has been experimentally verified on a test-rig. The output torque can be controlled accurately and smoothly. The nonlinear characteristics of the drive line are compensated by the controller.

The most critical situation is driving at a low, constant speed. The experimental results show that a low output torque can be realized by a small continuous change of the CVT ratio and, hence, smooth driving at low and constant speed is achieved. The results also show that the behaviour of the CVT in a drive line strongly depends on its operating conditions.

Experiments show that torque control without an explicit torque measurement can yield a sufficiently accurate and smooth response. During this set of experiments the torque sensor was not used and the output torque was estimated, based on the drive line model and the speed measurements. Further improvements in the output torque response can be achieved by a more accurate torque estimation algorithm and more accurate CVT control. The corresponding numerical simulations show that, in this case, the closed-loop could become unstable if large load changes are encountered. Therefore, a reliable estimation algorithm is vital.

8.2. Conclusions

The research presented in this thesis has been summarized in the previous section. Several conclusions concerning the CVT and the drive line control can be drawn.
Conclusions with respect to the CVT control are:

- Fairly simple first order models are sufficient for the design of a CVT controller.
- In the CVT, the required pulley sheave velocity and the clamping pressure can be controlled independently.
- The rate of CVT ratio change can be controlled with an error smaller than 0.02 s^{-1}, independent of the operating conditions. This error is sufficiently small for use in the flywheel-hybrid drive line.
- The dynamic response of the rate of ratio change is characterized by a 20 Hz bandwidth. Thus, the CVT can be considered as an independent component in the hybrid drive line.
- The clamping pressure in the CVT can be controlled by an adaptive control algorithm. Pressure control is straightforward and minimum clamping pressures can be maintained.

The conclusions with respect to the drive line controller are:

- The basic concept to separate the CVT controller from the drive line controller is justified by test-rig experiments. This concept yields good results for the drive line torque controller.

- In order to design a controller for the output torque, a nonlinear dynamic model is required. The essential characteristics of the CVT in the drive line should be incorporated in this model. The drive line model can be obtained by means of physical modelling and model reduction.
- The controller design model is obtained by reducing a complex drive line model. Analytical reduction techniques, which can deal with local nonlinearities, are advantageous to reduce these complex models. Such a reduction technique is an important design tool for this control problem.
- Accurate estimation of the state variables, based on model prediction, is essential for output torque control. Especially for those states which are not measured.
- Feedback linearization of the drive line controller design model enables the use of a linear PD-type control law. This control law yields good vehicle driveability and high passenger comfort levels.
- CVT overloading caused by non-predictable load changes, for instance hill climbing, can be prevented by adding an I-action to the PD-controller. This enables accurate control of the output torque. The numerical simulations, with the explicit torque measurement, show stability of the system, even when operating with large load changes.
- Numerical simulations show that wheel slip on a slippery surface can lead to large torques in the drive line, once traction is regained. Traction control of flywheel driven vehicles must be considered in order to guarantee safe vehicle driving.
- The measured torque responses show that the designed drive line controller yields good results for the vehicle driveability and high levels of passenger comfort can be achieved. The simple dynamic model is sufficient to design the closed-loop output torque controller.
- The construction of the metal V-belt can cause undesirable behaviour in the drive line response at low torques. A simple adjustment of the control law is sufficient to avoid oscillations in the output torque.
- Inaccuracies in the CVT rate of ratio change immediately appear as errors in the output torque in the drive line.
- The output torque control based on speed measurements is very promising. The output torque can be controlled smoothly. The obtainable accuracy depends on the quality of the drive line model, on the CVT rate of ratio change performance and on the output torque estimation algorithm.

The controller, presented in this thesis, has been designed for the dynamic behaviour of the 'low speed' hybrid mode. The obtained experimental results are satisfactory and justify the controller to be used directly in the hybrid vehicle proto-type. In order to control the entire drive line, also a controller for the 'high speed' hybrid mode must be available. This controller can be designed, based on the theory and formulation given in this thesis. In the steering and control strategy for the hybrid drive line also clutch control must be included together with a procedure to guarantee safe vehicle operation.

8.3. Recommendations

The proposed controller for the hybrid drive line, including the CVT controller, can be implemented and used in the hybrid vehicle. During the realization of the proto-type hybrid vehicle further research into the dynamic behaviour can be carried out to improve the accuracy and enhance the obtainable passenger comfort levels. To improve the torque response, several options are available:

- The accuracy of the drive line model can be improved. The behaviour of the CVT, can be modelled more accurately. The nonlinearities which are inherent to the CVT should be quantified.
- The CVT controller uses fairly simple, perhaps insufficient, models based on pressure response measurements. Further modelling, in combination with experiments, should clarify the dynamic behaviour of the combination of the hydraulic and mechanical components of the CVT.
- The dynamic behaviour of the hydraulic system of the CVT depends, for instance, on the stiffness of the oil cylinders. An understanding of the underlying relations could lead to an optimal CVT construction and, hence, could enhance the performance of future electronically controlled CVT's.
- The CVT controller basically consists of two separate single-input single-output controllers, one for the axial pulley sheave velocity and one for the clamping pressure. Integration of both controllers in one multiple-input multiple-output controller could be advantageous. It can use the interaction between the CVT pulleys and enhance the response of the CVT. For instance, an increase in flow at the driving pulley can be compensated directly at the driven pulley. This type of control strategy might be required when less expensive and slower, pulse width modulated, hydraulic valves are to be used.
- Errors in the obtained rate of ratio change immediately appear as torque errors in the drive line. Therefore, a fast and accurate CVT rate of ratio change response is essential. Further optimization of this CVT response enhances the attainable drive line controller performance.
- The output torque can be measured by a torque sensor in the output shaft of the drive line. However, such sensors are not suited for use in mass produced vehicles, because of their costs and vulnerability. Therefore, an output torque estimation algorithm should be used which employs speed measurements only. Further research should be carried out on suitable estimation algorithms and on their influence on the stability of the closed-loop system.
- Traction control must be considered in order to guarantee vehicle stability. In contrast to conventional vehicles the output torque can be reduced immediately and accurately. This allows traction control to be incorporated relatively simple and at low costs.
- In this thesis control of the hybrid drive line has been achieved by separating the CVT controller and the drive line torque controller. This requires a fast CVT rate of ratio change response compared to the drive line dynamics. The major advantage is that it enables the drive line controller to be designed without explicit knowledge of the CVT response. A disadvantage is that errors in the CVT response can deteriorate the drive line controller performance. The local CVT controller must not only be fast

but also be accurate over the entire range of operating conditions. Integration of the CVT controller and the drive line controller allows the complete drive line system to be controlled by a single control loop. In this case, a low bandwidth for the rate of ratio change is sufficient and a CVT model must be used explicitly in the drive line controller. The CVT controller will compensate for the nonlinearities and guarantees a predictable response for all operating conditions. The measured rate of CVT ratio change can be considered as an additional output of the system and may be used in the drive line controller. The disadvantage of this approach is the increased complexity and a loss of the modularity of CVT controller and drive line controller.

Appendix A

Reduction of gear ratios

Two inertias connected by a (time varying) ratio i are given in Figure A-1. The angle φ_1 is chosen as independent variable for this system. Reduction of the gear ratio yields a combined inertia expressed in the variable φ_1. The momentum p_1 of the first inertia J_1 is given by:

$$p_1 = J_1\dot{\varphi}_1, \tag{A-1}$$

and the momentum p_2 of the second inertia by:

$$p_2 = J_2\dot{\varphi}_2. \tag{A-2}$$

Taking the time derivative of these momenta and adding these to the external forces yields Newton's second law of motion for the first inertia:

$$J_1\ddot{\varphi}_1 + iJ_2\ddot{\varphi}_2 = T_{in}. \tag{A-3}$$

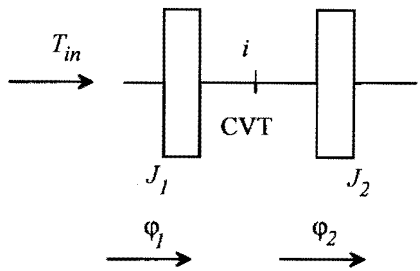

Figure A-1. A gear ratio connecting two inertias.

Including the coordinate transformation: $\dot{\varphi}_2 = i\,\dot{\varphi}_1$ and rewriting this equation yields:

$$\left(J_1 + i^2 J_2\right)\ddot{\varphi}_1 = T_{in} - J_1\, i\, \dot{\varphi}_1 \frac{di}{dt}, \tag{A-4}$$

which is a form of Lagrange's equation (Meirovitch, 1967), where the left hand expression for the inertia represents the instantaneous inertia associated with the generalised velocity :

$$J_1 + i^2 J_2. \tag{A-5}$$

The expression:

$$-J_1\, i\, \dot{\varphi}_1 \frac{di}{dt}, \tag{A-6}$$

is associated with the time dependent characteristic of the CVT ratio, which is a time dependent constraint for the system of Figure A-1. This latter expression is known as a 'gyristor' element (Allen, 1979) in bondgraph literature and appears whenever a time dependent coordinate transformation is applied to an inertia.

Appendix B

Model reduction of drive line models

In Chapter 3 the torsional model for the 'low speed' hybrid mode has been reduced. Here, reductions are derived for the torsional models of the 'engine' mode and 'high-speed' hybrid mode of the flywheel-hybrid drive line (van der Ven, 1988). As means of verification, the modal analysis reduction technique as well as the balanced truncation reduction process, have been applied to these models.

Model reduction objectives and boundaries
The closed-loop bandwidth of the drive line controller is 2.5 Hz. Therefore, an upper frequency boundary of 10 Hz is considered sufficiently high to act as a reduction boundary. In order to obtain the modal shapes, a CVT ratio of i = 1 has been chosen. Applying the balanced truncation reduction technique on the model requires a definition of inputs and outputs of the linear system. The torque generated by the CVT ratio change has been chosen as input signal to the system. The wheel torque in the drive line has been chosen as output signal. In order to obtain a solution with the balanced truncation reduction routine, the rigid body motion of the drive line models has been eliminated.

Reduction of the 'high speed' hybrid mode model
A torsional model of the 'high speed' hybrid mode is given in Figure B-2 (van der Ven, 1988). The model has been derived under similar assumptions as the 'low speed' hybrid drive line model. The model has been linearized in a suitable operating point.

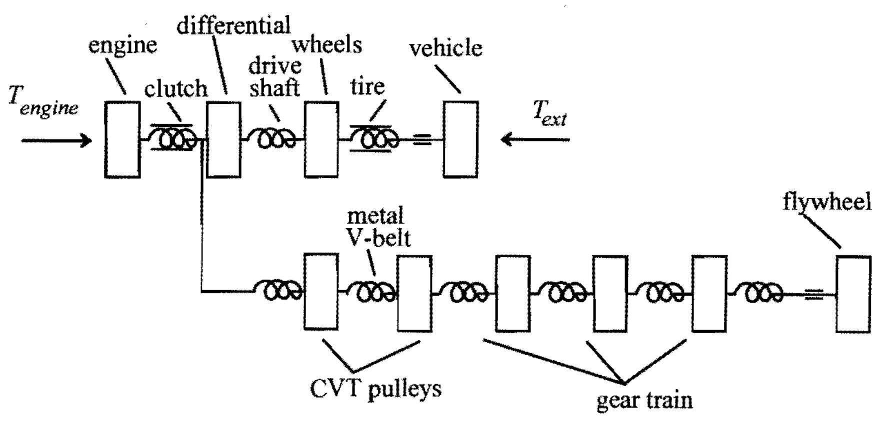

Figure B-2. Torsional model of 'high-speed' hybrid mode of drive line. Important subsystems are indicated.

The balanced truncation algorithm yields a second order model with a relative reduction error χ of 20%. This reduction error is fairly large. This is caused by the higher resonance frequencies in the original model. The results of the balanced truncation reduction process are summarized in the Bodeplot of Figure B-3.

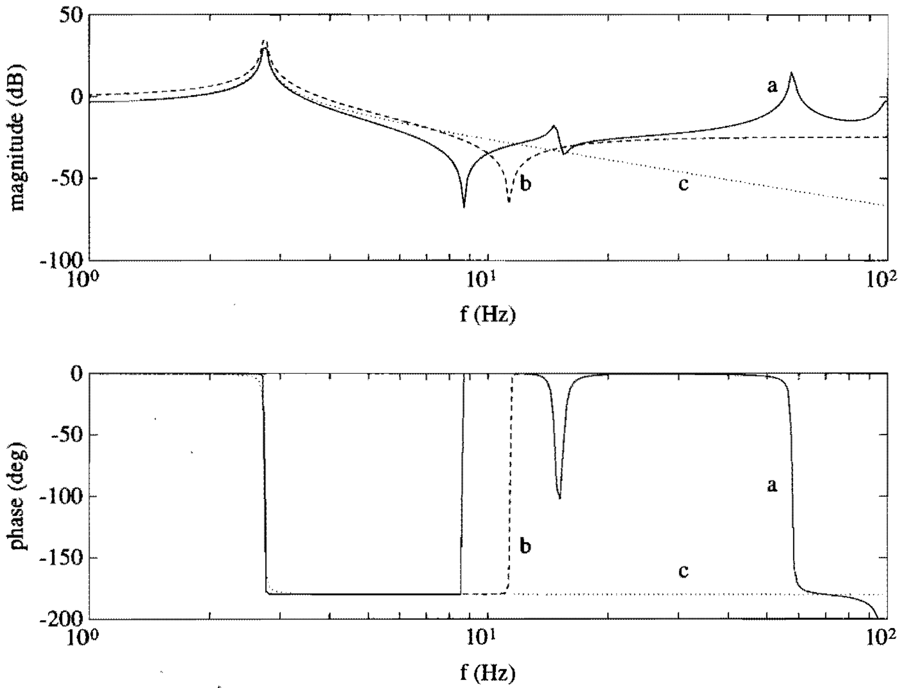

Figure B-3. Bodeplot of the 'high speed' hybrid mode original a) torsional model (solid line), b) reduced model obtained through balanced truncation (dashed line), and c) modal analysis (dotted line).

The Bodeplots show that the lower resonance frequency in the reduced models matches that of the original model. Above the first resonance frequency both reduced models deviate considerably from the original model. The resonance frequency at 9 Hz is represented in the model obtained by balanced truncation (Figure B-3b) and not represented by the model obtained by modal analysis.

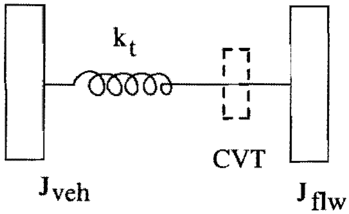

Figure B-4. Reduced undamped drive line model of the 'high speed' hybrid mode.

As controller design model, the model obtained after reduction by the modal analysis techniques can be used. This model is given in Figure B-4. The remaining inertias J_{flw} and J_{veh} are dominated by, respectively, the flywheel inertia and vehicle inertia. The CVT ratio i is time dependent. The torsional stiffness k_t is dominated by the combined stiffness of the drive shaft and tire. It is concluded that this reduced model can be used for controller design, but its limitations in frequency range and accuracy should be acknowledged.

Reduction of 'engine' mode model

A torsional model of the 'engine' mode has been given by van der Ven (1988). The model is given in Figure B-5. The model has been derived under similar assumptions as the 'low speed' hybrid drive line model and appropriate linear elements are used to obtain a linear model. The vehicle is operated differently in the 'engine' mode, as compared to the hybrid mode. In this case the vehicle is accelerated on the engine torque. This torque is a controller input of the drive line. Therefore, the engine torque has been used as an additional input variable for the balanced truncation reduction algorithm.

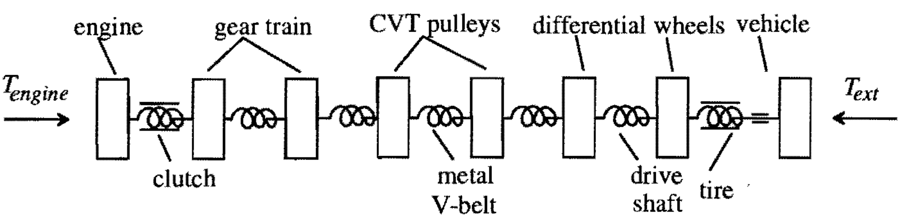

Figure B-5. Torsional model of 'engine' mode of drive line. Important subsystems are indicated.

The reduced model obtain by balanced truncation has a relative reduction error χ of 2% which is very small. The results of the balanced truncation reduction process are summarised in the Bodeplot of Figure B-7. The reduced models yield similar Bodeplots, they almost coincide and these plots show a good correspondence with the original model over a large frequency range up to the reduction boundary of 10 Hz.

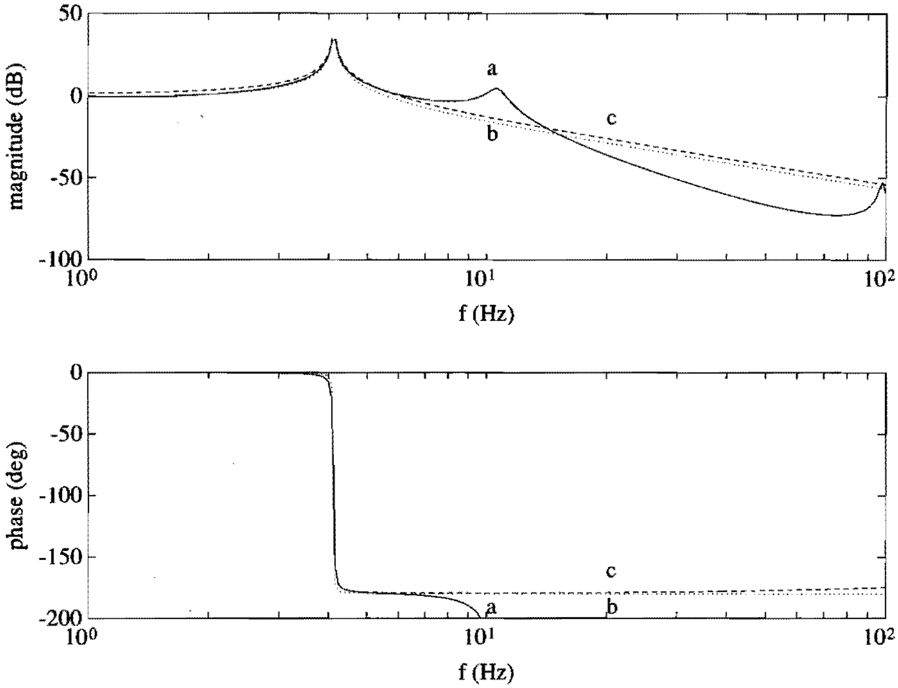

Figure B-7. Bodeplots of the 'engine mode' original a) torsional model (solid line), b) reduced model by modal analysis (dotted line), and c) obtained through balanced truncation (dashed line).

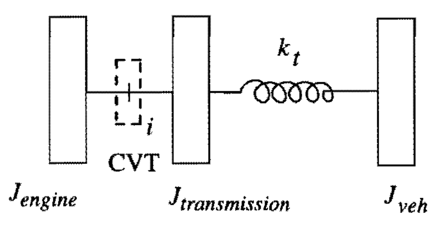

Figure B-6. Reduced drive line model of 'engine' mode.

The reduced model derived by the modal analysis is given in Figure B-6, the remaining inertias J_{engine}, $J^*_{transmission}$ and J_{veh} are dominated by, respectively, the engine inertia, transmission inertia and vehicle inertia. Because the lowest resonance frequency strongly varies with the transmission ratio, the ratio dependence of the transmission inertia is represented explicitly. The torsional stiffness k_t is dominated by the combined stiffness of the drive shaft and tire. It is concluded that this reduced model can be used for controller design.

Appendix C

CVT Specifications

The CVT specifications of the T165 are summarised in this section. The geometrical data which is used for the CVT controller is given in Table C-1. The centre distance of the T165 input and output shaft exceeds the centre distance of the CVT in the hybrid drive line by 10.0 mm. Hence, the belt for the T165 is slightly longer in order to fit in the transmission.

Table C-1. Data of T165.

shaft centre distance	$a = 165.0$ mm
nominal belt length	$L = 703.7$ mm
pulley sheave angle	$\beta = 11°$
maximum pulley sheave displacement	17.1 mm
pressure area of pulleys	$A = 0.010$ m^2
belt-pulley friction coefficient	$\mu = 0.09$

The multiple disc clutch enables starting from zero speed. It protects the CVT from overloading by slipping if the maximum torque is exceeded.

Table C-2. Clutch characteristics.

nominal pressure	6.5 bar
maximum torque at nominal pressure	120 Nm
valve type	proportional, pulse width modulated

The characteristics of the hydraulic circuit of the test-rig are given in Table C-2.

Table C-3. Hydraulic circuit characteristics.

accumulator volume	0.7 litre
CVT high pressure circuit	70 bar
lubrication low pressure circuit	8 bar
maximum pump capacity	23 litre/min at 350 bar
Helmholz resonator frequency	168 Hz

References

Chapter 1

- Bullock, K.J., 'Design Characteristics of Hybrid Vehicles with Road Test Results from Several Prototypes', SAE paper 852276.
- Bullock, K.J., 'The Technological Constraints of Mass, Volume, Dynamic Power Range and Energy Capacity on the Viability of Hybrid and Electric Vehicles', SAE paper 891659.
- Gelb, G.H., Richardson, N.A., Wang, T.C., Berman, B, 'An electromechanical transmission for hybrid vehicle powertrains - design and dynamometer testing', SAE paper 710235.
- Graaf, R. van der, 'An ic engine-flywheel hybrid drive for road vehicles', Proceedings of the "International Conference on New Developments in power train and chassis engineering", EAEC paper 87031, pp. 150-167, Strasbourg, 1987.
- Harbolla, B., Buschhaus, W. 'Konzeptauswahl und Entwicklung eines PKW-Hybrid-antriebs', ('Concept selection and development of a passenger car hybrid drive'), in German, 3. Aachener Kolloqium Fahrzeug- und Motorentechnik '91, pp. 515-536, 1991.
- Hoogovens groep, Light-weight sandwich project, Automotive design support, Netherlands, 1992.
- Höhn, B.-R., 'Möglichkeiten und Vorteile der stufenlosen Getriebe in Kraftfahrzeugen', (Options and advantages of CVTs in vehicles'), in German, Automobiltechnisches Zeitschrift 91, pp. 267-276, 1989.
- Martini, S., 'The MAN Hydrobus, a drive concept with hydrostatic brake energy recovery', International symposium - Advanced and Hybrid Vehicles, Department of Dynamics and Control, University of Strathclyde, pp. 227-234, Glasgow, Scotland, 1984.
- Masding, P.W., 'Some drive train control problems in hybrid i.c. engine/battery electric vehicles', University of Durham, Ph.D. Thesis, chap. 1, 1988.
- McGuinness, T.H., 'Utilities/Government/Manufactures: New partners for solution and environmental solutions', Proceedings of the ISATA 'Zero emissions vehicles - the electric/hybrid and alternative fuel challenge', ISATA paper 92029, Florence, Italy, pp. 209-214, 1992.

- Mitcham, A.J., 'A flywheel energy storage system for trolleybuses', Proceedings of the International symposium - Advanced and Hybrid Vehicles, Department of Dynamics and Control, University of Strathclyde, pp. 130-140, Glasgow, Scotland, 1984.
- Myers, P.S. 'Reducing transportation fuel consumption: how far should we go?', Automotive Engineering, pp. 89-95, September 1992
- Narumi, N., Suzuki, H., Sakakiyama, R. 'Trends in powertrain control', SAE paper 901154, 1990.
- Nationaal Milieubeleidsplan - kiezen of verliezen, in Dutch, Tweede Kamer, vergaderjaar 1988-1989, 21 137, No. 1-2, SDU uitgeverij, 1989.
- Nationaal Milieubeleidsplan-plus, in Dutch, Tweede Kamer, vergaderjaar 1989-1990, 21 137, No. 20-21, SDU uitgeverij, 1990.
- Oetting, H., 'Challenges to power train development in the late nineties', EAEC paper 91042, Proceedings of the EAEC congress Strasbourg, 1991.
- Reuyl, S.J., 'XA-100 hybrid electric vehicle', SAE paper 920440.
- Sampson, H.T., Killian H.J., 'Evaluation for hybrid heat engine/electric vehicles', SAE paper 720194, 1972.
- Schaik, M.A.M. 'Trends in aluminium applications in automobiles', Yearbook Autotechnical Trends, Apeldoorn, section 7.1, The Netherlands, 1992.
- Schilke, N.A., DeHart, A.O., Hewko, L.O., Matthews, C.C, Pozniak, D.J. and Rohde, S.M., 'The design of an engine-flywheel hybrid drive system for a passenger car', SAE paper 841306.
- Thoolen, F.J.M., 'Development of an advanced high speed flywheel energy storage system', Eindhoven University of Technology, Ph.D. thesis, chap. 5, 1993.
- Trummel, M.C., Mazor, S.D., Freeman, R.J., 'DOE hybrid test vehicle- Results of fuel economy emissions and engineering characterization testing', SAE paper 841251, 1984.
- Whitelaw, R.L., 'Three imperatives in the automobile future', Proceedings of the second Int. Conf. on Vehicle Mechanics, pp. 37-57, Paris, 1971.

Chapter 2

- Beachly, N.H., 'Control strategies for an internal combustion engine /accumulator energy-storage automobile', Proceedings of the International symposium - Advanced and Hybrid Vehicles, Department of Dynamics and Control, University of Strathclyde, pp. 72-82, Glasgow, Scotland, 1984.
- Devens, W.E.L. 'Computersimulaties omtrent brandstofbesparing en prestaties vliegwielhybride voertuigaandrijving ten opzichte van een handgeschakelde 5-versnellingsbak', ('Computer simulations regarding fuel savings and performance of flywheel-hybrid vehicle transmission compared to manual 5 speed transmission'),

in Dutch, Master's thesis, Laboratory for Automotive Engineering, Faculty of Mechanical Engineering, Eindhoven University of Technology, Report No. WV 155-091, The Netherlands, 1984.

- Douven, H.W.C., 'Regeling en besturing van een vliegwielhybride voertuigaandrijving', ('Control and steering of a flywheel-hybrid vehicle transmission'), in Dutch, Master's thesis, Laboratory for Automotive Engineering, Faculty of Mechanical Engineering, Eindhoven University of Technology, Report No. WV 155-106, The Netherlands, 1984.
- Falzoni, G.L., 'The "Unomatic" transmission', SAE paper 841307, 1984.
- Graaf, R. van der, 'An ic engine-flywheel hybrid drive for road vehicles', Proceedings of the EAEC 'International Conference on New Developments in power train and chassis engineering', EAEC paper 87031, pp. 150-167, Strasbourg, 1987.
- Greve, P., Liesner, W.P., 'Der neue VW Golf Ecomatic', ('The new VW Golf Ecomatic'), in German, Automobiltechnisches Zeitschrift 95, pp. 438-446, 1993.
- Hermans, A.A.M., 'De natte plaatkoppeling in de aandrijving van het vliegwielhybridevoertuig', ('The wet plate clutch in the transmission of a flywheel-hybrid vehicle'), in Dutch, Laboratory for Automotive Engineering, Faculty of Mechanical Engineering, Eindhoven University of Technology, Report No. WV 155-105, The Netherlands, 1984.
- Hermans, A.A.M., 'Regeling/besturing van de vliegwielhybride-aandrijving', ('Control/steering of a flywheel-hybrid vehicle transmission'), in Dutch, Master's thesis, Laboratory for Automotive Engineering, Faculty of Mechanical Engineering, Eindhoven University of Technology, Report No. WV 155-105 deel 1, 1985.
- Höhn, B.-R., 'Möglichkeiten und Vorteile der stufenlosen Getriebe in Kraftfahrzeugen', in German, Automobiltechnisches Zeitschrift 91, pp. 267-276, 1989.
- Hofbauer, P., Oberpichler, G.A., Sendzik, K. 'GA 1 - Glider automatic' SAE paper 830529, 1983.
- Ketelaars, G.J., 'Het langscomfort in een personenvoertuig, een literatuur onderzoek', ('The ride comfort in a passenger vehicle, a literature survey'), in Dutch, Laboratory for Automotive Engineering, Faculty of Mechanical Engineering, Eindhoven University of Technology, Report No. WOC/VT/R91.42, The Netherlands, 1991.
- Langereis, R., 'Het dynamisch regelgedrag van de vliegwielhybride voertuigaandrijving', ('The dynamic behaviour of a flywheel-hybrid vehicle transmission'), in Dutch, Master's thesis, Laboratory for Automotive Engineering, Faculty of Mechanical Engineering, Eindhoven University of Technology, Report No. WV 155-113, The Netherlands, 1985.
- Liebrand, N.J., 'Future developments in push belts for CVT application', IMechE paper C389/212, 1992.
- Main, J.J., 'Ford ELTEC integrated powertrain control', SAE paper 860652, 1986.

- Narumi, N., Suzuki, H., Sakakiyama, R. 'Trends in powertrain control', SAE paper 901154, 1990.
- Nijnatten, A. van, 'Ontwerp en beproeving van een synchronisatiekoppeling', ('Design and experimental verifcation of a synchrosing clutch'), in Dutch, Master's thesis, Laboratory for Automotive Engineering, Faculty of Mechanical Engineering, Eindhoven University of Technology, Report No. WV 155-129, The Netherlands, 1986.
- Riet, A. van der, 'Simulatieberekening aan de ophanging van de hybride aandrijfeenheid', ('Numerical simulations of the mounting of the hybrid transmission unit'), in Dutch, Master's thesis, Laboratory for Automotive Engineering, Faculty of Mechanical Engineering, Eindhoven University of Technology, Report No. WV 155-135, The Netherlands, 1988.
- Van Doorne's Transmissie, General product description, VDT, Tilburg, The Netherlands, 1988.
- Wade, J.M.A., 'An integrated electronic control system for a CVT based powertrain', ISATA paper 84006, 1984.

Chapter 3

- Berg, R. van den, 'Modellering van het gemiddelde uitgaande koppel van een ottomotor met Single Point Injectie', ('Modelling of the mean engine torque of a single point injection i.c. engine'), in Dutch, Eindhoven University of Technology, Laboratory for Automotive Engineering, Report No. WOC/VT/R/93.102, 1993.
- Bosch, S.P. van den, 'Model reduction methods, in theory and applied on a hybrid-drive line', Eindhoven University of Technology, Systems and Control Group, Faculty of Mechanical Engineering, Report No. 93.133, 1993.
- Catchpole, A.P., Healy, S.P., Hodgetts, D., 'Torsional vibrations of a vehicle drive line', Trans. of the ASME, Vol 100, October 1987.
- Chan, C., Yang, D., Voltz, T., Breitweiser, D., Jamzahdeh, F.S., Frank, A., Omitsu, T. 'System design and control of automotive continuously variable transmissions', SAE paper 840048, 1984.
- Custers, A.A.P.M., 'Onderzoek naar de invloed van de eigenschappen van een rubberband op de torsietrillingen in een vliegwielhybride aandrijving', ('Research at the influence of a rubber tire on the torsional vibrations of a flywheel-hybrid transmission'), in Dutch, Eindhoven University of Technology, Laboratory for Automotive Engineering, Report No. WOC/VT/R/92.82, 1992.
- Graaf, R. van der, 'An ic engine-flywheel hybrid drive for road vehicles', Proceedings of the EAEC "International Conference on New Developments in power train and chassis engineering", EAEC paper 87031, Strasbourg, pp. 151-167, 1987.

- Hendricks, E., Sörenson, S., 'Mean value modelling of spark ignition engines', SAE paper 900616, 1990.
- Hendrikx, R.T.W.M., 'Implementatie van een drijflijnmodel van het TUE hybride voertuig in DADS', ('Implementation of a drive line model of the EUT hybrid vehicle in DADS'), in Dutch, Eindhoven University of Technology, Systems and Control Group, Faculty of Mechanical Engineering, Report No. 93.034, 1993.
- Jones, R.P., Kuriger, I.F., Hughes, M.T.G., Holt, M.J, Ironside, J.M., Langley, P.A., 'Modelling and simulation of an automotive powertrain incorporating a Perbury continuously variable transmission', IMechE paper C200/86, IMechE conference publications on Integrated engine transmission systems, 1986.
- Laschet, A., 'Simulation von Antriebssytemen', (Simulation of propulsion systems') in German, Fachberichte Simulation, chap. 4, Springer-Verlag, 1988.
- MATLAB, Control Toolbox, users Guide, The MathWorks, Inc., South Natick.
- Meirovitch, L, *'Analytical methods in vibrations'*, chap. 4, The MacMillan Company, New York, 1967.
- Muiderman, H., 'Regeltechnisch model van een voertuigaandrijving', ('Control design model of a vehicle transmission'), Master's thesis ,in Dutch, Eindhoven University of Technology, Systems and Control Group, Faculty of Mechanical Engineering, August 1991.
- Moore, B.C., 'Principal component analysis in linear systems: controllability, observability, and model reduction', IEEE Transactions on Automatic control, Vol. AC-26, No. 1, February 1981.
- Nijnatten, A. van, 'Ontwerp en beproeving van een synchronisatiekoppeling', ('Design and verification of a synchronising clutch'), Master's thesis, in Dutch, Eindhoven University of Technology, Laboratory for Automotive Engineering, Report No. WV 155-129, 1986.
- Ogasawara, T, Yonekawa, T. 'A study of vehicle acceleration shock', Int. J. of Vehicle Design, Vol. 8. No. 4/5/6, 1987.
- Riet, A. van der, 'Simulatieberekening aan de ophanging van de hybride aandrijfeenheid', ('Numerical simulations of the mounting of the hybrid transmission unit'), in Dutch, Master's thesis, Laboratory for Automotive Engineering, Faculty of Mechanical Engineering, Eindhoven University of Technology, Report No. WV 155-135, The Netherlands, 1988.
- Sakai, Y., 'The "ECVT" Continuously Variable Transmission', VDI Berichte No. 803, pp. 235-261, 1990.
- Spijker, E., van der Graaf, R., Banens, J.P.A., Kriens, R.F.C, 'Measuring the dynamic behaviour of electronically controlled CVT's in hybrid vehicle drive lines', Zero emission vehicles - electric /hybrid and alternative fuel challenge Conference, pp. 48-52, ISATA paper 920216, Florence, Italy, 1992.
- Ven, A.A.P. van der, 'Analyse van torsietrillingen in de aandrijflijn van een hybride aangedreven voertuig', ('Analysis of torsional vibrations in the transmission of a

hybrid vehicle'), Master's thesis, in Dutch, Eindhoven University of Technology, Laboratory for Automotive Engineering, Report No. WV-155-137, 1988.

- Yang, D., Frank, A.A., 'An optimization technique for the design of a continuously variable transmission control system for automobiles', Int. J. of Vehicle design, Vol. 6, No. 1, 1985.

Chapter 4

- dSpace, 'DSP-CITpro Impex User's Guide', Vs 3.0; 'DS1002 TMS320C30 Systems hardware and software User's Guide', Vs. 2.1; 'Trace30 User's Guide', Vs. 2.0, dSpace GmbH, Paderborn, Germany, 1992.
- Egberts, T, 'Ontwerp en realisatie van een hybride aandrijf proefstand', ('Design and realization of a hybrid drive line test-rig'), in Dutch, Master's thesis, Laboratory for Automotive Engineering, Faculty of Mechanical Engineering, Eindhoven University of Technology, The Netherlands, 1993.
- Mannesmann Rexroth, Technical information RD 29586/09.89, 1989
- Overbeek, M.J., 'Vliegwiel-hybride aandrijving, motorregeling en wervelstroomrem', ('Flywheel-hybrid propulsion, motor control and eddy current brake'), in Dutch, thesis Hogeschool Eindhoven sector TC-Elektrotechniek, No. E 92070, The Netherlands, 1992
- Spijker, E., van der Graaf, R., Banens, J.P.A., Kriens, R.F.C, 'Measuring the dynamic behaviour of electronically controlled CVT's in hybrid vehicle drive lines', Proceedings of the Zero emission vehicles - electric /hybrid and alternative fuel challenge Conference, ISATA paper 920216, pp. 48-52, Florence, Italy, 1992.
- Stubbe, D.R. 'Onderzoek aan een continu variabele transmissie', ('Research on a continuously variable transmission') ,in Dutch, Master's thesis, Faculty of Mechanical Engineering, Delft University of Technology, Report No. A432, The Netherlands, 1987.
- Telma, Technical specification of C30 retarder, 0C461000, edition 12/85, Compagnie Françaíse Telma, 1985.
- Veen, S.C. van der, 'Stufenloser Drehmoment/Drehzahlwandler Transmatic', ('Continuously Variable Transmission Transmatic'), in German, Antriebstechnik 16, No. 4, pp. 217-222, 1977.

Chapter 5

- Abromeit, G. 'Konzept einer elektronischen Steuerung für ein stufenloses mechanisches Getriebe', ('Concept of an electronic controller for a mechanical CVT'), in German, Antriebstechnik 24, No. 2, pp.49-51, 1985.
- Åström, K.J., Wittenmark, B., *'Adaptive control'*, Addison-Wesly Publishing Company, 1989.

- Becker, H.-J., 'Mechanik des Van-Doorne-Schubgliederbandes', ('Functioning of the Van-Doorne push belt'), in German, Antriebstechnik 26, No. 8, pp. 47-52, 1987.
- Bonthron, A., 'CVT-Efficiency measured under dynamic running conditions', SAE paper 850569, 1985.
- Cadee, T., personal communication, 1992.
- Dittrich, O., 'Das Stufenlose Kettengetriebe als Hauptantrieb im Kraftfahrzeug', ('The CVT as main driver in a car'), in German, VDI Berichte No. 803, pp. 181-196, 1990.
- Elzinga, T. 'Voortgezette modelvorming en regeling van een continu variabele transmissie', ('Extended modelling and control of a continuously variable transmission'), in Dutch, Master's thesis, Faculty of Mechanical Engineering, Delft University of Technology, Report No. A-490, The Netherlands, 1988.
- Falzoni, G.L. 'The 'Unomatic' transmission', IMechE C423/84, 1985.
- Gerbert, G., 'Metal V-belts Mechanics', ASME paper 84-DET-227, 1985.
- Graaf, R. van der, 'An ic engine-flywheel hybrid drive for road vehicles', Proceedings of the EAEC "International Conference on New Developments in power train and chassis engineering", EAEC paper 87031, pp. 150-167, Strasbourg, 1987.
- Gieles, W.T.M. 'Electronic control of continuously variable transmission and its extension to engine transmission management', IMechE C382/048, 1989.
- Grewal, M.S., Andrews, A.P., *'Kalman filtering, theory and practice'*, chap. 7, Prentice Hall, Englewood Cliffs, New Jersey, USA, 1993.
- Hendriks, E., Ter Heegde, P., van Prooijen, T., 'Aspects of a metal pushing V-belt for automotive cut application', SAE paper 881735.
- Hirano, S, Miller, A.L., Schneider, K.F. 'SCVT - A state of the art electronically controlled continuously variable transmission', SAE paper 910410, 1991.
- Kok, J.E.M. 'Voortgezet onderzoek naar een regeling van een continu variabele transmissie voor een hybride aandrijving', ('Continued research for a controller for a continuously variable transmission'), in Dutch, Master's thesis, Systems and Control group, Faculty of Mechanical Engineering, Eindhoven University of Technology, Report No. WFW-89.036, The Netherlands, 1989.
- Kwakernaak, H., Sivan, R, *'Linear Optimal Control Systems'*, chap. 5, John Wiley & Sons, Inc., New York, 1972.
- Namuri, N., Suzuki, H., Sakakiyama, R. 'Trends of powertrain control', SAE paper 901155.
- Nijnatten, A. van, 'Ontwerp en beproeving van een synchronisatiekoppeling', ('Design and experimental verification of a synchronizing clutch'), in Dutch, Master's thesis, Laboratory for Automotive Engineering, Faculty of Mechanical Engineering, Eindhoven University of Technology, Report No. WV 155-129, The Netherlands, 1986.

- Pinches, M.J., Ashby, J.G., *'Power hydraulics'*, Prentice Hall, London, 1988.
- Rooij, J.H.M. van, 'Volvo Car's new chain concept', EAEC paper 91032, 1991.
- Rooij, J.H.M. van , Schearlaeckens, W.P.M., 'De metalen V-band (duwband), een theoretische benadering' ('The metal V-belt (push belt), a theoretical approach'), in Dutch, publication of GCI and NedCar, 1992.

  also published as 'Kräfte und Wirkungsgrad beim Schubgliederband', in German, Antriebstechnik 32, No. 8, 9 and 10, 1993.
- Röper, H. 'Anforderungen an die Druckölversorgungseinheit hydraulisch gesteuerter CVT-Getriebe', ('Requirements on the power hydraulics of a hydraulically controlled CVT'), in German, Antriebstechnik 26, No. 8, pp. 41-47, 1989.
- Sakai, Y., 'The "ECVT" Continuously Variable Transmission', VDI Berichte No. 803, pp. 235-261, 1990.
- Slotine, J.-J., Li, W.P. *'Applied nonlinear control'*, chap. 8, Prentice-Hall International, 1991.
- Spijker, E., Graaf, R. van der, Banens, J.P.A., Kriens, R.F.C, 'Measuring the dynamic behaviour of electronically controlled CVT's in hybrid vehicle drive lines', Proceedings of the ISATA Zero emission vehicles - electric /hybrid and alternative fuel challenge Conference, ISATA paper 920216, pp. 48-52, Florence, Italy, 1992.
- Spijker, E, Graaf, R. van der, Rooij, J.H.M. van, Kriens, R.F.C, 'Electronic control of a CVT for a flywheel-hybrid vehicle transmission', Proceedings of the ISATA Mechatronics Conference, paper 93ME033, pp. 281-288, Aachen, 1993a.
- Spijker, E, 'An electronically controlled CVT for a flywheel-hybrid vehicle: Design, development and validation of control algorithms, Laboratory for Automotive Engineering, Eindhoven University of Technology, Report No. WOC/VT/R/93.150, 1993b.
- Stubbe, D.R. 'Onderzoek aan een continu variabele transmissie', ('Analysis of a continuously variable transmission'), in Dutch, Master's thesis, Faculty of Mechanical Engineering, Delft University of Technology, Report No. A432, 1987.
- Sun, D.C., 'Performance analysis of a variable speed-ratio metal V-belt drive', Trans. of the ASME, Vol. 110, pp.472-481, December 1988.
- Viersma,T.J., *'Analysis, synthesis and design of hydraulic servosystems and pipelines'*, Elseviers Scientific Publishing Company, Amsterdam, 1980.
- Wade, J.M.A., 'An integrated electronic control system for a CVT based powertrain', ISATA paper 84006, Proceedings of the ISATA Confernce, 1985.
- Wang, G., 'Untersungen an Stufenlos einstellbaren Zug- und Schubgliedergetrieben', ('Analysis of continuously variable transmissions with chains and metal V-belts'), in German, Ph.D. thesis Technical University Clausthal, Clausthal, Germany, 1991.

Chapter 6

- ACSL, Advanced Continuous Simulation Language, Reference Manual, Mitchell and Gaulthier Associates, Concord, Mass., USA, 1986.
- Berg, R. van den, 'Modellering van het gemiddelde uitgaande koppel van een ottomotor met Single Point Injectie' ('Modelling of the mean engine torque of a single point injection i.c. engine'), in Dutch, Eindhoven University of Technology, Laboratory for Automotive Engineering, Report No. WOC/VT/R/93.102, 1993.
- Custers, A.A.P.M., 'Onderzoek naar de invloed van de eigenschappen van een rubberband op de torsietrillingen in een vliegwielhybride aandrijving', ('Research at the influence of a rubber tire on the torsional vibrations of a flywheel-hybrid transmission'), in Dutch, Eindhoven University of Technology, Laboratory for Automotive Engineering, Report No. WOC/VT/R/92.82, 1992.
- Dalmaijer, J.W., 'Modelvorming van de dynamische koppelrespons van een Volvo viercylinder viertakt motor' (Modelling of the dynamic torque response of a Volvo four cylinder four stroke engine'), in Dutch, Eindhoven University of Technology, Laboratory for Automotive Engineering, 1986.
- Franklin, G.F., Powell, J.D., *'Digital control of dynamic systems'*, chap. 5, Addison-Wesley Publishing Company, 1980.
- Grewal, M.S., Andrews, A.P., *'Kalman filtering, theory and practice'*, Prentice Hall, Englewood Cliffs, New Jersey, USA, 1993.
- Isidori, A., *'Nonlinear control systems: an introduction'*, 2nd ed., Springer Verlag, Berlin, 1989.
- Hendricks, E., Sörenson,.S., 'Mean value modelling of spark ignition engines', SAE paper 900616, 1990.
- Hendrikx, R.T.W.M., 'Implementatie van een drijflijnmodel van het TUE hybride voertuig in DADS', ('Implementation of a drive line model of the EUT hybrid vehicle in DADS'), in Dutch, Eindhoven University of Technology, Systems and Control Group, Faculty of Mechanical Engineering, Report No. 93.034, 1993.
- Kemenade, L.H.A. van, 'Studie naar het optimaal regelen van de energiestroom in een vliegwiel hybride aandrijflijn', ('Study at optimal control of the powerflow in a flywheel hybrid transmission'), in Dutch, Eindhoven University of Technology, System and Control Group, Faculty of Mechanical Engineering, WFW-Report No. 92.108, 1993.
- Ketelaars, G.J., 'Het langscomfort in een personenvoertuig, een literatuur onderzoek', ('The ride comfort in a passenger vehicle, a literature survey'), in Dutch, Eindhoven University of Technology, Laboratory for Automotive Engineering, Faculty of Mechanical Engineering, Report No. WOC/VT/R91.42, The Netherlands, 1991.
- Kwakernaak, H., Sivan, R, *'Linear Optimal Control Systems'*, chap. 5, John Wiley & Sons, Inc., New York, 1972.

- Masmoudi, R.A., Hedrick, J.K., 'Estimation of vehicle shaft torque using nonlinear observers', ASME Journal of Dynamic Systems, Measurement, and Control, Vol. 114, pp. 394-400, 1992.
- Misawa, E.A., Hedrick, J.K., 'Nonlinear observers - A state of the art survey', ASME Journal of Dynamic Systems, Measurement, and Control, Vol. 111, pp. 344-352, 1989.
- Moskwa, J.J., Hedrick, J.K., 'Nonlinear algortihms for automotive engine control', IEEE Control Systems Magazine, pp. 88-93, April 1990.
- Schols, E., 'Metingen aan een tweetal Volvo motoren in stationair bedrijf', (Measurements on two Volvo engine at stationary operating conditions'), in Dutch, Eindhoven University of Technology, Laboratory for Automotive Engineering, Report No. WV 155-119, 1985.
- Schols, E., 'Metingen aan de dynamische koppelrespons van een Volvo viercylinder viertakt motor' (Measurements of the dynamic torque response of a Volvo four cylinder four stroke engine'), in Dutch, Eindhoven University of Technology, Laboratory for Automotive Engineering, Report No. WV 155-126, 1986.
- Slotine, J.J.E., Li, W., *'Applied nonlinear control'*, chap. 6, Printice-Hall International, Inc., New York, 1991.
- Spijker, E., van der Graaf, R., Banens, J.P.A., Kriens, R.F.C., 'Measuring the dynamic behaviour of electronically controlled CVT's in hybrid drive lines', Proceedings of the ISATA Zero Emission Vehicles Conference, ISATA paper 920216, pp. 48-52, Florence, Italy, 1992.
- Spijker, E., Veldpaus, F.E., Kriens, R.F.C., 'Closed loop control of a CVT based hybrid vehicle transmission', Proceedings of the 4th International Conference on 'Vehicle and traffic systems technology', pp. 561-574, Strasbourg, France, 1993.
- Sweet, L.M., Anhalt, D.A., 'Optimal control of flywheel hybrid transmissions', Transactions of the ASME, Journal of Dynamic Systems, Measurements, and Control, Vol. 100, pp. 24-33, March 1978.
- Van Doorne's Transmissie, General product description, VDT, Tilburg, The Netherlands, 1988.
- Ven, A.A.P. van der, 'Analyse van torsietrillingen in de aandrijflijn van een hybride aangedreven voertuig', ('Analysis of torsional vibrations in the transmission of a hybrid vehicle'), Master's thesis, in Dutch, Eindhoven University of Technology, Laboratory for Automotive Engineering, Report No. WV-155-137, 1988.

Chapter 7

- Egberts, T.L.T.M., 'Ontwerp en realisatie van een equivalente vliegwielhybride voertuigaandrijflijn op een simulatie proefstand' (Design and realization of an equivalent flywheel-hybrid vehicle transmission on a test-rig'), in Dutch, Laboratory for Automotive Engineering, Report No. WOC/VT/R/93.142, Eindhoven University of Technology, 1993.

- Gerbert, G., 'Metal V-belt mechanics', PTG Conference in Boston, ASME paper 84-DET-227, 1984.
- Gerbert, G, 'Influence of flexible pulleys on V-belt mechanics', Report No. 1985-09-02, Division of Machine Elements, Chalmers University of Technology, 1985.
- Gerbert, G, 'How the metal V-belt works', Report No. 1983-03-08, Division of Machine Elements, Chalmers University of Technology, 1983.

Appendix A

- Allen, R.R. 'Multiport Representations of Inertia Properties of Kinematic Mechanisms', J. of the Franklin Institute, Vol. 308, No. 3, September 1979.
- Meirovitch, L, *'Analytical methods in vibrations'*, chap. 4, The MacMillan Company, New York, 1967.

Appendix B

- Ven, A.A.P. van der, 'Analyse van torsietrillingen in de aandrijflijn van een hybride aangedreven voertuig', ('Analysis of torsional vibrations in the transmission of a hybrid vehicle'), Master's thesis, in Dutch, Eindhoven University of Technology, Laboratory for Automotive Engineering, Report No. WV-155-137, 1988.

Acknowledgements

I want to thank all persons who have contributed to the work presented in this thesis.

I am grateful to Roel van der Graaf for initiating the project and for the guidance and advice during the project. Furthermore, I also want to thank Frans Veldpaus for his support and advice. The discussions with Roel and Frans were time consuming but always very enlightening.

My promotors Prof.dr.ir. R.F.C. Kriens and Prof.dr.ir. J.J. Kok are acknowledged for their valuable comments during the project and during the preparation of this thesis.

Furthermore, I want to thank Jacques van Rooij and Theo Cadee of GCI and Willy Schaerlaeckens of NedCar Technology who gave advice and technical support for the experimental work. I also want to thank Riné Pelders and Harry Cuijten of Van Doorne's Transmissie and Ed van Looij, Ad de Beer, Theo Duisters and Theo Egberts who all contributed and enabled the experimental verification. My fellow Ph.D. students at the Laboratory of Automotive Engineering are acknowledged for their suggestions and pleasant working atmosphere.

Finally, I want to thank my parents and my wife who supported me and encouraged me to complete this work.

Engbert

Curriculum vitae

Engbert Spijker was born at June 26th, 1965 in Oldemarkt, The Netherlands. Between 1978 and 1982 he attended the Scholengemeenschap Gelderingen and he continued his education from 1982 to 1984 at the Rijksscholengemeenschap Jan Hendrik Tromp Meesters at Steenwijk. In 1984 he started his study Electrical Engineering at the Twente University of Technology. There, he got the opportunity to participate in an E.G. student exchange program. This allowed him to carry his graduation project out at the University of Strathclyde, Glasgow (Scotland), at the Control Unit of the faculty of Electrical Engineering. The graduation project was about the control of a ship propulsion system. In this period, his interest in control of technical applications was established. In 1989 he received his M.Sc. degree in Electrical Engineering. In 1990 he started his Ph.D. project on control of a hybrid vehicle drive line at the Laboratory for Automotive Engineering, faculty of Mechanical Engineering, Eindhoven University of Technology. The result of this work is reported in this thesis.

STELLINGEN

behorende bij het proefschrift

Steering and control of a CVT based hybrid transmission for a passenger car

1. Voor het ontwerpen van een regeling voor de CVT met duwband zijn de complexe modellen van het krachtenspel op en in de metalen duwband van ondergeschikt belang *(dit proefschrift)*.

2. Op grond van de moeilijke regelbaarheid wordt de combinatie van vliegwiel en mechanische CVT slechts zelden toegepast in hybride voertuigen. Dit is vanuit het oogpunt van rendementen volkomen onjuist *(dit proefschrift)*.

3. Een wezenlijk probleem bij het regelen van complexe technische systemen is niet het kiezen van een specifieke regelwet maar het verkrijgen van voldoende en nauwkeurige informatie over het systeemgedrag *(dit proefschrift)*.

4. Regelingen voor het aandrijfkoppel worden slechts zelden toegepast in voertuigen omdat het gebruik van koppelmeetassen, in technisch en financieel opzicht, ongewenst is. Men vergeet hierbij dat robuuste schattingsalgoritmen, in combinatie met eenvoudig te meten signalen van toerentallen, het meten van koppels overbodig maken *(dit proefschrift)*.

5. Het gebruik van een vliegwiel in een voertuig is volstrekt ontoelaatbaar als niet aan de strengste veiligheidseisen is voldaan. Hierbij zijn zowel het bezwijkgedrag als de gyroscopische effecten van het vliegwiel essentieel.

6. Bij populaire publikaties over CVT's in voertuigen worden de belangrijke voordelen zoals brandstofverbruik, bedieningsgemak en comfort, volledig overschaduwd door de aandacht die wordt gegeven aan de in de CVT toegepaste duwband.

7. Voertuigen met hoogrendement aandrijfsystemen kunnen, door hun complexiteit, niet op kostprijs concurreren met de huidige conventionele voertuigen. Introductie is alleen mogelijk indien de overheid een actief stimuleringsbeleid voert.

8. De huidige trend naar steeds snellere en luxueuzere voertuigen wordt hoofdzakelijk veroorzaakt door de voorkeur van de autojournalisten voor deze types voertuigen.

9. Voor een goede concurrentiepositie van academici op de internationale arbeidsmarkt is meer aandacht voor de beheersing van de Engelse taal noodzakelijk.

10. De temperatuurstijging ten gevolge van het broeikaseffect zal in de nabije toekomst het gebruik van energieverslindende airconditioners stimuleren.

E. Spijker
Eindhoven, 14 maart 1994